Model Predictive Control of Water Level and Salinity in Coastal Areas

Aydin, B.E.

Important note
To cite this publication, please use the final published version (if applicable).
Please check the document version above.

MODEL PREDICTIVE CONTROL OF WATER LEVEL AND SALINITY IN COASTAL AREAS

MODEL PREDICTIVE CONTROL OF WATER LEVEL AND SALINITY IN COASTAL AREAS

Dissertation

for the purpose of obtaining the degree of doctor
at Delft University of Technology,
by the authority of the Rector Magnificus, Prof. dr. ir. T.H.J.J. van der Hagen
chair of the Board for Doctorates,
to be defended publicly on Friday 28 August 2020 at 15:00 o'clock

by

Boran Ekin AYDIN

Master of Science in Civil Engineering
Middle East Technical University, Ankara, Turkey
born in Maçka, Trabzon, Turkey

This dissertation has been approved by the promotors.

Composition of the doctoral committee:

Rector Magnificus,   chairperson
Prof. dr. ir. N.C. van de Giesen   Delft University of Technology, promotor
Dr. ir. E. Abraham   Delft University of Technology, copromotor
Dr. ir. G.H.P. Oude Essink   Deltares, University of Utrecht, copromotor

Independent Members:

Prof. dr. ir. H.H.G. Savenije   Delft University of Technology
Prof. dr. ir. M.F.P. Bierkens   University of Utrecht
Prof. dr. ir. A. Weerts   Deltares
Dr. J.M. Maestre Torreblanca   University of Seville, Spain
Prof. dr. ir. S.C. Steele Dunne   Delft University of Technology, reserve member

To my mother Semra,
my father Ali,
and in the memory of dr. ir. Peter Jules van Overloop

SUMMARY

P OLDERS are low-lying and artificially drained areas surrounded by water storage canals. In low-lying delta areas such as the Mississippi delta in Louisiana (USA), the Ganges-Brahmaputra delta (Bangladesh), or the Rhine-Meuse delta (The Netherlands), polders experience surface water salinization problem due to saline groundwater exfiltration, which is the upward flow of saline groundwater from the subsurface. A significant increase in surface water salinization is expected globally driven by rising sea levels, leading to a decreasing freshwater availability. Land subsidence, climate change induced decrease in precipitation and sea level rise are expected to accelerate salinization of groundwater and surface water systems. To counteract surface water salinization, freshwater diverted from rivers is used for flushing the canals and ditches in coastal areas. Sustaining freshwater-dependent agriculture in such areas will entail an increased demand for flushing, while the demand of a better water quality will tend to increase. On the other hand, freshwater usage is not explicitly considered for polder operation and results in excessive use. Decreasing the amount of freshwater usage for polder flushing can create additional supply opportunities for industrial users, drinking water companies or other irrigation systems. To meet the increasing demand for flushing due to expected increase of salinization while the freshwater availability is decreasing, new operational designs are required for polders that will use the available freshwater resources efficiently.

Efficient water management in polders aims to regulate water levels, salinity levels and the water usage by manipulating the intake and pump flows. In accordance with that, the control objectives for a polder may be summarized as:

- surface water level needs to stay between predetermined thresholds for safety (always), demand satisfaction, and keeping groundwater levels in operational limits for the drainage system,

- salinity level needs to stay below a certain threshold (when necessary) for agricultural and ecological use, and

- freshwater use and pumping cost should be minimized, given the water level and salinity concentration constraints described above are satisfied.

The relation between these sub-objectives could be conflicting: additional freshwater from the intakes is necessary to satisfy the salinity level objective, which results in increased usage of freshwater and pump flows. This may result in violations of water levels, resulting in a complex multi-objective control problem. An advanced control algorithm for polder flushing to control salinity level and quantity can increase the efficiency of the system. Model Predictive Control (MPC) is such an optimization-based control strategy, which makes use of a model of the system controlled to predict the future behavior of

the system over a finite prediction horizon. The ability of MPC to handle multiple objectives and constraints makes it an attractive tool for optimal control of water systems. Therefore, the main research question of this thesis is:

> *How to apply Model Predictive Control to polder flushing satisfying the constraints on water level and salinity concentrations while minimizing the freshwater intake?*

The research presented in this thesis focuses on control of the surface water system, which is affected by saline groundwater exfiltration. The open channel system (single pool or network of channels) consists of freshwater intakes and pumping stations for drainage of the polder. Using these structures, the salinity and surface water level is controlled by adjusting the flushing and pumping discharges in the system. Polder flushing is modeled using one dimensional De Saint Venant (SV) and Advection Dispersion (AD) equations. For saline groundwater exfiltration, existing models and data in the literature are used for the case study areas.

Chapter 2 analyses the use of linearized SV and AD equations as the internal model of the MPC for salinity and water level control. Coupling the MPC with a saline groundwater exfiltration model, three different scenarios are presented using data from two representative Dutch polders. To minimize the usage of freshwater for flushing, a combination of soft constraints on salinity concentration and flushing discharge are introduced. It is shown that MPC can successfully be used to control salinity and water level of water courses. A comparison with a fixed flushing strategy, which is very common in practice, is provided showing the flexibility and advantages of using MPC.

In Chapter 3, control of a real polder network is presented. The MPC formulation applied in Chapter 2 was limited to the control of channels connected in series. In a real polder network, multiple channels with different salinity concentrations are connected with or without hydraulic structures in between. Mixing at the connection nodes, spatial and temporal variation of salinity and nonlinear dynamics of salinity transport has to be considered in optimization for polder flushing. Therefore, in Chapter 3, a Nonlinear Model Predictive Control (NMPC) is presented and applied to the control of the Lissertocht catchment, Haarlemmermeer Polder, Province of North-Holland, The Netherlands. The results showed that the network of canals could not be made sufficiently fresh with the current intake capacity. A posteriori analysis of the results is used for an update of the intake capacity of the catchment, and with these proposed capacities, the NMPC was shown to achieve satisfactory salinity control performance within the constraints of the network.

MPC uses real time measurements at every control time step to update the current state of the system. The controller needs to be coupled with a monitoring network (for salinity and water level measurements) to update the system states in real time for calculation of the optimum control action. Water level in a polder system is kept within a predefined narrow margin and does not vary too much throughout the polder and therefore can be monitored easily. On the other hand, the spatial and temporal variation of salinity can be high and depends on the season of the year, access to flushing water and distance from salty boils resulting in a requirement of an efficient salinity monitoring network. However, considering the economic feasibility, an optimal monitoring

network is required for the estimation of the salinity states at unmeasured points of interests of the system using the minimum number of sensors. In Chapter 4, an optimal salinity sensor placement is presented for the Lissertocht catchment. Salinity dynamics are represented by a low-order Principal Component Analysis (PCA) model and a greedy algorithm is used for placing minimum number of sensors for reconstructing salinity in all main channels.

Chapter 5 summarizes the contributions of this thesis and recommendations for future research directions that are expected to be important for the real application of MPC in polder management.

Samenvatting

Een polder is een over het algemeen laaggelegen gebied dat omgeven is door één of meerdere waterkeringen, waarvan het waterpeil kunstmatig beheerst wordt. In deltagebieden waar deze polders voorkomen, zoals de Mississippi Delta in Louisiana (Verenigde Staten), de Ganges-Brahmaputra Delta (Bangladesh) of de Rijn-Maas Delta (Nederland), kan zout grondwater naar de oppervlakte stromen en het zoete oppervlaktewater verzilten. Wereldwijd wordt door de zeespiegelstijging een significante toename van de verzilting van het zoete oppervlaktewater verwacht. Dit leidt tot een afname van de beschikbaarheid van zoet water. Bodemdaling, afnemende neerslag als gevolg van klimaatverandering zullen naar verwachting de verzilting van grond- en oppervlaktewatersystemen verder versnellen. Om het zoute water uit de polders te verwijderen, wordt zoet water uit rivieren gebruikt om de kanalen, waterlopen en sloten in kustgebieden door te spoelen. Dit wordt gedaan omdat agrariërs zoet water van voldoende kwaliteit op het juiste moment nodig hebben om zoetwaterlandbouw te kunnen bedrijven. Bij het doorspoelen van polders wordt niet expliciet rekening gehouden met het zoetwatergebruik. Om aan de toenemende doorspoeldebieten te voldoen, zijn nieuwe operationele systemen voor de polders nodig om de totale zoetwaterbehoefte te verminderen.

Efficiënt waterbeheer in polders heeft als doel het waterpeil, het zoutgehalte en het watergebruik te reguleren door de in- en uitlaatstromen te manipuleren. De controle subdoelstellingen van een polder zijn samen te vatten als:

- oppervlaktewaterpeil moet (altijd) tussen vooraf bepaalde drempels blijven voor veiligheid en watervoorziening voor gebruik in de landbouw,

- het zoutgehalte moet (indien nodig) onder een bepaalde drempel blijven voor agrarisch en ecologisch gebruik, en

- zoetwaterverbruik en pompkosten moeten geminimaliseerd worden, terwijl voldaan wordt aan (met name) de oppervlaktewaterpeil- en zoutconcentratie-eisen.

De relaties tussen deze subdoelstellingen kunnen tegenstrijdig zijn. Een geavanceerd algoritme voor polderspoeling om het waterpeil en het zoutgehalte te regelen, kan de efficiëntie van het systeem verhogen. Model Predictive Control (MPC) is een op optimalisatie gebaseerde methode die gebruik maakt van een intern model van het watersysteem, waarmee optimale regelacties worden berekend over een voorspelhorizon. Het vermogen van MPC om meerdere doelstellingen en beperkingen aan te kunnen, maakt het een aantrekkelijk hulpmiddel voor een optimale controle van watersystemen. De belangrijkste onderzoeksvraag van dit proefschrift is zodoende:

Hoe kan Model Predictive Control toegepast worden bij het efficiënt doorspoelen van polders, terwijl de oppervlaktewaterpeil- en zoutconcentratie eisen en zoetwaterverbruik geminimaliseerd worden?

Het onderzoek in dit proefschrift richt zich op de beheersing van het oppervlakte-watersysteem. Het open kanaalsysteem bestaat uit zoetwaterinlaten en pompstations. Deze structuren worden gemanipuleerd om het waterpeil en het zoutgehalte te beheersen. Polder doorspoelen wordt numeriek gemodelleerd met De Saint Venant (SV) en Advection Dispersion (AD) vergelijkingen.

Hoofdstuk 2 toont resultaten van simulaties die gelineariseerde SV- en AD-vergelijkingen gebruiken als het interne model van de MPC. We tonen resultaten van drie scenario's. We gebruiken verziltingsgegevens uit twee Nederlandse polders. Het gebruik van zoet water wordt geminimaliseerd met behulp van de MPC. In dit hoofdstuk wordt de flexibiliteit en voordelen van het gebruik van MPC gedemonstreerd.

Hoofdstuk 3 toont de resultaten van simulaties van de besturing van een echt pol-dernetwerk. In de polder is het mengen van zout water in de verbindingsknooppunten belangrijk. Bovendien wordt de ruimtelijke en temporele variatie van het zoutgehalte gemodelleerd. Dit hoofdstuk presenteert nieuwe methode, genaamd een Nonlinear Model Predictive Control (NMPC). We passen de methode toe in het stroomgebied van de Lissertocht, dat een peilvak is in het zuiden van de Haarlemmermeer Polder, Provincie Noord-Holland, Nederland. De resultaten laten zien dat de capaciteit van het systeem niet voldoende is. Na een aanpassing van het ontwerp voor de innames bestuurt NMPC de polder echter met bevredigende prestaties.

MPC gebruikt real-time metingen bij elke controletijdstap om de huidige status van het systeem bij te werken. Daarom heeft het een meetnetwerk nodig voor metingen van zoutgehalte en waterpeil. Het waterpeil in een polder varieert niet te veel en is daarom gemakkelijk te meten. De ruimtelijke en temporele variatie van het zoutgehalte kan echter hoog zijn. Het hangt af van het seizoen van het jaar, toegang tot zoet water en afstand tot zoute wellen. Zodoende is een optimaal meetnetwerk nodig om het zoutgehalte in de polder goed in te schatten. Hoofdstuk 4 laat de optimale plaatsing van de zoutwater sensoren voor het Lissertocht zien. We gebruiken een Principal Component Analysis (PCA)-model (een multivariate analysemethode in de statistiek om een grote hoeveel-heid gegevens te beschrijven met een kleiner aantal relevante grootheden, de principale componenten) en een Greedy Algorithm (een algoritme dat probleemoplossende heuristieken volgt om in elke fase de lokaal optimale keuze te maken) om de sensoren optimaal te plaatsen. Met behulp van het PCA-model plaatsen we een minimaal aantal sensoren waarmee het zoutgehalte in alle hoofdkanalen van een polder voldoende kan worden gereprocudeerd.

Hoofdstuk 5 worden de conclusies van dit proefschrift gepresenteerd. Het bevat bovendien aanbevelingen voor toekomstige onderzoeksrichtingen die belangrijk zijn voor de toepassing van MPC op polders.

CONTENTS

1

INTRODUCTION

Science is the only true guide in life.

Mustafa Kemal Atatürk

This thesis is concerned with the optimal control of salinity and water level in low-lying delta areas by explicitly considering freshwater use. Here, the motivation of the thesis and the optimal control problem applied to polder flushing is described and followed by the research objectives.

1

1.1. Salinization Problem in Low-Lying Delta Areas

More than 35% of the world's population lives within 100 km of the coast [1], having access to transport connections, fish stocks and fertile inlands [2]. Fresh groundwater resources in these areas are mostly the main source for domestic, industrial and agricultural use. Due to growing populations, increasing food demands and economic development, freshwater consumption is expected to increase [3]. The total water consumption for agriculture purposes, which has around 70 % share in total freshwater demand, is expected to increase by more than half by 2090s [4]. In coastal areas, unless properly managed, this increase will cause over-exploitation of aquifers and salinization of extraction wells [5]. Due to the artificial drainage, groundwater table lowering causes an upward flow of brackish and nutrient rich groundwater adversely affecting the surface water quality [6]. Moreover, the river discharges delivering freshwater to coastal areas will likely to decrease due to climate change induced decrease in precipitation patterns [7] and increased water demand for agriculture, both locally and upstream [8]. In low-lying delta areas such as the Mississippi delta in Louisiana (USA), the Ganges-Brahmaputra delta (Bangladesh), and the Rhine-Meuse delta (Netherlands) [9–13], saline groundwater will increasingly move towards the ground surface and exfiltrate to the surface water system [14] resulting in salinization. Land subsidence, climate change and sea level rise accelerate salinization [12].

To counteract surface water salinization, freshwater diverted from rivers is used for flushing the canals and ditches in coastal irrigation networks. However, decreasing freshwater availability [8] and expected increase of surface water salinization [12, 14] will force water managers to reconsider the current water management practice in polders facing salinization; they will likely aim to minimize the intake of diverted river water for flushing. In The Netherlands, the locations where the largest saline groundwater exfiltration, which is the upward flow of saline groundwater from the subsurface to surface water, occur in low-lying polders [15]. Nowadays, freshwater from the rivers Rhine and Meuse is used for flushing these polders during agricultural growing seasons, with about 15% of the total freshwater supply in The Netherlands [16]. Increasing the efficiency of flushing is regarded as a promising way to decrease surface water demand in [17], where the importance of water management in polders is highlighted. Therefore, the main objective of this thesis is how to apply Model Predictive Control to polder flushing satisfying the constraints on water level and salinity concentrations while minimizing the freshwater intake? The research presented in this thesis uses real-world data of two representative Dutch polders as case studies. The methodologies developed are not case specific and are therefore also relevant to low-lying delta areas around the world.

1.2. Polders and Saline Groundwater Exfiltration

Polders are low-lying and artificially drained areas surrounded by water storage canals (Fig. 1.1). Although The Netherlands is associated with polders (totaling around 4000 nationwide [18]), polders are found in coastal areas across the world [19]. Elevations of polders are generally below the surrounding area resulting in a necessity for continuous drainage of excess water using a dense network of water canals or ditches in the polder [19]. Dominant land use in polders is mostly agriculture. Accumulated storm water in
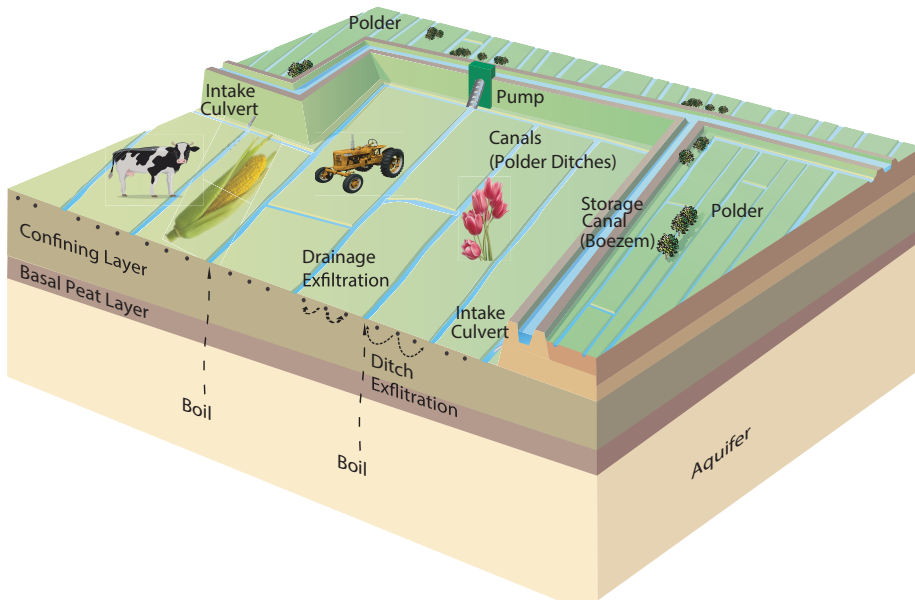
Figure 1.1: Schematic overview of a polder system (Adapted from [19])

the polder is transported to the pumping station and is pumped out of the polder onto the surrounding water storage canals (the so-called boezems). Water storage canals are used for providing extra freshwater during dry periods to replenish precipitation deficits, and for creating storage space for the surplus water from polders during wet periods. Water levels in polders and surrounding water storage canals are maintained within a given narrow margin so that the groundwater levels in the polders are kept close to a target level, to avoid dike failures in water storage canals and to prevent acceleration of land subsidence [20]. Deep polders experience a significant groundwater inflow, generally over the entire season in the same order of magnitude as the precipitation surplus [21]. Saline groundwater exfiltration threatens agricultural activities and the freshwater ecosystem in the polders by salinization of the surface water used for irrigation. Additional freshwater from the water storage canals is supplied to the polders that are experiencing water quality problem due to the saline groundwater exfiltration. In this way, salinity concentration levels in the ditches and canals of the polder are diluted and flushed out of the system using the pumping stations at the downstream end of the polders.

In the coastal zone of The Netherlands, exfiltration of brackish to saline groundwater

is the main input of salt to the surface water in polder systems [21, 22]. Three different sources of saline groundwater exfiltration are considered in this thesis as defined in [23]: ditch and drain exfiltration and boils. Boils are the small vents directly connecting the deep aquifer with the surface water. They are the dominant source of salinity in some of the deep polders in The Netherlands [22]. Concentration and discharge of the boils is rather constant since the groundwater head and the surface water level do not vary much. Other sources of salt in deep polders are the groundwater flows through pale-ochannel (i.e. drain exfiltration (also called drainage)) and diffuse (i.e. ditch exfiltration) seepage [22]. The salinity concentrations of these latter two sources, viz. ditch and drain exfiltration, are location specific and depend on the depth of the interface between fresh and saline groundwater.

1.3. CONTROL OF WATER SYSTEMS

Water systems are managed for different objectives such as maintaining water levels in a river or a canal for shipping or flood protection, reservoir management for energy production or supplying water for irrigation or drinking water supply. To manage and real-locate water resources, hydraulic structures like weirs, gates and pumps are constructed in many water systems. Over the last decades, automatic control of these structures has been extensively studied using different control techniques. There are two classical control approaches used for operational water management: feedback control and feedforward control (see also Figure 1.2).

Figure 1.2: Classical control approaches. a) Feedback control, b) Feedforward control, c) Combined feedforward and feedback control.

Feedback Control

Feedback controllers measure the system output (controlled variable) and compare it with the target level to compute the control action to counter the error (Figure 1.2-(a)).
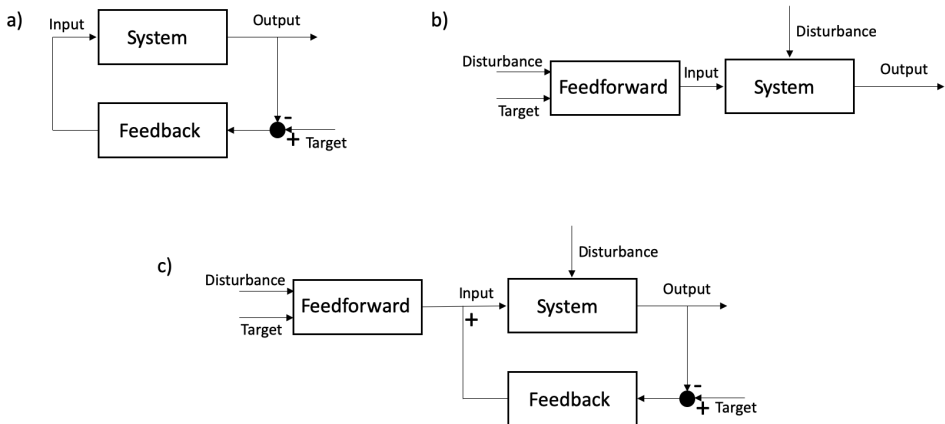
A feedback controller constantly corrects the error between the measured and target values of the controlled variable. For this reason, it is known as the closed loop control (as depicted in the closed feedback loop of Figure 1.2-(a)). Application of feedback controllers on water systems have many examples such as water level and flow control in canals [24–28], aquifer management [29], water delivery in water distribution systems [30] and control of water quality in water distribution systems [31, 32]. Feedback controllers can be robust to a certain types of uncertainties (i.e. the system states will not deviate much from set points if the errors are within a certain range). On the other hand, feedback controllers are reactive and cannot anticipate the delayed deviations in measured variables from current disturbances resulting in time delays. For example, a typical water level feedback control is a downstream water level control, where the upstream structure setting is adjusted according to the downstream water level. For this kind of control, although an adjustment will be made immediately reacting to an error in the water level, the actual effect on the downstream water level can be delayed.

Feedforward Control

Feedforward controllers on the other hand allow the use of measurements or prediction of the disturbances before they enter the system, and use this information to take corrective action to counter the future influence of the disturbances on the system [33] (Figure 1.2-(b)). Using an inverse model of the disturbance on the system, feedforward controllers compute the adjustments on the control inputs [28]. Some of the applications in water systems include: downstream feedback water level control for open canals [27, 34] and feedback control of irrigation canals [35]. Since the controller uses a prediction of the disturbances, the control action is calculated and implemented in advance. However, as the inverse model used for disturbance prediction is usually not accurate, the adjustments made to the control structures cannot guarantee reaching the reference level.

Ideally, a combination of feedforward and feedback controllers (Figure 1.2-(c)) can be used to compensate the limitations of each one [28]. These controllers are easy to tune, and practical to use for simple single input single output systems [36]. However, in the operation of most of the water systems, multiple objectives have to be met simultaneously, which may be conflicting with each other. Moreover, there are physical constraints of the system such as the maximum capacity of intake or pump or operational constraints like the minimum flow required to be released from a reservoir for environmental flows, which cannot be handled by classical feedback or feedforward controllers. Therefore, a more advanced control method is necessary for more complex water management problems, such as the integrated water quality and quantity control in polders considered in this thesis.

1.4. MODEL PREDICTIVE CONTROL

Model Predictive Control (MPC) is an advanced control strategy that originated in the late seventies and has since been developed and used in different industries [37]. MPC is an optimization-based control strategy, which makes use of a model of the system controlled to predict the future behavior of the system over a finite prediction horizon [37]. MPC combines feedback control on the measured controlled states, which can be

1
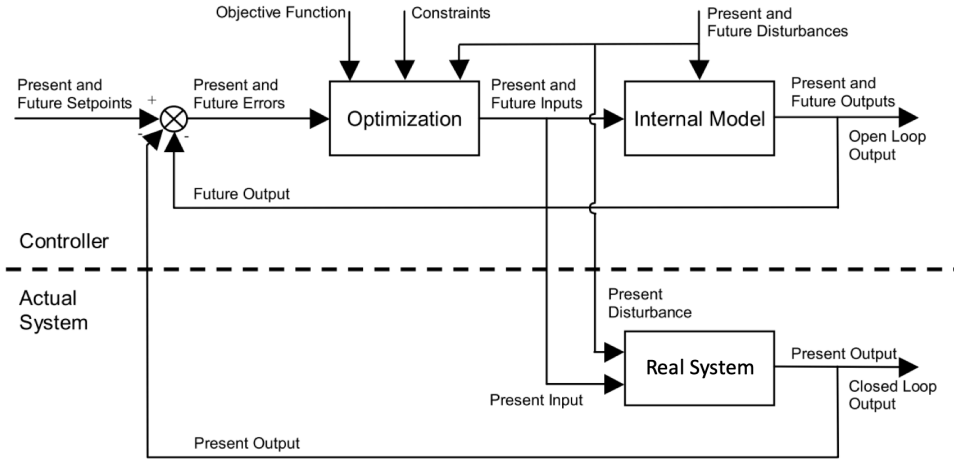
Figure 1.3: Structure diagram of model predictive control of an actual system [28]

seen in Figure 1.3 as the difference between the present output of the actual system and the present and future desired set points and feedforward control on the predicted disturbances in a repetitive optimization process that also takes constraints of the system into account [28]. As can be seen in Figure 1.3, MPC includes several components such as an internal model, objective function, constraints and optimization.

The internal model in MPC is the representation of the real system and it is used to predict the future states of the system. As an input, the internal model uses the present and future disturbances and the present and future inputs (control actions) calculated by the optimization that optimizes the objective function subject to the system states and the constraints. The outputs of the internal model are the present and future system outputs (states) (Figure 1.3). Accuracy of the internal model directly influences the control performance and a trade off exists between model accuracy and computational efficiency. The actual water systems controlled are nonlinear and the system dynamics are represented with nonlinear partial differential equations such as De Saint Venant equations for water transport in open channels. For certain MPC applications, required accuracy of the internal model can be achieved by using linear approximations of system dynamics, such as an Integrator Delay (ID) [25] model used for water level control in long canals [28]. MPC with a linear internal model can be categorized as a linear MPC and has been applied to water resources management problems such as irrigation and drainage system control [28, 38, 39], flood defence [40–42], water quality and quantity control [43, 44] and reservoir management [45, 46]. Linearized and discretized versions of the non-linear governing equations describing the dynamics of the actual water system can also be used as the internal model. This kind of internal models are applicable for processes that remain around a fixed operating point, which allows linearization of the process model and thus the application of linear MPC [47] as described in Chapter 2 of this thesis for optimal salinity and water level control of water courses. On the other

hand, for some water systems, the required accuracy for control calculation cannot be obtained by using linear internal models due to the nonlinearities in the system. As an alternative, governing nonlinear differential equations can be used as the internal model resulting in to a nonlinear MPC (NMPC) formulation. In Chapter 3, a NMPC scheme is used to control salinity and water level of a real polder network.

In most MPC applications, the objective function is usually a quadratic cost function, as also formulated in this thesis in Chapters 2 and 3. Combined with a linear internal model, the optimal control problem can be solved by using a Quadratic Programming (QP) algorithm [28]. On the other hand, if a nonlinear internal model is used, as in Chapter 3, the optimal control problem becomes a Nonlinear Programming (NLP) problem, which has to be solved using a nonlinear optimization solver.

At each control time step, k, MPC solves the following optimal control problem over the prediction horizon N_p:

$$(\mathbf{u}^*, \mathbf{x}^*) := \min_{\mathbf{u}, \mathbf{x}} J = \sum_{i=0}^{N_p-1} f(x(k+i+1), u(k+i)) \tag{1.1}$$

subject to

Initial conditions

$$x(k) \tag{1.2}$$

System dynamics

$$x(k) = g(x(k-1), u(k), d(k)) \tag{1.3}$$

Physical and operational constraints

$$c(x(k), u(k)) \leq 0 \tag{1.4}$$

where $\mathbf{u} = \{u(k), \ldots, u(k+N_p-1)\}$ is a control input sequence, which we can manipulate to bring the system to the state $\mathbf{x} = \{x(k+1), \ldots, x(k+N_p)\}$; $u(k) \in \mathbb{R}^{n_u}$ is the control variable at time k, $x(k) \in \mathbb{R}^{n_x}$ is the state vector at time k and $d(k) \in \mathbb{R}^{n_d}$ is the disturbance vector at time step k where n_u, n_x and n_d represent the number of control inputs, states and disturbances, respectively. The optimal control signal, $\mathbf{u}^*$, minimizes the objective function, $f(\cdot)$, given in (1.1), to bring the system to the desired state $\mathbf{x}^*$ subject to the initial conditions (1.2), system dynamics (1.3) and physical and operational constraints (1.4).

System dynamics, $g(\cdot)$, given in (1.3) represents the internal model in MPC as depicted in Figure 1.3. Constraints, $c(\cdot)$, represent the physical and operational limitations on the controlled system. The optimization calculates the optimal control signal considering the constraints of the system. Some constraints are not allowed to be violated because of physical limitations such as maximum pump or intake capacity. These constraints are called the hard constraints. On the other hand, soft constraints are not that rigid and can be violated if necessary. For example, the salinity concentration at a certain time can be higher than the required threshold and can be violated. In this thesis, we use combinations of soft and hard constraints for water levels, salinity concentrations and intake and pump capacities to find the optimal solutions in Chapters 2 and 3.

1

In the closed loop application of MPC depicted in Figure 1.3, at time step, k, the procedure starts with taking measurements or estimates of the states, $x(k)$, and the prediction of the disturbances, $\{d\}_k^{k+N_p}$ over the prediction horizon. Then the optimal control problem given in the equations (1.1)-(1.4) are solved and the optimal control signal, $\mathbf{u}^*$ is obtained. Only the first control action, $u(k)$, is implemented until the next control time step when new measurements are available. At the next time step, $k+1$, the horizon is shifted and the optimal control problem is solved again using the updated measurements and predictions (Figure 1.4). For this reason, MPC is also known in literature [37] as receding horizon control.
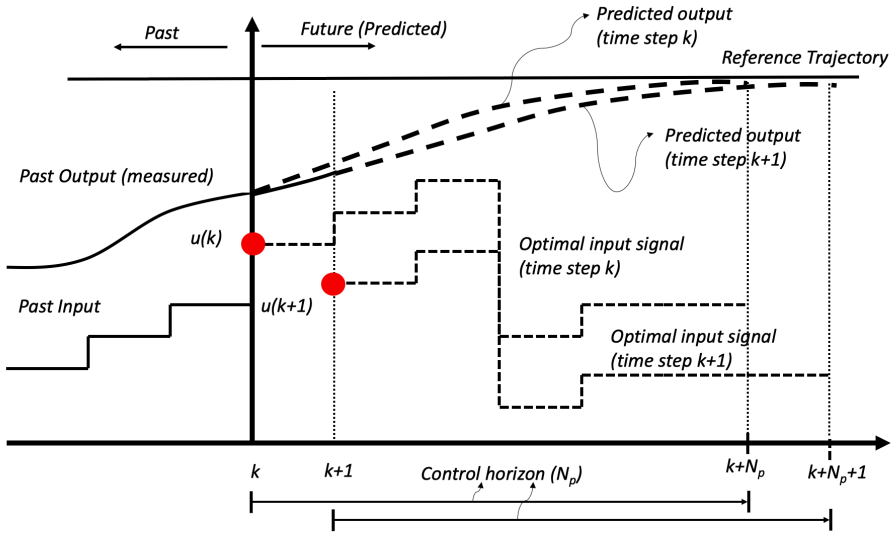
Figure 1.4: Receding horizon strategy of MPC

1.5. MONITORING AND MODEL PREDICTIVE CONTROL OF WA-
TER QUANTITY AND QUALITY

Both water quantity and quality are influenced by the natural conditions such as climate, geography, topography, and geology, and human activities [48]. Water quantity control of water systems can be formulated by keeping the water levels around the set points. Disturbance flows, inflow or outflow from the water system, will cause the water level to drift from the set points, which will be corrected by the controller. Using water level measurements to control and manage water quantity including flood and drought management, MPC has been widely used for canals [49–51], rivers and deltas [40, 52, 53] and reservoir operations [54–56].

To control both water quality and quantity, Xu et al. [43, 44], applied MPC on open channels (connected in series). In their discussion, excessive use of freshwater for flushing was pointed out as an important topic for further research. MPC formulations presented by Xu et al. [43, 44], considered a simple reservoir model for average salinity

and a simple low order model as the internal models for water quality. Using virtual salinity exfiltration scenarios, they illustrated the first successful applications of MPC for integrated water quality and quantity control applied to open channels. However, a need still exits for the development of MPC schemes for controlling real polder networks experiencing saline groundwater exfiltration. Different sources of saline groundwater exfiltration combined with the nonlinear looped dynamics of salinity transport in the polder networks require modeling the polder flushing processes using physically-based network models. A network model for salinity and water transport coupled with saline groundwater exfiltration models can improve the accuracy of predictions and optimal control actions calculated by MPC that will also minimize the freshwater usage for flushing.

An important component of MPC are the measurements that are used to update the system states at every control time step. To control salinity and water level in a polder network, water level and salinity sensors have to be placed efficiently to monitor the system state with the required precision. Water level in a polder system is kept within a predefined narrow margin and does not vary too much throughout the polder and therefore can be monitored easily. On the other hand, where and how to measure salinity is an open research question. Recent advances for monitoring salinity make the application of advanced control methods like MPC possible. To measure salinity, Electrical Conductivity (EC) is a surrogate measure, which can be converted to the dissolved salinity concentration in water. For example, a CDT-diver (Conductivity - Depth - Temperature) together with a wireless connection allows a real time profiling of EC measurements that can be used to update the salinity states of the water system. Using the real time measurements of salinity, MPC schemes can optimize the operation of control structures while satisfying the constraints of the system. However, considering spatial and temporal variability of salinity in polders, an efficient placement of sensors is necessary. Using the salinity measurements of a minimum number of sensors that are optimally placed in the polder, salinity states at all locations of interest can be updated and used by the MPC for optimal control.

1

1.6. RESEARCH QUESTIONS AND THESIS OUTLINE

Globally, low-lying deltas are under stress due to rising sea levels and decreasing fresh-water availability. As a result of these stresses, triggered by the saline groundwater exfiltration, surface water salinization is expected to increase in these areas. As a common practice, freshwater diverted from the rivers is used for flushing the canals and ditches in coastal areas to overcome the salinization problem. To meet the increased demand for flushing in these areas, new operational designs are required that will reduce the need for diverted freshwater. Due to the expected freshwater availability deficits, decreasing the total amount of freshwater used for flushing becomes more important for the sustainable operation of low-lying polders. For a real polder network, open research questions on "how to optimally monitor and control salinity?" exists and has to be addressed. Therefore, in this thesis we focus on monitoring and control of a real low-lying polder with a problem of salinization of the surface water system. We aim to better understand and control the surface water salinity and quantity in low-lying polder networks using Model Predictive Control by explicitly considering the amount of freshwater used. This thesis aims to answer the main research question:

> *How to apply Model Predictive Control to polder flushing satisfying the constraints on water level and salinity concentrations while minimizing the freshwater intake?*

Using tools of modeling and optimization, the following sub-questions are answered:

- Chapter 2: Can physically-based model as the internal model of a Model Predictive Control scheme be used effectively and computationally feasibly for real time control of the the salinity and water level of polders??

- Chapter 2: Can excessive use of freshwater (over-flushing) be avoided by using Model Predictive Control?

- Chapter 3: How to model and control the flushing of a real polder network using Model Predictive Control?

- Chapter 3: Can the results of Model Predictive Control be combined with system characteristics and used for updating the surface water system for better control performance?

- Chapter 4: Can a Principal Component Analysis based model be used to represent the salinity dynamics in a polder network and be used for salinity sensor placement optimization?

- Chapter 4: What is the optimal placement of salinity sensors for estimating unmeasured salinity levels in a real polder network?

Finally, Chapter 5 summarizes the contributions of this thesis and provides an outlook for future research.

2

OPTIMAL SALINITY AND WATER LEVEL CONTROL OF WATER COURSES

Yaşamak bir ağaç gibi tek ve hür
ve bir orman gibi kardeşçesine,
bu hasret bizim.

Nazım Hikmet Ran

In this chapter, we demonstrate a Model Predictive Control (MPC) scheme to control salinity and water levels in a water course while minimizing freshwater usage. A state space description of the discretized De Saint Venant and Advection-Dispersion equations for water and salt transport, respectively, is used as the internal model of the controller. The developed MPC scheme is tested using groundwater exfiltration data from two different representative Dutch polders. The tests demonstrate that water levels and salinity concentrations can successfully be controlled within set limits while minimizing the freshwater used.

2.1. INTRODUCTION

Efficient water management in polders is a challenging process since the water level should be kept within a narrow margin while the saline groundwater exfiltration triggers the salinization problem and deteriorates the water quality. Saline groundwater exfiltrates to the ditches through boils (direct pathways between deep saline aquifer and the surface water), drains (exfiltration of shallow phreatic groundwater) and through diffusive seepage directly below the ditches [22, 23]. When the salinity level in the polder ditch exceeds a certain threshold, to maintain acceptable surface water quality, freshwater is introduced through the upstream structure of the ditch to flush the surface water system. However, current practice of salinity control in polders generally involves constant flushing during the growing season, manually opening the inlet culverts at the start and closing them at the end of the growing season [19]. Water level control is achieved by the operation of a pumping station, responding to water level measurements. Flushing is generally not considered in operation and this results in excess use of freshwater and unnecessary pumping.

In this chapter, we demonstrate a Model Predictive Control (MPC) scheme for optimal operation of a water course or called here test polder ditch (Figure 2.2) for flushing by explicitly considering freshwater conservation. The focus of our research is to find a solution for supplying the available freshwater resources in a more efficient way for real polders. To the best knowledge of the authors, previous studies controlling water level and water quality did not consider the amount of freshwater supply. Xu et al., [43, 44] merely mentioned over-flushing as an important topic in their discussion. Therefore, in this study we proposed a solution to this problem by introducing an additional control objective as the minimization of freshwater use and demonstrated how much freshwater can be saved if flushing is done only when it is necessary. Another novelty of this chapter is using physically-based models in real time control, as opposed to low order numerical models derived using proper orthogonal decomposition (POD). We employed the discretized Saint Venant (SV) and advection dispersion (AD) equations as the internal model of the real time controller. Finally, we coupled an exfiltration model with the controller to deal with real exfiltration scenarios driven by real precipitation and hydrological data instead of using arbitrary exfiltration flux and concentration. All these three aspects of this chapter are important steps for application of the developed MPC scheme to a real polder system in a follow-up research.

An internal model employed a coarse discretization of SV and AD equations. A detailed state space description is given in section 2.3. For the simulations, we solved the discretized SV and AD equations programmed in MATLAB. We tested the developed control scheme in closed-loop simulations for two representative Dutch polders with different saline groundwater exfiltration characteristics (Figure 2.1). As described in section 2.2 the simulation models are abstractions of real-world ditches (Schermer polder [58] and the Lissertocht catchment [23]) and are used to simulate the system dynamics based on discretized SV and AD equations, where the scenarios are designed with real precipitation and hydrological data for the areas using the Rapid Saline Groundwater Exfiltration Model (RSGEM). The Lissertocht catchment (surface level 6 3.5 m below sea level (BSL), water depth 6.4 m BSL, salinity concentration variation in the ditches 136 5453 g/m^3 [23]) represents of deep polders, where the main salinity input is deep saline
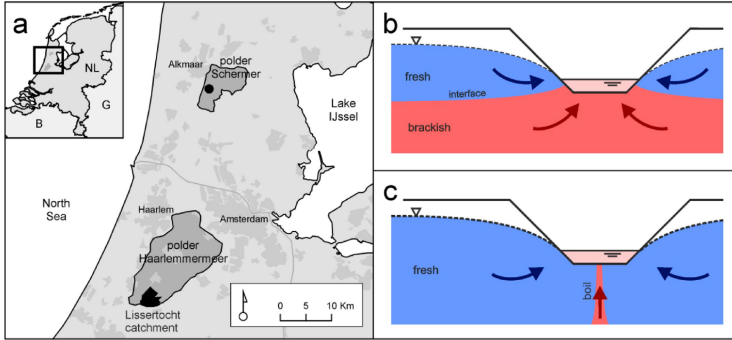
Figure 2.1: a) Locations of the two polders in the Netherlands used for testing the developed MPC scheme: i) Schermer Polder, ii) Lissertocht Catchment (adapted from Delsman, 2015), b) conceptualization of fresh and brackish groundwater flow to a ditch in the Schermer Polder, and c) conceptualization of fresh and brackish groundwater flow and a boil connecting the deep saline aquifer to a ditch in the Lissertocht catchment.

groundwater exfiltration through boils [59] (Figure 2.1(c)). In this catchment, two different layouts are observed: main ditches that receives the drained water directly from the drains and main ditches without drain connection but connected to stagnant ditches (collected excessive water in the surrounding area is drained to these stagnant ditches). We considered both layouts in this study. On the other hand, the Schermer polder (surface level 4.14 3.86 m BSL, water depth 5 m BSL, salinity concentration variation in the ditches 700 7700 g/m^3 [14] is representative of polders where the main salinity input derives from shallow saline groundwater, viz. exfiltrating towards ditches and tile drains (Figure 1b). Interested readers are referred to Delsman et al. [23, 58] for further information about the areas considered in this study. The saline groundwater exfiltration is modeled by the RSGEM [58].

MPC uses an internal model to predict the states of the surface water system over the prediction horizon. The accuracy of the internal model affects the control performance of the MPC in terms of accuracy and computation time. Simple models exist for water quantity control like Integrator Delay model [25] and Integrator Resonance model [50]. For water quality control, Xu et al. [43, 44] used a simple reservoir model assuming full mixing to control the average salinity concentration in a ditch and proceeded by applying a model reduction technique and achieve a simple internal model decreasing computational time requirements to control the downstream water salinity concentration. Moreover, no previous studies pay attention to the minimal freshwater use of polder flushing assuming an unlimited source. Decreasing the freshwater intake to the ditch for flushing will directly decrease the amount of pumping water from the system. This is considered as a surrogate for saving energy. Therefore, in this study we develop a scheme to regulate water level and salinity of a test polder ditch by minimizing the freshwater use. We present an internal model and a state space description for a MPC scheme to control the flushing of the ditch. Multiple objectives (water level and salinity control and minimization of freshwater use) while meeting the constraints of the system are satisfied. We use the discretized SV and ADE equations as the internal model for the

controller, which enables us to regulate the water level and salinity concentration in any discretization point of the test polder ditch.

2.2. Modeling for the simulations

In this section, we described the groundwater exfiltration model used to estimate the ditch and drain exfiltration to the ditch, and the models used for the simulation of the flushing of a ditch.

2.2.1. Modeling the saline groundwater exfiltration - RSGEM

Saline groundwater exfiltration in low-lying polders is governed by the regional hydraulic gradient in the upper groundwater system. Saline groundwater moves upward and mixes with the surface water, increasing the salinity of the surface water. Existing groundwater models require long run times and limit the application in operational freshwater management. To support operational water management of freshwater resources in coastal lowlands, Delsman et al. [58] formulated a hydro(geo)logical model for fast calculation of groundwater exfiltration flux and salinity in a low-lying catchments. RSGEM recognizes that groundwater exfiltration salinity critically depends on both the fast-responding pressure distribution, and the slow-responding salinity distribution in the shallow groundwater. The model was developed for a test site in Schermer polder, and was validated using both measured groundwater levels, exfiltration rates and salinity response and results of a previously applied detailed, complex model to the same area [58]. RSGEM is a lumped water balance model used for determining the saline groundwater ditch and drain exfiltration discharges and salinity concentrations. The model aimed to include the saline groundwater exfiltration dynamics in coastal lowlands and is suitable for densely drained polders where fresh rainwater overlies shallow saline groundwater. RSGEM uses precipitation, evaporation and groundwater levels as the input and the output is the groundwater exfiltration concentration (Figure 2.5(a) and 2.7(a)) and discharge (Figure 2.5(b) and 2.7(b)). Other parameters necessary for running RSGEM for the given cases are taken from Delsman et al. [23, 58]. Interested readers can refer to [58] for detailed information about RSGEM.

In this study, we forced RSGEM with real-world data (precipitation, evaporation and groundwater levels) from two Dutch polders (Schermer polder [58] and the Lissertocht catchment [23]) to obtain realistic exfiltration scenarios. The modeled exfiltration discharge and the concentration are used as known disturbance for the developed controller. We assumed full system knowledge and perfect predictions for the exfiltration calculated by the RSGEM, thus, no uncertainty assessment is conducted.

2.2.2. Modeling the flushing of a polder ditch

To model the flushing of a polder ditch, transport of water and transport of dissolved matter have to be considered [60]. These dynamics can be described by the SV equations given in (2.1) for water transport and a one-dimensional AD equation given in (2.2) for salt transport.
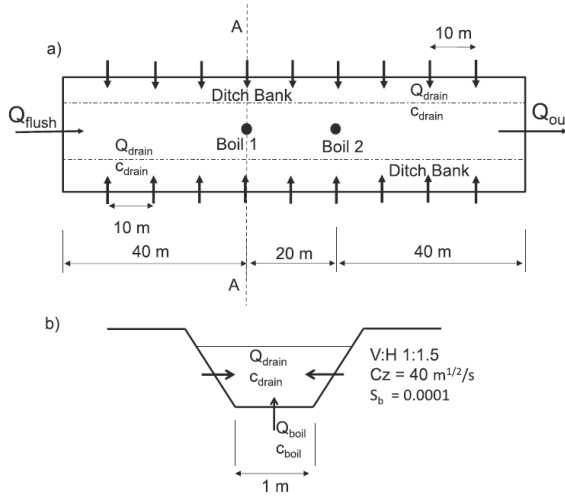
Figure 2.2: a. Schematization of the test polder ditch (not to scale) for the first scenario, 10 m drainage spacing, 1 m bed width, 1:1.5 side slope, Chezy coefficient 40 $m^{1/2}$/s and bottom slope 0.0001 [-] with flushing discharge (Q_{flush}), outflow discharge (Q_{out}), groundwater drain exfiltration discharge (Q_{drain}) and concentration (c_{drain}), locations of the two boils and two locations used in controller design that are 40 m and 60 m downstream of the flushing inlet, b. Cross section of the ditch (A-A in (a)) with drain exfiltration discharge (Q_{drain}) and concentration (c_{drain}), boil discharge (Q_{boil}) and concentration (c_{boil}).

$$\frac{\partial A}{\partial t} + \frac{\partial Q}{\partial x} = q_l \tag{2.1}$$

$$\frac{\partial Q}{\partial t} + \frac{\partial (Qu)}{\partial x} + gA\frac{\partial \zeta}{\partial x} + g\frac{Q|Q|}{C_z RA} = 0$$

$$\frac{\partial AC}{\partial t} + \frac{\partial QC}{\partial x} = \frac{\partial}{\partial x}(KA\frac{\partial C}{\partial x}) + q_l C_l \tag{2.2}$$

where A is the cross sectional area [m^2], Q is the flow [m^3/s], q_l is the lateral inflow per unit length [m^3/s/m], u is the mean velocity (Q/A) [m/s], ζ is the water depth above the reference plane [m], $C_z = 40$ is the Chezy coefficient [$m^{1/2}$/s], R is the hydraulic radius (A/P_f) [m], P_f is the wetted perimeter [m] and g is the gravity acceleration [9.8 m/s^2], K is the longitudinal dispersion coefficient [m^2s], C is the salt concentration [kg/m^3], C_l is the lateral flow concentration [kg/m^3], t is time [s] and x is horizontal length [m]. The longitudinal dispersion coefficient (K) is given by Fischer et al. [61] as:

$$K = 0.011\frac{B^2 v^2}{du_s} \tag{2.3}$$

where B is the mean width [m], d is the mean water depth [m], $us = (gRS_b)^{1/2}$ is the shear velocity [m/s] and S_b is the bottom slope of the canal [-]. The parameters used for discretization of the test ditch are given in Figure 2.2.

These partial differential equations can be discretized using a staggered grid [62] with a combination of first order upwind and theta method for time integration. This discretization is explained in detail by Xu et al. [43]. The equations are implemented in MATLAB to simulate the surface water system using initial conditions for the water level, concentrations and updated inflow and outflow discharges by the controller. For every simulation time step, the discretized SV equation calculates the water levels and velocities at the discretization points, followed by calculating the concentrations using the discretized AD equations.

The stability of the used models is important for a reliable control design and stable simulation of the system. In this study, we used a staggered grid discretization that is unconditionally stable [62]. The spatial discretization used in both simulation and control model is 10 m representing the drain spacing of the considered ditch. For the time discretization, 1 min time steps are used for the simulations and 2 min time steps are used for the controller. Normally, for testing the model performance of real time controllers the control time step can be much larger than the simulation time step; in this study we used a smaller control time step in order to capture the fast response of the controlled downstream water level and downstream salinity concentration to a change in flushing discharge because the length of the test polder ditch was only 100 m. In case of a longer ditch (where the travel time of the flushing water is much larger) the control time step can be selected to be appropriately larger. The second reason was to force the controller with a smaller control time step to illustrate that the computation time of control action is not a limitation for the scheme described in this chapter. Computation time is discussed in Section 2.5.

2.3. CONTROLLER DESIGN

MPC is an optimization based control scheme that uses an internal model to predict the future process outputs within a specified prediction horizon [37]. We used discretized SV and AD equations, which serve as the internal model of the controller. Using the internal model equations, a time variant state space description (2.4) is obtained and used to describe and predict the states over the prediction horizon.

$$x(k+1) = A(k)x(k) + B(k)u(k) + B_d(k)d(k) \tag{2.4}$$

where x is the state vector of the system, u is the controlled variable, d is the disturbance and k is the discrete time step index. A, B and B_d are the time dependent matrices associated with system states, control input and disturbance input, respectively.

In the following paragraphs, the steps to achieve a time variant state space description for optimal flushing control is described and then the used objective function is defined. The controller controls the amount of flushing discharge, salinity and the water level at the downstream end of the polder ditch by manipulating the flushing and outflow discharges. According to the state space description given in equation (2.4); the states (x) are the water levels (h_i), concentrations (c_i), flushing discharge (Q_{flush}) and outflow discharge (Q_{out}) where i represents the discretization point in space; the inputs (u) are the change of flushing and outflow discharges (ΔQ_{flush}, ΔQ_{out}); and the disturbance (d) include all the remaining terms that are not associated with the states or

inputs.

The internal model proposed uses the discretized SV and ADE as the basis. First, a discretization matrix is introduced that has similar terms like the state space description given in equation (2.4). At this stage, the water levels (h_i) and concentrations (c_i) are replaced with the deviation from water level set point ($eh_i = h_i - h_{ref}$) and deviation from concentration set point ($ec_i = c_i - c_{ref}$) since the controller aims to keep the water level and concentrations around the set point. Later, using algebraic operations, a state space description as equation (2.4) is achieved from the discretization matrix. Finally, additional states and inputs are introduced that are necessary for minimising the freshwater usage.

2.3.1. DISCRETIZATION MATRIX

Based on the discretization for SV and ADE given in Xu et al. [43] and following a similar approach for combined open water quantity and quality model described in Xu et al. [44], the discretized SV and AD equations are written in a compact matrix form including the flushing (Q_{flush}) and outflow discharges (Q_{out}) as the states and the change of these discharges (ΔQ_{flush}, ΔQ_{out}) as the control input of the system. For the sake of simplicity, a discretization matrix with three discretization points is introduced here (2.5) and a general notation is provided in the Appendix A. All the terms with the next time step ($k+1$) are written on the left side and the terms with the current time step (k) are left on the right side such that the states ($x(k+1)$ and $x(k)$), controlled variables ($u(k)$) and the disturbances ($d(k)$) in equation (2.4) are also present in the discretization matrix.

$$
\begin{bmatrix}
sv_{11} & sv_{12} & & & & & sv_f & \\
sv_{21} & sv_{22} & sv_{23} & & & & & \\
& sv_{32} & sv_{33} & & & & & sv_o \\
& & & ad_{11} & ad_{12} & & ad_f & \\
& & & ad_{21} & ad_{22} & ad_{23} & & \\
& & & & ad_{32} & ad_{33} & & ad_o \\
& & & & & & 1 & \\
& & & & & & & 1
\end{bmatrix}^{k+1}
\begin{bmatrix}
eh_1 \\ eh_2 \\ eh_3 \\ ec_1 \\ ec_2 \\ ec_3 \\ Q_{flush} \\ Q_{out}
\end{bmatrix}^{k+1} =
$$

$$
\begin{bmatrix}
1 & & & & & & & \\
& 1 & & & & & & \\
& & 1 & & & & & \\
& & & ad_{11} & & & & \\
& & & & ad_{22} & & & \\
& & & & & ad_{33} & & \\
& & & & & & 1 & \\
& & & & & & & 1
\end{bmatrix}^{k}
\begin{bmatrix}
eh_1 \\ eh_2 \\ eh_3 \\ ec_1 \\ ec_2 \\ ec_3 \\ Q_{flush} \\ Q_{out}
\end{bmatrix}^{k}
+
\begin{bmatrix}
\\ \\ \\ \\ \\ \\ 1 \\ 1
\end{bmatrix}
\begin{bmatrix} \Delta Q_{flush} \\ \Delta Q_{out} \end{bmatrix}
+ [I]d^k \quad (2.5)
$$

where sv_{ij}, ad_{ij} (i,j=1:3), sv_f, sv_o, ad_f, ad_o and $ad_i j^k$ (i,j=1:3) are the time dependent terms from linearized equations associated with each state or control variable (see the Appendix A for the details). To obtain these terms, every control time step, a pre-simulation of the system is conducted using the control variables of the optimization

calculated at the previous control time step. This simulation is run for the entire prediction horizon such that the calculation of the water level and salinity concentration for every discretization point is conducted that will be used in the discretization matrix. These procedure is referred as forward estimation in [43].

2.3.2. STATE SPACE DESCRIPTION

Equation (2.5) can be showed in a compact form as:

$$D_1 x(k+1) = D_2 x(k) + D_3 u(k) + d(k) \tag{2.6}$$

where D_1, D_2 and D_3 are compact forms of the corresponding matrices in (2.5). All the diagonal elements of D_1 are non-zeros, thus, the inverse of this matrix exists. After multiplying equation (2.6) with the inverse of D_1 matrix, the state space description given in equation (2.5) can be achieved with $A = D_1^{-1}D_2$, $B = D_1^{-1}D_3$ and $B_d = D_1^{-1}$ matrices and the state space description is achieved as:

$$x(k+1) = D_1^{-1}D_2 x(k) + D_1^{-1}D_3 u(k) + D_1^{-1}d(k) \tag{2.7}$$

This description relates the deviation of water level and the concentrations at the discretization points according to the change of flushing and outflow discharges and can be used only to control water level and salinity deviations from their set point. To achieve the third objective of minimization of freshwater use additional states and control variables are required and explained in the next section.

2.3.3. OBJECTIVE FUNCTION AND CONSTRAINTS

Objective function is used to formulate the goals of the controller subject to the constrains of the system. The controller has to bring the states to their desired states by manipulating the control variables. Therefore, control actions also have to be considered in the objective function to limit the change of the control setting. In MPC formulation, the objective function is formulated as a quadratic function to deal with the positive and negative deviations from set points of the variables [28]. A finite horizon objective function over the prediction horizon N_p with weighting matrices Q and R for states and the control variables respectively can be expressed as:

$$\min J = X^T Q X + U^T R U \tag{2.8}$$

The most important aspect of the developed control scheme in this study is to control water level and salinity by minimizing the freshwater use. To achieve that, the controller should limit itself to use freshwater only when it is necessary by flushing only if the salinity is above the given threshold and stop flushing when it is below the threshold. This can be achieved by introducing two soft constraints to the objective function. Soft constraints are used for variables that are allowed to violate their limitations [28, 63]. Thus, they become active in the objective function only if they violate their limitations. For example, a soft constraint on flushing discharge with upper limit of 0 m^3/s will let the controller to violate this upper limit and use flushing if necessary. However, after the violation this use will be penalised by the objective function, thus, the controller will try to avoid this violation as much as possible.

Soft constraints are implemented as additional virtual input and virtual state variables into the system dynamics. Therefore, we used e*c to limit flushing only when the salinity concentration is below the set point and e*q to limit the amount of flushing. Virtual input has no physical meaning and it is subtracted from the state that needs to be constrained to achieve the virtual state. The objective function that is used in this study is given below:

2

$$\min J = \sum_{i=1}^{N_p} e_h(k+i|k)^T Q_{eh} e_h(k+i|k) + (e_c(k+i|k) - e_c^*)^T Q_{ec}(e_c(k+i|k) - e_c^*) +$$

$$\sum_{i=1}^{N_p} (Q_{flush}(k+i|k) - e_q^*)^T Q_{eq}(Q_{flush}(k+i|k) - e_q^*) +$$

$$\sum_{i=1}^{N_p-1} \Delta Q_{flush}(k+i|k)^T R_{\Delta Q_{flush}} \Delta Q_{flush}(k+i|k) +$$

$$\sum_{i=1}^{N_p-1} \Delta Q_{out}(k+i|k)^T R_{\Delta Q_{out}} \Delta Q_{out}(k+i|k) +$$

$$\sum_{i=1}^{N_p-1} e_c^*(k+i|k)^T R_{e_c^*} e_c^*(k+i|k) + e_q^*(k+i|k)^T R_{e_q^*} e_q^*(k+i|k)$$

subject to

$$\begin{bmatrix} x(k+1) \\ e_c(k+1) - e_c^* \\ Q_{flush}(k+1) - e_q^* \end{bmatrix} = \begin{bmatrix} A & 0 & 0 \\ A_6 & 0 & 0 \\ A_7 & 0 & 0 \end{bmatrix} \begin{bmatrix} x(k) \\ e_c(k) - e_c^* \\ Q_{flush}(k) - e_q^* \end{bmatrix} +$$

$$\begin{bmatrix} B & 0 & 0 \\ B_6 & -1 & 0 \\ B_7 & 0 & -1 \end{bmatrix} \begin{bmatrix} u(k) \\ e_c^* \\ e_q^* \end{bmatrix} + \begin{bmatrix} B_d \\ B_{d_6} \\ B_{d_7} \end{bmatrix} \begin{bmatrix} d(k) \\ d_6(k) \\ d_6(k) \end{bmatrix}$$

$$e_h(k) = h(k) - h_{ref}$$

$$e_c(k) = c(k) - c_{ref}$$

$$h_m in \le h_{ref} \le h_m ax$$

$$-c_{ref} \le e_c^* \le 0$$

$$-Q_{flush}^{max} \le e_q^* \le 0$$

$$0 \le Q_{out} \le Q_{out}^{max}$$

$$\Delta Q_{i,min} \le \Delta Q_i \le \Delta Q_{i,max}$$

(2.9)

where N_p is the prediction horizon; e_h and e_c are the water level and concentration deviations from set points at the last discretization point downstream of the polder ditch; $e_c - e_c^*$ and $Q_{flush} - e_q^*$ are the virtual states necessary for the soft constraints; $Q_{e_h}, Q_{e_c^*}, Q_{e_{q^*}}$ are the weights penalizing the corresponding states; $R_{\Delta Q_{flush}}, R_{\Delta Q_{out}}, R_{e_c^*}$ and $R_{e_q^*}$ are the weights penalizing the corresponding input variables; h_{ref} and c_{ref} are the water level and concentration set points at the last discretization point; Q_{flush}^{max} is

the maximum capacity of flushing; Q_{flush}^{max} is the maximum pumping capacity; ΔQ_i is the maximum allowed structure setting in a control time step for any control structure; h_{min} and h_{max} are the minimum and maximum allowed water levels. Updated state space description is also given here using the example given in equation (2.5) with three discretization points. $A_6, A_7, B_6, B_7, B_{d_6}$ and B_{d_7} are the 6th or 7th rows of the original A, B and B_d matrices given in equation (2.7). Similarly, d_6 and d_7 are the 6th and 7th rows of the disturbance vector d.

2.4. CASES AND SCENARIOS

To test the proposed controller under different representative conditions, we apply it to three different exfiltration scenarios at two locations. For all scenarios, we control a simple one pool test polder ditch (Figure 2.2-2.4) with a length of 100 m (the length of the ditch is selected such that it is representative of a small polder ditch and the length is not a limitation for the developed method). A spatial discretization spacing of 10 m is used for both simulations and the internal model calculations.

For the first two scenarios, we used exfiltration data from the Lissertocht catchment [23]. This catchment is a deep polder where the main salinity input is deep saline groundwater exfiltration through boils [22]. The drainage and ditch exfiltration salinity concentrations were calculated with RSGEM, leading to a mean of 75 g/m^3 and 336 g/m^3, respectively; boils have a mean salinity concentration of 5453 g/m^3 [23]. In the first scenario, we modeled and controlled a main channel directly collecting drainage water from the surrounding areas (Figure 2.2). Saline groundwater exfiltration through the drains and ditches are modeled by RSGEM with daily time scales. We immediately represent the drain and ditch exfiltration modeled by RSGEM entering the test polder ditch. To test the controller, we selected a 24-day period (17 August 2010 9 September 2010). In addition to the drain and ditch exfiltration modeled by RSGEM, two boils with a discharge of 0.002 m^3/s were added at locations 40 m and 60 m downstream of the flushing inlet. See Figure 5a-b for the exfiltration concentrations and discharge, respectively, used in the first scenario.

In the second scenario, we illustrate the performance of the controller in case of stagnant ditches (that collects the drained water from the surrounding areas) connected to a main channel without drains, an often-occurring surface water layout in Dutch polders (Figure 2.3). Some of the stagnant ditches with boils present in them are observed in the Lissertocht catchment; they store high salt loads during dry periods. After an intensive rainfall event, these ditches are flushed naturally by the collected water from the drains. Therefore, in this scenario we first simulated the stagnant ditch for the same full dry period without an inflow discharge given in the first scenario and recorded the outflow discharge and concentrations at the end of the ditch every minute. We selected a test period with the highest surface water outflow salinity concentration and discharge for the simulations (8 April 2010 5 May 2010); these model inputs are shown in Figure 2.6(a)-(b), respectively. We assumed two stagnant ditches that are used to collect the drained water on the left and right banks of the polder ditch. The stagnant ditches are connected to the controlled main polder ditch at 40 m and 60 m downstream of the flushing inlet.

For the third scenario (Figure 2.4), exfiltration data from a different polder is used
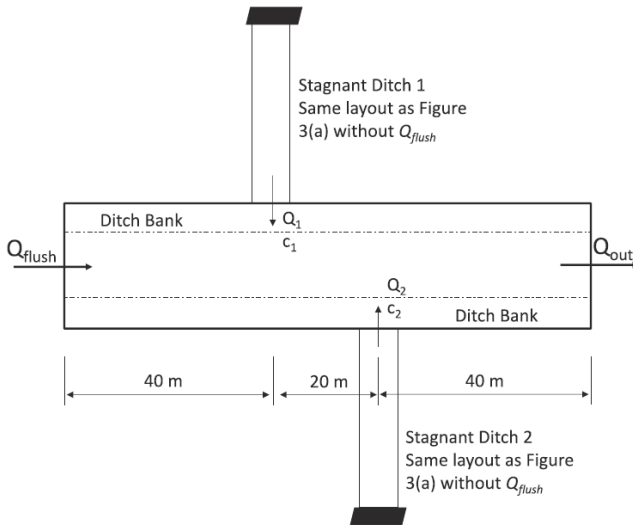
Figure 2.3: Schematization of the test polder ditch (not to scale) for the second scenario with flushing discharge (Q_{flush}), outflow discharge (Q_{out}), outflow discharge ($Q_{1,2}$) (see Fig 2.6(b)) and concentration ($c_{1,2}$) (see Fig 2.6(a)) of the two stagnant ditches. The stagnant ditches have the same layout as the first scenario except no flushing discharge (shown as black block in this figure)
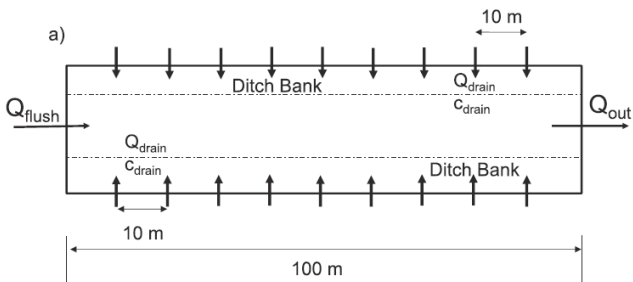

Figure 2.4: Schematization of the test polder ditch (not to scale) for the third scenario with flushing discharge (Q_{flush}), outflow discharge (Q_{out}), drain exfiltration discharge (Q_{drain}) and concentration (c_{drain})

	Q_{e_h}	$Q_{e_c^*}$	$Q_{e_q^*}$	$R_{\Delta Q_{flush}}$	$R_{\Delta Q_{out}}$	$R_{e_c^*}$	$R_{e_q^*}$
Scenario 1	16	62.5	0.01	80	80	10^-4	10^-4
Scenario 2	16	62.5	0.01	80	80	10^-4	10^-4
Scenario 3	16	6.25	0.01	4	4	10^-4	10^-4

Table 2.1: Weights [-] used in the objective functions for the three scenarios

(Schermer polder, location A in Figure 2.1). Contrary to the Lissertocht catchment, the main salinity input derives from shallow saline groundwater, exfiltrating towards ditches and tile drains. Tile drain and ditch exfiltration concentrations average 321 g/m^3 and 829 g/m^3 respectively and reach up to 5665 g/m^3 for both of them [58]. Using RSGEM, ditch and drain exfiltration discharge and concentration is modeled hourly and a test period with the highest salt load entering the system is selected (13-24 July 2012). See Figure 2.7(a)-(b) for the ditch and drain exfiltration salinity concentration and discharge modeled by RSGEM, respectively.

For all three scenarios, drains with a spacing of 10 m are used to collect the excess water (fresh and saline groundwater) from the nearby areas. All of the ditches considered in this study have the same cross section as given in Figure 2. The water level (h_{ref}=-0.41 m) and the salinity concentration (c_{ref}=550 g/m^3) at the downstream end (last discretization point) of the ditch is controlled by manipulating flushing (Q_{flush}) and outflow (Q_{out}) discharges. The reference levels for water level and concentration are arbitrary and in the control calculation the deviations from the reference level are considered, therefore, they are not crucial for the method. A simulation time step of 1 min, a control time step of 2 min and a prediction horizon (N_p) of 30 steps (equal to 1-hour prediction horizon) are used in the simulations. To determine the weights used in the objective functions, we used the maximum allowed value estimate approach described by van Overloop [28] as an initial guess and arranged them accordingly as summarized in Table 2.1.

2.5. RESULTS AND DISCUSSIONS
2.5.1. SCENARIO 1
In this scenario, we used the proposed MPC scheme to control the test polder ditch with drains using the exfiltration data from the Lissertocht catchment for 24-day period. In this catchment the main source of salinity is the boils. The drain and ditch exfiltration are fresh after a rain event because of the shallow freshwater lens in the catchment. This causes a decrease of modeled groundwater exfiltration concentration after 23/08 in Figure 2.5(a) while the exfiltration discharge increases (Fig 2.5(b)). This natural flushing due to rainfall is noticed by the controller, and it reduces the flushing during this time. The results of the MPC scheme can be seen in Figure 2.5(c)-(e).

As can be seen in Figure 2.5(c), the controller reacts to the groundwater exfiltration modeled by RSGEM (Figure 2.5(a)-(b)) and keeps the water level (Figure 2.5(d)) around the set point without any violation in salinity concentration (Figure 2.5(e)). As expected, the controller anticipates the additional fresh drain water entering the ditch after 23/08 and reduces the flushing discharge (Q_{flush}) accordingly for this period, thus achieving
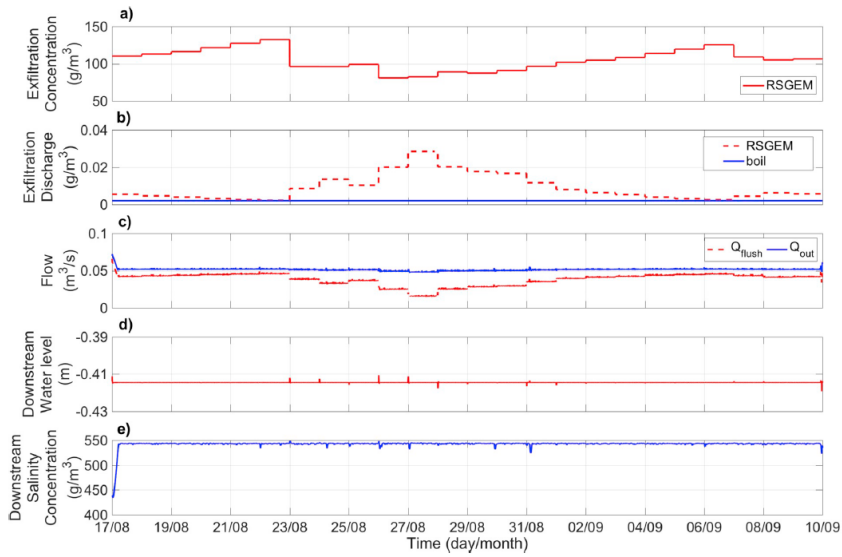
Figure 2.5: Disturbance data and results of the controller for the first scenario. Groundwater exfiltration a) concentration (c_{boil}=5453 g/m^3 is constant and not shown in the figure) and b) discharge used for the first scenario (dashed lines shows the first location 40 m downstream of the flushing inlet, which is a combination of the first boil and the exfiltration modeled by RSGEM and the solid line shows the second location, which is 60 m downstream of the flushing inlet with the second boil only). c) Controlled flushing and outflow discharge, d) downstream water level and e) downstream salinity concentration.
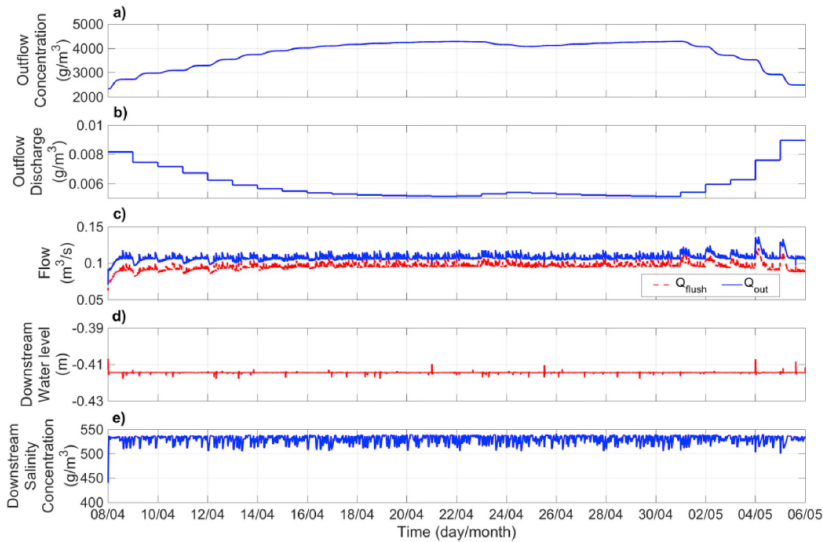
Figure 2.6: Disturbance data and results of the controller for the second scenario. Surface water outflow a) concentration and b) discharge of the stagnant ditch connected to the controlled test polder ditch. c) Controlled flushing and outflow discharge, d) downstream water level, e) and downstream salinity concentration.

the goal of flushing only when it is necessary.

2.5.2. SCENARIO 2

In this scenario, we wanted to see the effect of stagnant ditches connected to the main ditches in the Lissertocht catchment. Stagnant ditches are used to collect the drained water and transfer it to the main channels. The upstream ends of the stagnant ditches are closed, and they are naturally flushed during the rainfall events resulting in an inflow to the main ditch (outflow from the stagnant ditch). There is no control structure in between, therefore, the water levels at the stagnant ditches also stays at the target value of the polder system. Similar saline groundwater exfiltration is modeled and simulated as the first scenario for two stagnant ditches without an inflow at the upstream end, using the water level at the connections as a boundary condition. The outflow discharge (Figure 2.6(a)) and salinity concentrations (Fig 2.6(b)) at the connections of the stagnant ditches to the controlled test polder ditch of the stagnant ditches (see Figure 2.3) are simulated and used as a disturbance to the main channel controlled by the MPC scheme. Results are presented in Figure 2.6(c)-(e) for a 28-day simulation.

As presented in Figure 2.6(c), the controller does not change the flushing discharge except for the small fluctuations throughout the simulation. This is due to the inverse relation between the exfiltration discharge and the concentration (Figure 2.6(a)-(b)) resulting in a more or less constant salt load entering the system. Therefore, without a step change in flushing or outflow discharge the controller is able to keep the water level around the set point and the salinity concentration below the threshold.
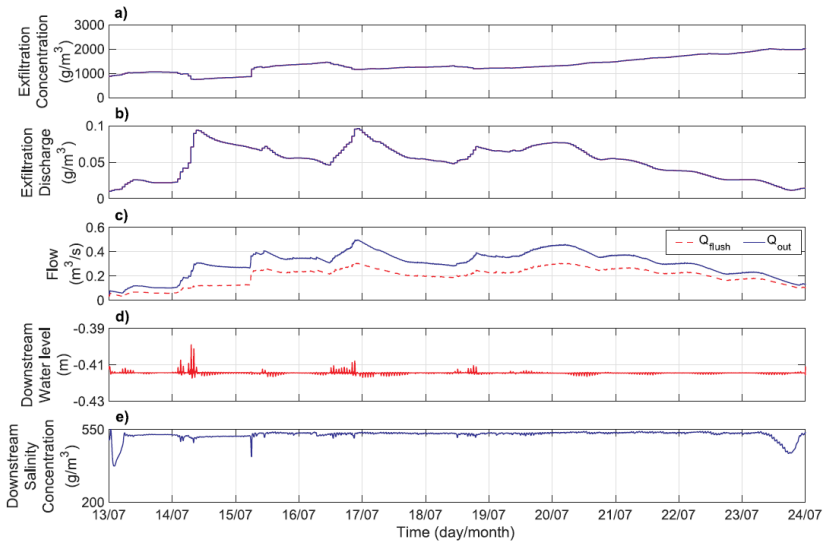
Figure 2.7: Disturbance data and results of the controller for the third scenario. Groundwater exfiltration a) concentration and b) discharge used for the second scenario. c) Controlled flushing and outflow discharge, d) downstream water level, e) and downstream salinity concentration.

2.5.3. SCENARIO 3

In the last scenario, we examined the performance of the controller in a polder with different saline groundwater exfiltration dynamics. Using data from the Schermer polder (with shallow saline groundwater), the MPC scheme is tested for a 11-day period. The results of the simulations are presented in Figure 2.7(c)-(e).

The results of this scenario show the ability of the proposed MPC scheme to deal with both increased exfiltration discharge fluxes (e.g. Figure 2.7(b) after 14/07) and increased exfiltration concentration (e.g. Figure 2.7(a) after 15/07). The initial salinity concentration is 500 g/m^3 at the downstream end of the ditch (Figure 2.7(e)) while the exfiltration concentration is almost 1000 g/m^3 (Figure 2.7(a)). The concentration drops below the threshold at the beginning of the simulation and the controller decreases the flushing until the controlled downstream concentration gets close to the threshold of 550 g/m^3. Moreover, as can be seen in Figure 2.7(c), the outflow discharge Qout after 14/07 is increased while the flushing discharge Q_{flush} does not change considerably. This is due to the fact that the controller needs to pump the excess water out of the ditch while the current flushing is enough to keep the salinity concentration below the threshold. On the other hand, after 15/07 the controller introduces additional freshwater into the system by a step increase of flushing discharge Q_{flush}. The outflow discharge is adjusted with a similar increase to keep the water level at set point. With similar arrangements on flushing and outflow discharges the controller keeps the water level (Figure 2.7(d)) and concentration (Figure 2.7(e)) in accordance with the objective of the controller. Moreover, as can be seen clearly after 20/07, the flushing and outflow discharges are decreased,

c_{ref} (g/m³)	Q_{max} (m³/s)	$\sum Q_{flush}$ (10³ m³/s)		$\sum Q_{pump}$ (10³ m³/s)		% Saved	
		MPC	Fixed	MPC	Fixed	Q_{flush}	Q_{pump}
550	0.384	198.1	365.2	296.8	463.9	45.7	36.0
750	0.172	105.6	163.4	204.3	262.0	35.3	22.0
900	0.115	67.7	109.2	166.4	207.9	38.0	19.9
1000	0.096	49.2	91.6	147.9	190.2	46.2	22.2

Table 2.2: Comparison between flushing with MPC and current practice of fixed flushing with different salinity threshold.

as the saline groundwater exfiltration after this point requires less freshwater to achieve the salinity concentration control objective. This shows that the third objective of the controller to use a minimum of freshwater is also achieved.

To demonstrate how much freshwater and pumping water can be saved by using the developed control scheme, we compared results of the simulations with different salinity concentration to the current fixed flushing practice. We did the analysis only for the third scenario due to its high dependency on exfiltration dynamics. We assumed the maximum flushing discharge achieved during the simulations using the proposed MPC scheme is the maximum capacity of the intake of the test polder ditch and used this as the fixed flushing discharge for comparison. The results are presented in Table 2.2.

For all the simulations presented in Table 2.2, similar results are obtained as in Figure 2.7. Flushing with MPC kept the salinity level close to the set point without any violations and the water level was always around the set point with fluctuations within the range of maximum and minimum water levels defined in the objective function. As can be seen in Table 2.2, increasing salinity set points resulted in less need for flushing discharge. Although in this study we used a given fixed threshold for the salinity concentration over the whole simulation period, in practice the concentration requirement will be varying, depending on the requirements. With a known but spatially and temporally varying demand for quantity and quality, the developed MPC scheme can be modified such that the demand is satisfied using the predictive behavior of the controller. By this way additional savings in freshwater and pumping use can be achieved. Simulations with fixed flushing always resulted in more flushing and pumping than the flushing with MPC. More than 35% savings in freshwater use is achieved by using the proposed MPC scheme. Similarly, the savings in total pumping volume reached up to 36% in case of using MPC. With fixed flushing, the average salinity concentration over the simulation period is below the set point, which results in a better water quality. However, as discussed earlier this is due to the unwanted excessive freshwater usage, resulting in unnecessary pumping and energy use.

Using a discretized internal model (as opposed to an internal model achieved by model reduction as proposed by Xu et al. [44]) is also an important outcome of this research, which will give the operator to modify the controller such that the water level and the salinity concentration can be controlled in any discretization points. In this study we used 10 m discretization spacing for the internal model, resulting in total of 24 states and 4 control variables. We used a control time step of 2 minutes with 1-hour prediction hori-

zon (i.e. 30 control time steps) resulting in total of 24*30 states and 4*30 control variables, respectively. To illustrate the computational time, one closed loop simulation (calculation of control actions over the whole prediction horizon followed by simulation of the system dynamics with the calculated control action) ended in less than 0.1 seconds. All the computations performed within MATLAB R2017a-64 bit for macOS High Sierra (v 10.13.6) installed on a 2.9 GHz Intel Core i5. In a polder system without any intermediate structures between the ditches, the network of ditches is controlled by the intake structures and the pumps in the system only. However, a farmer can use the water in any intermediate location without a hydraulic structure, and therefore, this feature can be interesting by means of salinity and water availability. The flexibility of controlling the main structures according to the states of any intermediate location is an important outcome of the developed MPC scheme.

2.6. CONCLUSION

In this study, a MPC scheme was developed for optimizing flushing of a polder catchment. We provided a MPC scheme to control the salinity concentration and water level in a polder ditch also considering the freshwater usage. We tested the scheme on a test polder ditch layout. The controller was numerically tested for different scenarios and compared with the current operation practice in the field. The results showed that MPC of flushing of a polder ditch results in savings in the order of 35-45% freshwater use, depending on the salinity thresholds.

RSGEM is used to estimate the exfiltration flux and concentration for a realistic scenario using past data. However, this is not a limitation for the controller. The weather predictions and estimations of related events can be used to run the fast RSGEM as a predictive model with required uncertainty assessments and the developed MPC scheme can be used in real time.

Although in this study we focused on salinity as the source of water quality problem, other nutrients that are used in the fields and accumulated in the ditches by means of drained water can also be controlled with the developed MPC scheme. The limitation in such a control scheme will be obtaining real time measurements for the nutrient levels in the ditches.

3

NONLINEAR MODEL PREDICTIVE CONTROL OF POLDER NETWORKS

Hiç, yoktan iyidir.

Erkan Oğur

This chapter presents a novel network model based approach that uses De Saint Venant (SV) and Advection Dispersion (AD) equations to optimize multiple objectives on water level and salinity control using a Nonlinear Model Predictive Control (NMPC). The resulting NMPC problem is solved with a receding horizon implementation, where the nonlinear programming (NLP) problem at each iterations are solved using state-of-the-art large scale interior point solver (IPOPT). We showed the performance of the approach by comparing it with the traditional fixed flushing for a representative Dutch polder. The results have revealed that NMPC framework proposed is capable of controlling the water level and salinity level in the polder. Moreover, the results highlighted that the network of canals could not be made sufficiently fresh with current intake capacity. A simple design approach was used to identify appropriate new capacities for two of the gates and with these proposed capacities, the NMPC can guarantee the required water level and quality constraints.

3.1. INTRODUCTION

Polders are low-lying, artificially drained embanked lands surrounded by storage canals. Water levels in polder networks are kept within a predefined narrow margin using both intake structures and pumping stations. Agricultural activities as well as the freshwater ecosystem in the polders are threatened by surface water salinization due to saline groundwater exfiltration [6]. Land subsidence, climate change and sea level rise increase the salinization of polders by enhancing the salt water intrusion rate [12]. To maintain an acceptable salinity level, freshwater diverted from rivers is used to flush the polder and keep the surface water salinity levels below a certain threshold while not violating the water level constraints of the system. Current practice of flushing control generally relies on constant flushing where the inlet culverts are kept open while the resulting excess water is pumped out from the other side of the polder. This lasts from the beginning until the end of the crop growing season resulting in excess use of freshwater and unnecessary pumping. In the Netherlands, 15 % of total freshwater supply is used for surface water flushing [16] and efficient surface water flushing is listed as a necessity to decrease surface water demand [17]. Efficient water management in polders aims to regulate water levels, salinity levels and the water usage by manipulating the intake and pump flows. In accordance with that, the control objectives for a polder may be summarized as:

- water level needs to stay between predetermined thresholds (always) for safety, demand satisfaction and to maintain groundwater levels in operational limits for the drainage system,

- salinity level needs to be below a certain threshold (when necessary) for agricultural and ecological usage, and

- freshwater use and pumping cost should be minimized.

The relation between these sub-objectives may be conflicting: additional freshwater from the intakes is necessary to satisfy the salinity level objective, which will result in increased usage of freshwater and pump flows. This may result in violations of water levels, resulting in a complex multi-objective control problem. An advanced control algorithm for polder flushing to control salinity level and quantity will increase the efficiency of the system. This chapter considers the flushing problem of a polder with multiple objectives using nonlinear model predictive control (NMPC).

Model predictive control (MPC) is a popular technique and has been used in the control of water systems including drinking water networks [64], irrigation systems [38, 65, 66], flood control [40] and polders [44, 57]. If the processes that are controlled are staying around a fixed operating point, the process models can be linearized, which allows application of linear MPC [47] as applied in [57] for optimal salinity and water level control of water courses. However, in operation of a polder network, different salinity thresholds can be considered according to the farmer needs resulting in time-varying set points. Moreover, spatial and temporal variation of saline groundwater disturbances make local linearization inefficient in terms of future system behaviour predictions. Here we consider a NMPC strategy that is based on the receding horizon principle. It can optimize the predicted future system behaviour by solving a nonlinear program (NLP) on-line at

each control time step [67] and has been used for water systems in [68, 69]. The main advantage of NMPC is the ability to explicitly implement the constraints on inputs, outputs and states in the optimization problem.

For water quality (salinity) and quantity control, Xu et al. [43, 44], developed a MPC strategy to control the average salinity concentration in a ditch using a reservoir model. This study was followed by applying a model reduction technique for an internal model to control downstream salinity concentration in open channels. In a recent study, we achieved point salinity control in a single pool by explicitly considering freshwater conservation, using linearized Saint Venant (SV) and advection dispersion (AD) equations as the internal model of the MPC scheme [57]. We used real saline groundwater exfiltration data for the first time to test the developed MPC scheme. Although the results were promising, the formulation was limited to control of channels connected in series. In a real polder network, multiple channels with different salinity concentrations are connected with or without hydraulic structures in between. Mixing at the connection nodes is very important since the inflow concentration of downstream channels depend on the concentration of the upstream channels. Therefore, mixing at the connection nodes should be considered in optimization for polder flushing.

Motivated by the above-mentioned arguments, we propose in this study a novel NMPC framework for efficient flushing control in low-lying polders. To the best knowledge of the authors, this is the first case where a (real-world) polder network is controlled with a NMPC framework. We first formulate the NMPC problem based on SV and AD equations to model the dynamics of the water and salt transport in the polder for flushing. Subsequently, parameters and constraints of the model are defined. Simulation examples of flushing control of a representative Dutch polder, the Lissertocht catchment, are presented to illustrate the closed-loop performance of the developed NMPC scheme as a case study. Finally, we investigate the performance of the controller and employ a co-design approach to upgrade the fresh water intake capacities of the polder to increase the salinity control performance of the case study area.

3.2. SYSTEM MODEL

Transport of water and dissolved matter have to be considered to model the flushing of a polder [60]. For a signle channel, these dynamics are described by Saint Venant (SV) (3.1) and one-dimensional Advection Dispersion (AD) (3.2) equations, respectively:

$$\frac{\partial A}{\partial t} + \frac{\partial Q}{\partial z} = q_l, \tag{3.1}$$

$$\frac{\partial Q}{\partial t} + \frac{\partial (Qu)}{\partial z} + gA\frac{\partial \zeta}{\partial z} + g\frac{Q|Q|}{C_z RA} = 0,$$

$$\frac{\partial AC}{\partial t} + \frac{\partial QC}{\partial z} = \frac{\partial}{\partial z}(KA\frac{\partial C}{\partial z}) + q_l C_l, \tag{3.2}$$

where A is the cross sectional area [m^2], Q is the flow [m^3/s], q_l is the lateral inflow per unit length [m^3/s/m], u is the mean velocity (Q/A) [m/s], ζ is the water depth above the reference plane [m], $C_z = 40$ is the Chezy coefficient [m$^{1/2}$/s], R is the hydraulic radius

(A/P_f) [m], P_f is the wetted perimeter [m] and g is the gravity acceleration [9.8 m/s^2], K is the longitudinal dispersion coefficient [m^{2}s], C is the salt concentration [kg/m^3], C_l is the lateral flow concentration [kg/m^3], t is time [s] and z is horizontal dimension [m] (the choice of z instead of x as the horizontal dimension is to avoid confusion in the remainder of the chapter where x is a vector representing the states of a system). The longitudinal dispersion coefficient (K) is given by Fischer et al. [61] as:

$$K = 0.011 \frac{B^2 u^2}{d u_s} \tag{3.3}$$

where B is the mean width [m], d is the mean water depth [m], $u_s = (gRS_b)^{1/2}$ is the shear velocity [m/s] and S_b is the bottom slope of the canal [-]. In this chapter, equations (3.1) and (3.2) are discretized as in [44], using a staggered grid and applied for both simulating the polder system and as the dynamic model of the NMPC design, which is implemented in MATLAB$^{\circledR}$. Organizing the discretized SV and AD equations in a similar approach for the discretization matrix given in equation (2.5), the following system dynamics is achieved for a single channel j:

$$E_j^k x_j^{k+1} = A_j^k x_j^k + B_{u_j}^k u_j^k + d_j^k \tag{3.4}$$

where $x_j^k = [h_{j1}^k h_{j2}^k \ldots h_{jn}^k c_{j1}^k c_{j1}^k \ldots c_{jn}^k]^T \in \mathbb{R}^{2n}$ is the state vector corresponding to channel j and its water levels, h_{ji}, and salinity concentrations, c_{ji}, at all n discretization points ($i = 1, 2, \ldots, n$) at time step $k \in \mathbb{N}$, $u_j^k = [Q_{j_{in}} Q_{j_{out}}]^T$ is the input vector that consists of the inflow, $Q_{j_{in}}$, and outflow, $Q_{j_{out}}$, discharges to the channel j and finally $d_j i^k \in \mathbb{R}^{2n}$ is the disturbance vector, which has all the remaining terms that are not associated with states and inputs. The time variant matrices $E_j^k \in \mathbb{R}^{(2n)\times(2n)}$, $A_j^k \in \mathbb{R}^{(2n)\times(2n)}$ and $B_{u_j}^k \in \mathbb{R}^{(2n)\times 2}$ are associated with the states and the inputs and are filled by time dependent terms from the linearized SV and AD equations in (3.1)-(3.2)

Equation (3.4) is defined for a single channel and needs to be extended to a network of channels in order to represent the system dynamics of a polder network. As an example, here, we provide the full system dynamics of a simple three channel network shown in Figure 3.1 as:

$$\underbrace{\begin{bmatrix} E_1 & 0 & 0 \\ 0 & E_2 & 0 \\ 0 & 0 & E_3 \end{bmatrix}^k}_{\mathbf{E}^k \in \mathbb{R}^{n_x \times n_x}} \underbrace{\begin{bmatrix} x_1 \\ x_2 \\ x_3 \end{bmatrix}^{k+1}}_{\mathbf{x}^{k+1} \in \mathbb{R}^{n_x}} = \underbrace{\begin{bmatrix} A_1 & 0 & 0 \\ 0 & A_2 & 0 \\ 0 & 0 & A_3 \end{bmatrix}}_{\mathbf{A}^k \in \mathbb{R}^{n_x \times n_x}} \underbrace{\begin{bmatrix} x_1 \\ x_2 \\ x_3 \end{bmatrix}^k}_{\mathbf{x}^k \in \mathbb{R}^{n_x}} + \tag{3.5}$$

$$\underbrace{\begin{bmatrix} B_{u1} & 0 & 0 \\ 0 & B_{u2} & 0 \\ 0 & 0 & B_{u3} \end{bmatrix}^k}_{\mathbf{B_u}^k \in \mathbb{R}^{n_x \times (n_u)}} \underbrace{\begin{bmatrix} u_1 \\ u_2 \\ u_3 \end{bmatrix}^k}_{\mathbf{u}^k \in \mathbb{R}^{(n_u)}} + \underbrace{\begin{bmatrix} d_1 \\ d_2 \\ d_3 \end{bmatrix}^k}_{\mathbf{d}^k \in \mathbb{R}^{n_x}}$$

where $\mathbf{x} \in \mathbb{R}^{n_x}$ is the state vector of the channel network that has all of the water level and salinity concentrations at all of the discretization points of each channel, $\mathbf{u} \in \mathbb{R}^{n_u}$ is

the input vector for the network that has all of the inflow and outflow discharges of the channels. Total number of states, n_x, is the summation of the number of states of each channel determined by the number of discretization points. On the other hand, total number of the input, n_u, is two times the total number of channels (which is 6 for the network given in Figure 3.1 having one pair of inflow and outflow for each channel).
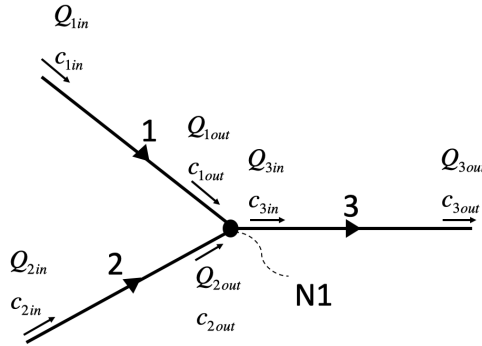

Figure 3.1: A simple network of three channels (labeled by 1, 2 and 3) connected at the connection node N1.

In addition to the system dynamics given in (3.5), mass conservation at connection nodes has to be considered to model a network of channels. As an example, for the network in Figure 3.1, mass conservation at node N1 assuming complete mixing is given as:

$$Q1_{out}^k + Q2_{out}^k = Q3_{in}^k \tag{3.6}$$

$$c3_{in}^k = \frac{Q1_{out}^k \times c1_{out}^k + Q2_{out}^k \times c2_{out}^k}{Q1_{out}^k + Q2_{out}^k} \tag{3.7}$$

where discharge and salinity concentration entering a channel are represented by $Q_{j\,in}$ and $c_{j\,in}$ while the ones leaving a channel are represented by $Q_{j\,out}$ and $c_{j\,out}$ (j=1,2,3). Equations (3.5) - (3.7) can be extended to model the dynamics of any polder network for flushing, with the size of the resulting state-space model and number of constraints depending on the number and connection of the channels. For the real case study shown in Figure 3.3, these additional mass balance and salinity concentrations are created from the network graph.

3.3. Nonlinear MPC Framework for polder Flushing

In this section we formulate the general NMPC problem followed by the definition and application of the control objectives for polder flushing.

3.3.1. NMPC FORMULATION

NMPC applications use a model of the system to be controlled to predict the future system behaviour. A cost function that combines the system states and control inputs is used as the objective function of the controller. Control action is calculated by the minimization of the objective function subject to both equality (system model) and inequality (limits of the states and inputs) constraints of the system over the prediction horizon. For a finite time interval $[t_k, t_f]$ discretized to N_p number of prediction steps where $N_p \times t_c = t_f - t_k$ and t_c is the control time interval, the NMPC problem can be expressed with the following objective function:

$$\min_{\mathbf{u},\mathbf{x}} \quad \sum_{i=0}^{N_p-1} ||\mathbf{x_r}(t_k + i + 1) - \mathbf{x}(t_k + i + 1)||_Q^2 +$$

$$||\mathbf{u}(t_k + i)||_R^2 + ||\mathbf{x_r}(t_k + N_p) - \mathbf{x}(t_k + N_p))||_{Q^f}^2$$

subject to:

the system dynamics, and

constraints   (3.8)

where $\mathbf{x_r}(i)$ is the reference for the states at time step i. System dynamics are given by equations (3.5)-(3.7) and the constraints of the system are defined in the next section in equations (3.9)-(3.14). The matrices $Q \in \mathbb{R}^{n_x \times n_x}$, $R \in \mathbb{R}^{n_x \times n_u}$ and $Q^f \in \mathbb{R}^{n_x \times n_x}$ are symmetric positive definite weighting matrices associated with states and inputs. The last part of the objective function, that is penalized by Q^f is known as the terminal cost and is added for stability reasons in NMPC [70].

3.3.2. CONTROL OBJECTIVES AND PROBLEM FORMULATION FOR POLDER FLUSHING

As discussed in the introduction, polder flushing is governed by three objectives: controlling the water level and salinity concentration while minimizing the freshwater use and pumping. For any discretization point, i, in channel j, described in (3.4), deviations of water level, $e_{h_{ji}}^k$, and salinity concentration, $e_{c_{ji}}^k$, from a given set point, h_{ref} and c_{ref}, at time step k are:

$$e_{h_{ji}}^k = h_{ji}^k - h_{ref}, \tag{3.9}$$

$$e_{c_{ji}}^k = c_{ji}^k - c_{ref}. \tag{3.10}$$

Water level in the polder should be kept around a predefined set point with an upper and lower limit. Violations of these water levels in a polder may result in overbank flooding or embankment failures. Therefore, lower ,$\underline{e_h}$, and upper ,$\overline{e_h}$, limits of water level deviation are implemented as hard constraints, which are described as:

$$\underline{e_h} \leq e_{h_{ji}}^k \leq \overline{e_h} \tag{3.11}$$

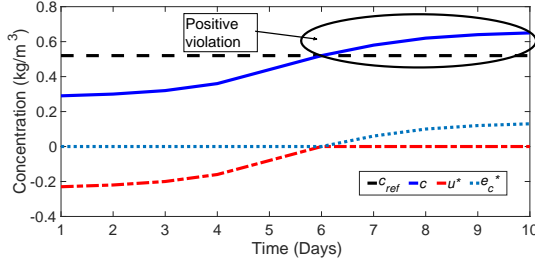In contrast to the implementation of water level constraints, using a hard constraint is

Figure 3.2: Illustrative figure for showing the application of the soft constraint for salinity control. Only the positive violations above the salinity threshold, c_{ref}, are penalized in the objective function with the virtual state, e_c^*. Virtual state is equal to zero if the salinity concentration is below or equal to the salinity threshold.

not feasible for salinity control. Due to the salinity characteristics of the polder system, at certain times salinity concentrations higher than the threshold can be observed, which sometimes may not be possible to flush out depending on the capacity of the system. On the other hand, salinity concentrations below the salinity threshold are fresher than what is required and, thus, they are not a problem in terms of salinity control. To penalize only the positive violations above the salinity threshold, we introduce a soft constraint as explained in [63] for salinity control and depicted in Figure 3.2. Soft constraints can be implemented for concentration values (at discretization points of a channel) using a combination of a virtual input, u^*, and a virtual state, e_c^*, which track distance to maximum salinity constraint and the level of constraint violation, respectively, as:

$$e_{c_{ji}}^{*k} = e_{c_{ji}}^k - u_{ji}^* \tag{3.12}$$

with constraints

$$\underline{e_{c_{ji}}^k} \leq e_{c_{ji}}^k \leq \overline{e_{c_{ji}}^k}$$
$$0 \leq e_{c_{ji}}^{*k} \leq \overline{e_{c_{ji}}^{*k}} \tag{3.13}$$
$$\underline{e_{c_{ji}}^k} \leq u_{ji}^* \leq 0$$

where $\underline{e_{c_{ji}}^k}$ and $\overline{e_{c_{ji}}^k}$ are the minimum and maximum salinity concentration deviations that are physically possible. Virtual state, $e_{c_{ji}}^{*k}$, has a very high penalty in the objective function and is activated only if there is a positive violation of the salinity concentration. For all the other cases, the virtual input, u_{ji}^*, will be equal to the distance below the set salinity threshold, $e_{c_{ji}}^k$, resulting in zero violation of the virtual state, $e_{c_{ji}}^{*k}$. Figure 3.2 illustrates a trajectory of salinity concentration (solid blue line), an upper threshold for

salinity levels (black dashed line), virtual input (red dash-dotted line), and the virtual state (light blue dotted line).

The last objective, minimizing the usage of freshwater and pumping flow, is achieved by penalizing the inputs corresponding to the flows through the intakes and the pumping station of the network in the objective function. For all m hydraulic structures in the polder (intakes and pumps), the structure setting can change between fully closed, resulting to zero flow, and fully open, resulting to a flow equal to the maximum capacity, $\overline{Q_i^k}$. Therefore, capacity constraints for all m structures in the network are given as:

$$0 \leq Q_i^k \leq \overline{Q_i^k}, \quad i = 1, 2, \ldots, m \tag{3.14}$$

In this work, we follow the direct collocation approach of 'first discretize and then optimize' [71], where the optimal control problem is discretized and parametrized resulting in a NLP problem. At each control time step, the NLP problem is solved over the prediction horizon and only the first control action is implemented with a receding horizon principle, where the prediction and optimal control calculations are repeated as the prediction horizon slides along. In this study, we use a state-of-the-art open-source optimization software IPOPT [72] to solve the resulting NLPs.

3.4. Test Case Description and Results

3.4.1. Lissertocht Catchment

To illustrate the closed loop performance of the proposed NMPC scheme based on real-world saline groundwater exfiltration data, we performed simulations for controlling the flushing operation of the Lissertocht catchment. The catchment is located approximately 25 km southwest of the city of Amsterdam (Figure 3.3). It can be considered as a representative deep polder in the Netherlands where the main source of salinity is deep saline groundwater exfiltration through boils that are preferential flow paths intersecting the Holocene cover layer [22]. The discharge and concentration of the boils are rather constant while the other sources of salt, ditch and drain exfiltration, have temporal variations. Different sources of the saline groundwater exfiltration in the Lissertocht catchment have been studied and modelled in [23]. Spatial variation of boils in the Lissertocht catchment (see red dots in Figure 3.3), results in heterogeneity in salinity disturbance. Upstream main channels close to the intakes have fresh water, while the downstream main channels are affected by the boils and higher salinity concentrations are observed. To decrease the surface water salinity, freshwater is supplied through five inlets with a total capacity of 0.0956 m³/s (see Table 3.1 for the capacity of each intake). A main pumping station with a capacity of 1.48 m³/s is used to maintain the water level around the set point, h_{ref}. In this study, we focused on these five intakes and the main pumping station as the control structures. The main land use in the area is agriculture and the salinity concentration and water quantity requirement of the farmers varies depending on the crop cultivated.

In [73], we used a SOBEK [74] model combined with a saline groundwater exfiltration model [58] of the area to optimize the salinity sensor placement for real time control of polder flushing in the main channels of the Lissertocht catchment. Similarly, in this study we focused on controlling the salinity concentration and water quantity of
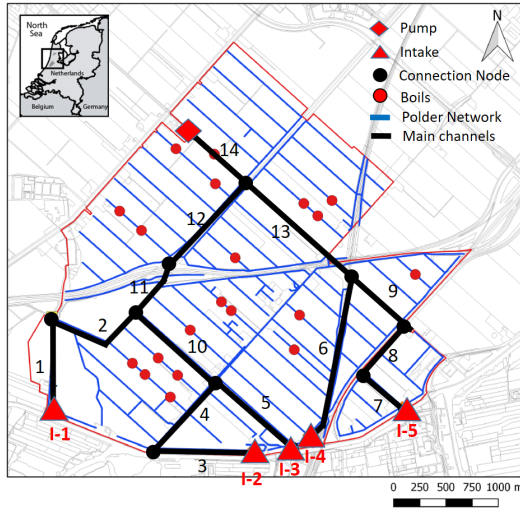
Figure 3.3: Location of the Lissertocht catchment (top left) and the layout of the controlled network of the main channels (14 in total with 9 connection nodes), intakes (labeled as I-1 to I-5), pump station and the boils in the area.

Table 3.1: Maximum Capacities of the Intakes

Structure	Maximum Capacity [m^3/s]
Intake 1	0.0162
Intake 2	0.0236
Intake 3	0.0306
Intake 4	0.0097
Intake 5	0.0155

the main channels of the Lissertocht catchment (Figure 3.3) that transfer the freshwater from intakes to the pumping station. To test the performance of the NMPC scheme, we selected a 30 day dry period (8 May 2013 - 6 June 2013 shown in Figure 3.4) with a very intense rainfall in between [73]. We model the Lissertocht catchment with 14 main channels, depicted with numbers in Figure 3.3, aggregating a number of connected main ditches. Drainage channels with a connection to the main channels are represented as lateral flows to the main channels transporting the excessive water in the polder parcels collected by the drainage system. Drainage channels can provide a buffer for water level variations and salt load in the polder and during severe drought, flow from main channels to the drainage channels can be observed. However, in accordance with the characteristics of the selected test period in this study, water flows and the associated inflow concentrations from these drainage channels to the main channels are used as known disturbances based on real-world saline exfiltration data of the catchment as modelled in [73].
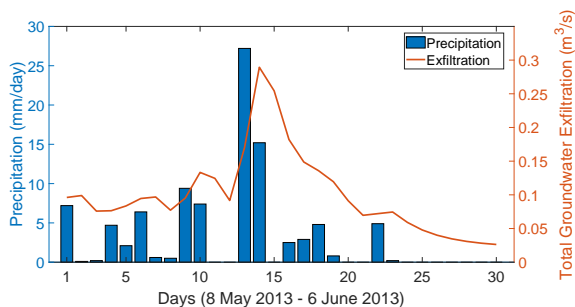
3

Figure 3.4: Selected test period for the NMPC scheme. Daily precipitation (mm/day) is shown on the left and the resulting total groundwater exfiltration (m^3/s), as we modeled in [73], used as the disturbance is shown on the right.

Table 3.2: Properties of the channels of Lissertocht Catchment

Channel	Length [m]	Bed width [m]	Side slope [V:H]	Mean Water Depth [m]
1	822	1.40	1	1.12
2	931	2.50	2	0.95
3	915	1.65	1	1.12
4	850	1.40	1	1.12
5	970	1.65	1	0.62
6	1550	1.00	2	1.02
7	450	1.40	2	0.97
8	616	2.00	3	0.97
9	730	2.00	2	0.82
10	1000	1.45	2	1.02
11	550	4.00	2	0.82
12	1070	5.00	2	0.91
13	1330	4.20	2	0.95
14	657	4.20	2	0.95

Table 3.3: Weights in the objective function (3.8)

Description	In Matrix	Value [-]
Deviation of water level, e_h	Q	400
Deviation of virtual state, e_c^*	Q	5
Virtual input, u^*	R	10^{-5}
Flushing discharge, Q_{flush}	R	10^{-2}
Pumping discharge, Q_{pump}	R	10^{-2}
Water level stability, $e_h(t_f)$	Q_f	400
Concentration stability, $e_c(t_f)$	Q_f	5

3.4.2. PARAMETERS FOR MODELLING AND CONTROL

In this work, our control goal is to maintain the water level around the set point of -6.45 m in the polder with a maximum deviation of ±0.05 m. For salinity level control, a salinity threshold of 1.5 kg/m^3 (= 1500 mg/l) is imposed in accordance with the requirements of the responsible water authority of the area, the Rijnland District Water Control Board. We controlled the water level and salinity concentration at the end of each main channel.

For the spatial discretization of (3.8), we used a discretization spacing of 50 m and for the temporal discretization, we used 1 min as the simulation time step and 1 hour as the control time interval, t_c. To capture the slow dynamics of the salt transport, we implement a prediction horizon of 24 hours resulting in 24 prediction steps, N, for the controller. The system model consists of 12528 states (water level and salinity concentration deviations and the virtual states), 1008 control inputs (inflows, outflows and the virtual inputs), 9 connection nodes and 28 water level and salinity concentration control points.

The weighting matrices Q, R and Q^f in (3.8) are filled with the values given in Table 3.3 for each channel of the network depending on the state or input penalized. As an initial guess for the weights penalizing the states and the inputs used in this study, we used the maximum allowed value estimate (MAVE) described in [28]. An estimate of how much a state or a control input may vary is selected as the MAVE of that variable. For example, a MAVE of 0.05 m was used for the water level deviation, which is equal to the allowed deviation from the water level set point and the weight in the objective function is calculated as the reciprocal of the square of the MAVE as $1/(0.05)^2 = 400$. Following similar approaches for the other states and inputs penalized, and analyzing results of different settings, we decided on the values given in Table 3.3 that ensures no violation of the water level constraints. For the weights of the terminal cost, Q_f, we decided to use the same values as the original states penalized since we did not observe any stability problems in the results of the simulations.

3.4.3. RESULTS

The described NMPC framework is used to control the water level and the salinity concentration of the Lissetrocht catchment. The simulation results are presented in Figs. 3.6 - 3.7. To illustrate the difference between the current flushing practice in the Lissertocht catchment (fixed flushing during the crop growing season), the results of the

Table 3.4: Comparison of NMPC and fixed flushing water usage over the simulation period

	NMPC [m^3]	Fixed [m^3]	% Saved
Intake 1	3.33×10^4	4.19×10^4	20.6
Intake 2	5.14×10^4	6.11×10^4	15.7
Intake 3	6.30×10^4	7.92×10^4	20.4
Intake 4	1.61×10^4	2.51×10^4	35.5
Intake 5	3.53×10^4	4.01×10^4	12.0
Total	1.99×10^5	2.47×10^5	19.5
Pump	3.94×10^5	4.48×10^5	11.9

NMPC scheme is compared with fixed flushing. All computations were performed within MATLAB R2019a installed on a 3.50 GHz Intel Xeon machine with 16 GB of ram running Windows 10. The acceptable tolerance of constraint violation option of IPOPT was set to 10^{-3}. We limited the maximum number of iterations to 100, and the average control computation time resulted in 120 seconds, which is much smaller than the control time step of 1 hour.

Figure 3.5 shows the controlled water level at the downstream end of the catchment close to the pumping station. As can be seen, NMPC keeps the water level around the set point of -6.45 m. The fluctuations in the water level resulting from the changing control structure settings at all control time steps are in the order of millimeters and they never violate the water level constraint. The NMPC scheme successfully controls the water level by reacting to the disturbances from groundwater exfiltration shown in Figure 3.4.

The controlled discharges of the inlet gates are shown in Figure 3.6 for the whole test period (a moving average over 24 hours for better visualization). All of the gates have an initial flow of 0.05 m^3/s and the NMPC scheme immediately increases the flows at the beginning of the test period. Maximum capacities of the intakes, which are used by the fixed flushing strategy over the whole simulation period, are shown with dashed red horizontal lines in Figure 3.6(a)-(e). As can be seen, the NMPC scheme operates the system using flushing discharges close to the individual capacities of the intakes except intake I-4 (Figure 3.6(d)), which has the lowest capacity compared to the other intakes. The pumping discharge shown in Figure 3.6(f) shows similar behaviour for both options, fixed flushing resulting in a slightly higher pumping, as expected. The total volume of water used by each intake and the total volume of flushing and pumping are reported in Table. 3.4. The total freshwater savings compared to the fixed flushing is 19.5 % while the savings in pumping volume is lower at 11.9 %, since the system also pumps out later inflows that drain into the channels. The individual savings from each intake varied between 12.0 % to 35.5 %.

Figure 3.7 shows the salinity concentrations at the downstream end for six main channels. These six main channels either have saline boils in them (eg. main channel 14 in Figure 3.3) or have a direct connection to drainage channels with saline boils (eg. main channels 2,6,11,12, and 13). Therefore, the salinity concentration in these channels exceeds the salinity concentration threshold set by irrigation requirements. Moreover, depending on the location of the channel in the polder one or more intakes can provide
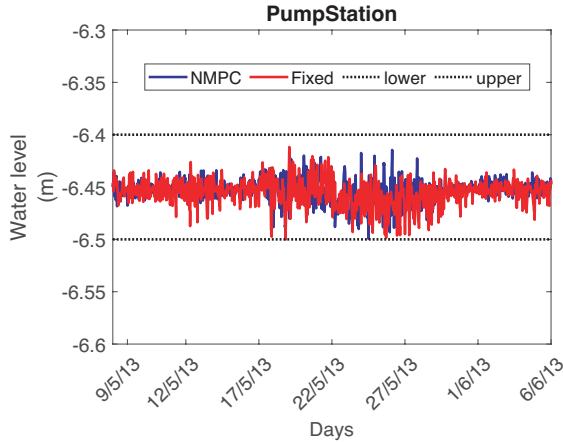
Figure 3.5: NMPC controlled water level at the downstream end of Lissertocht catchment compared with fixed flushing, together with upper and lower bound constraints on water level.

freshwater to these main channels. For example, main channel 2 can only be flushed using the intake I-1, while intakes I-1 to I-3 can provide freshwater for main channel 11 as can be seen in Figure 3.3, making this main channel fresh for the most of the considered time. The remaining eight main channels in the catchment (main channels 1 to 10 except 2 and 6) have no boils connected to them and the ditch exfiltration into these channels is fresh. Therefore, salinity in these channels remains fresher and within constraints.

In terms of salinity control, in this model run, it is clear that the NMPC scheme does not perform as well as the water level control. However, comparison with the fixed flushing gives much more information in terms of the capacity of the system and therefore the performance of the NMPC scheme. The dashed lines in Figure 3.7(a)-(f) show the salinity concentrations at the end of each channel with fixed flushing. This is a benchmark for the NMPC scheme, since the NMPC uses values close to the flushing capacity for most intakes. Salinity concentration at these points cannot drop below this level with the given flushing capacity of intakes. For example, as can be seen in Figure 3.7(a), the salinity concentration drops below the threshold of 1.5 kg/m^3 only around 20/05/13. This corresponds to the period of the simulation when the intensive rainfall results in a peak in (fresh) groundwater exfiltration, which flushes the catchment naturally. The NMPC scheme achieves the salinity level control goal in the main channels 11 and 13 (Figure 3.7(c)&(e)). On the other hand, the NMPC scheme fails to drop the salinity concentration below the threshold for the other four main channels presented in Figure 3.7. Main channels 12 and 14 are at the downstream end of the network, and they carry most of the high saline water to the pumping station. Therefore, higher salinity concentrations are observed in these two main channels. Moreover, as can be seen in Figure 3.7(d)&(f), the performance of the fixed flushing is also not good for main channels 12 and 14 and the salinity concentrations are close to the values achieved by the NMPC. The biggest difference in terms of salinity control performance between fixed flushing and NMPC is

3
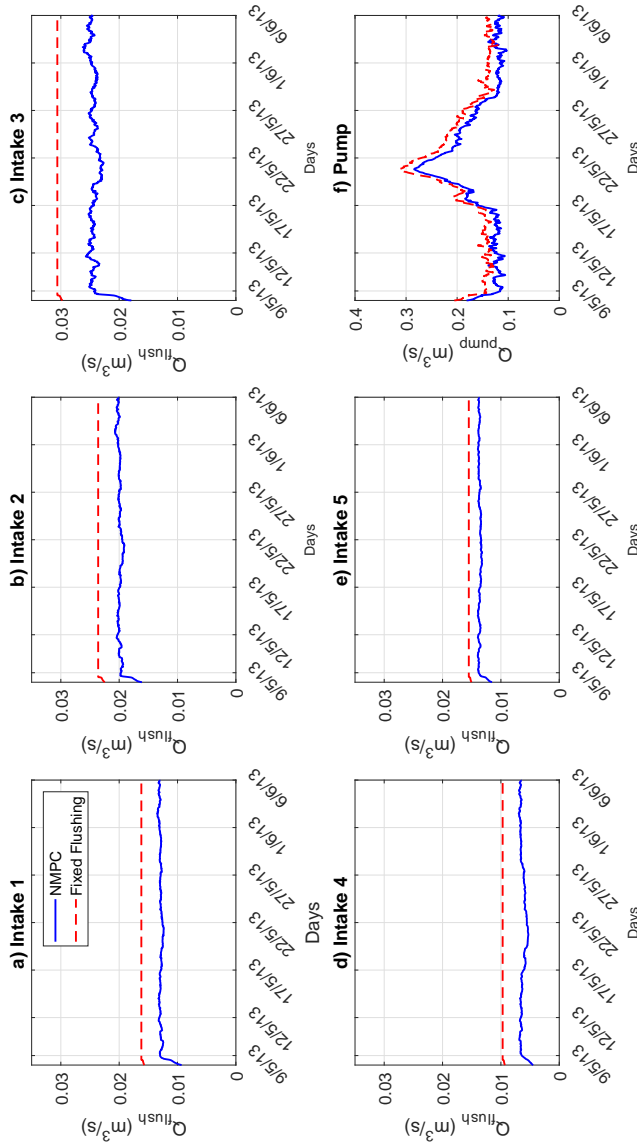

Figure 3.6: Controlled discharges (m³/s) of the intakes (a-e) and the pumping station (f) represented with a moving average of 24 hours for smoothing. Discharges used for fixed flushing are represented by the dashed lines, which are also the upper limit of the intakes.
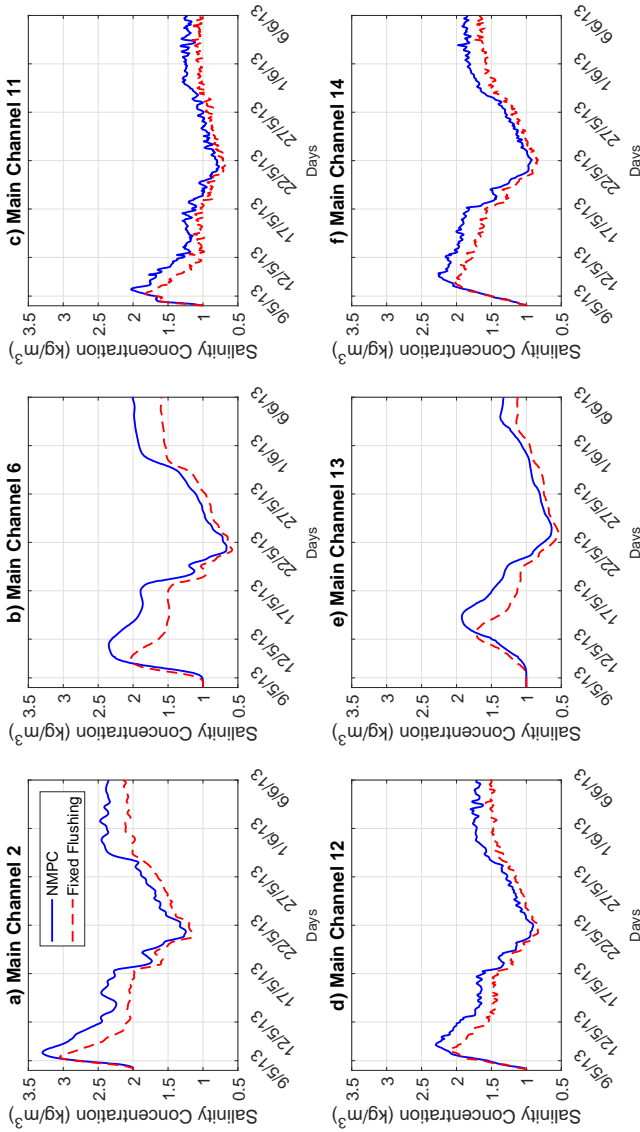
Figure 3.7: Controlled salinity concentrations over the simulation period at six different channels of the Lissertocht catchment. a) Main Channel 2, b) Main Channel 6, c) Main Channel 11, d) Main Channel 12, e) Main Channel 13 and f) Main Channel 14. (see Figure 3.3 for the locations of the main channels).

observed in main channels 2 and 6 (Figure 3.7(a-b)). These two main channels are on the upstream side of the catchment, where main channel 6 can only be flushed by intake I-4 (directly connected to main channel 6) and main channel 2 can only be flushed by intake I-1 (freshwater should first be transported through main channel 1) - see also Figure 3.3. The NMPC scheme prefers not to use the full capacity of intakes I-1 and I-4 and saves water in exchange for higher salinity in two main channels. This is a trade-off between salinity and freshewater usage and it is further elaborated in the next paragraph.

Salinity control performance is directly related to the amount of freshwater usage. Combining the information given in Table 3.4 and Figure 3.7, it can be concluded that there is more freshwater availability for intakes I-1 and I-4 that should be able to dilute the salinity concentration in main channels 2 and 6, respectively. However, as can be seen in Table 3.4, the capacities of intake I-1 and I-4 are utilized the least compared to the other intakes. At first, the reason why the NMPC does not utilize the maximum capacities of intakes I-1 and I-4 to decrease the higher concentrations in the upstream main channels 2 and 6 was not apparent. A posteriori analysis of the polder network and the results reveal a possible reason related to the flushing capacities and the salt transport dynamics described by the AD equations. When a channel is flushed, water with high salinity concentration in the channel is transferred to the downstream channels of the polder and finally pumped out of the system. If a channel is not flushed, salinity concentration in that channel will increase locally and later, through very slow dispersive mechanism, will spread to the rest of the polder. The NMPC makes use of this behaviour defined by the system dynamics in the constraints and decides to transport less salt water from main channels 2 and 6 to the downstream channels. By carrying less salt water downstream, it decreases the need for freshwater usage in the remainder of the polder. Alternative routes that carry fresher water are preferred to flush the downstream channels. For example, downstream of main channel 2 and 6 are main channels 11 and 13, respectively. As shown in Figure 3.7, salinity concentrations in these two downstream main channels are most of the time below the salinity threshold. Freshwater necessary to decrease the salinity is mostly provided by alternative routes through intakes I-2, I-3 and I-5. Freshwater provided by these three intakes travels without mixing with saline groundwater through at least one main channel and reaches downstream as a 'fresher' water source. In the considered case here, since the salinity concentrations are controlled in all main channels with equal weighting, the NMPC scheme allows higher concentrations in channels 2 and 6 in exchange for saving freshwater use, which is one of three weighted objectives for the controller.

In the next section, we consider upgrading intake capacity as a future possibility for the stakeholders to guarantee lower salinity levels. Based on simplistic mixing, we propose potential upgrades in intake capacity and test their performance both under fixed flushing and under the advanced NMPC schemes.

3.4.4. SYSTEM UPDATE TO IMPROVE THE SALINITY CONTROL PERFORMANCE

Results presented in the previous section showed that the salinity control performance was hampered by insufficient capacity of intakes I-1 and I-4. Therefore, in this section, we provide a simple system update by increasing the capacities of these intakes to im-

prove the salinity control performance of the NMPC framework. We focus on decreasing the salinity concentration at main channels 2 and 6. By considering the worst scenario of no rain to naturally flush the system and the number of existing boils discharging (directly or through drainage channels) to these two main channels, we estimated the necessary freshwater intake to dilute the high saline water in these main channels using Equations (3.6)-(3.7). We increased the capacities of intake I-1 from 0.0162 m^3/s to 0.0342 m^3/s and of intake I-4 from 0.0097 m^3/s to 0.0136 m^3/s, respectively to bring average salinity levels to below the threshold of 1.5 kg/m^3. Keeping the rest of the parameters as the original setting, we simulated the system and the results are presented in Figs. 3.8-3.9, where also results of the original configuration and fixed flushing with the updated capacities are included for comparison.

Figure 3.8 presents the controlled discharges of the intakes and the pumping station. Full capacity of all intakes were used by the fixed flushing and are shown with a dashed line. Similar to Figure 3.6, all of the intakes start with an initial flow and the NMPC immediately increases the flushing from all of the intakes. Due to the increased capacities, flushing through intakes I-1 and I-4 is increased as expected for the upgraded case where the NMPC scheme is applied. The rest of the intakes behave similarly to the original setting (i.e. Figure 3.6).

The salinity control performance of the updated system (both fixed flushing and NMPC) compared with the original configuration (NMPC) is shown in Figure 3.9. The NMPC scheme utilized the increased capacities of intakes I-1 and I-4 and additional freshwater from these intakes is used to dilute and flush the high saline water in the main channels 2 and 6 (Figure 3.9(a)-(b)). As a result of additional flushing water used, salinity control performance of the NMPC scheme significantly improved and the salinity concentrations in all channels are below or around the salinity threshold for the updated design. Fixed flushing also used full capacities of the intakes resulting in the lowest salinity concentrations, which were lower than the set threshold.

For the updated system, the NMPC scheme used around 20% less freshwater compared to the fixed flushing (2.46 × 10^5 m^3 for the NMPC and 3.05 × 10^5 m^3 for fixed flushing). For both fixed flushing and NMPC, the better salinity performance comes at the price of using more freshwater from the increased capacities (around 19% increase).

3.5. CONCLUSION

In this chapter, we propose a novel NMPC framework for optimal flushing control in polders. We presented a network model to optimize multiple objectives and tested the controller in a low-lying Dutch polder, the Lissertocht catchment as a case study. The proposed NMPC scheme is mathematically explained, implemented and used for this case study to control salinity concentration and water quantity in all main channels of the network in simulation experiments. Sufficient performance for water level control was achieved by keeping the water level always within set boundaries. Salinity control performance of the NMPC, however, appeared to be limited due to the intake capacity. Further analysis of the network and the results allowed us to set up a simple design update of the system. We achieved a satisfactory salinity control performance by updating the intake capacity of two intakes. Both in the original and updated system, freshwater usage is reduced by around 20% using the NMPC compared to the fixed flushing strategy

3

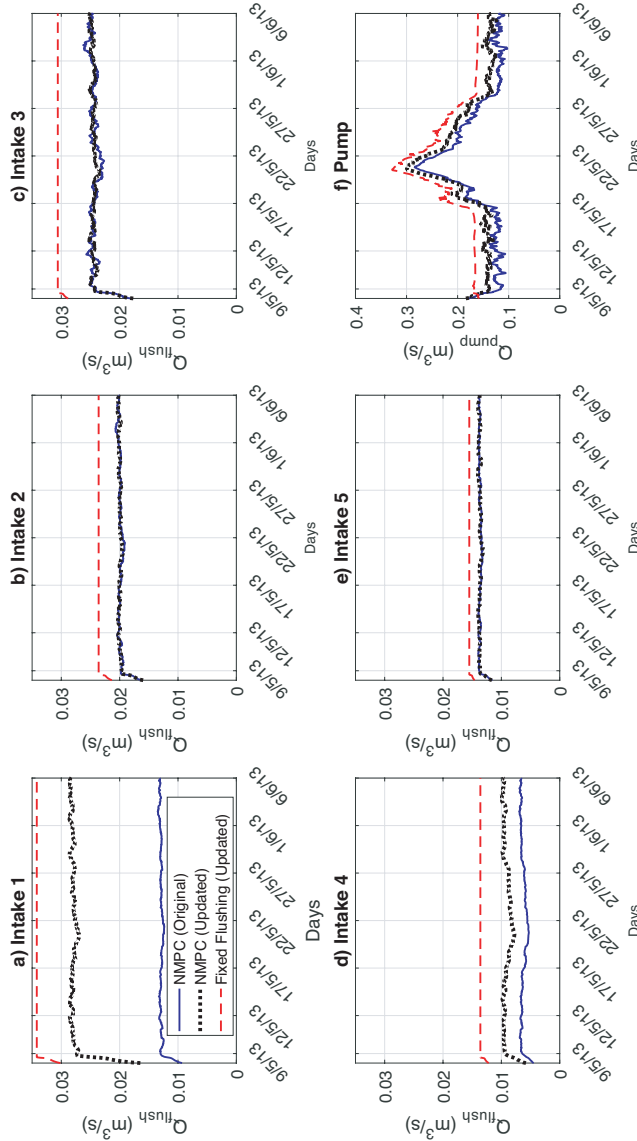Figure 3.8: Controlled discharges (m³/s) of five intakes (a-e) and the pumping station (f) for the updated system (black dotted line) compared with the original configuration (blue continuous line) and fixed flushing using the updated capacities (red dashed line). For smoothing and better representation of the results, all discharges are represented with a moving average of 24 hours in this figure.
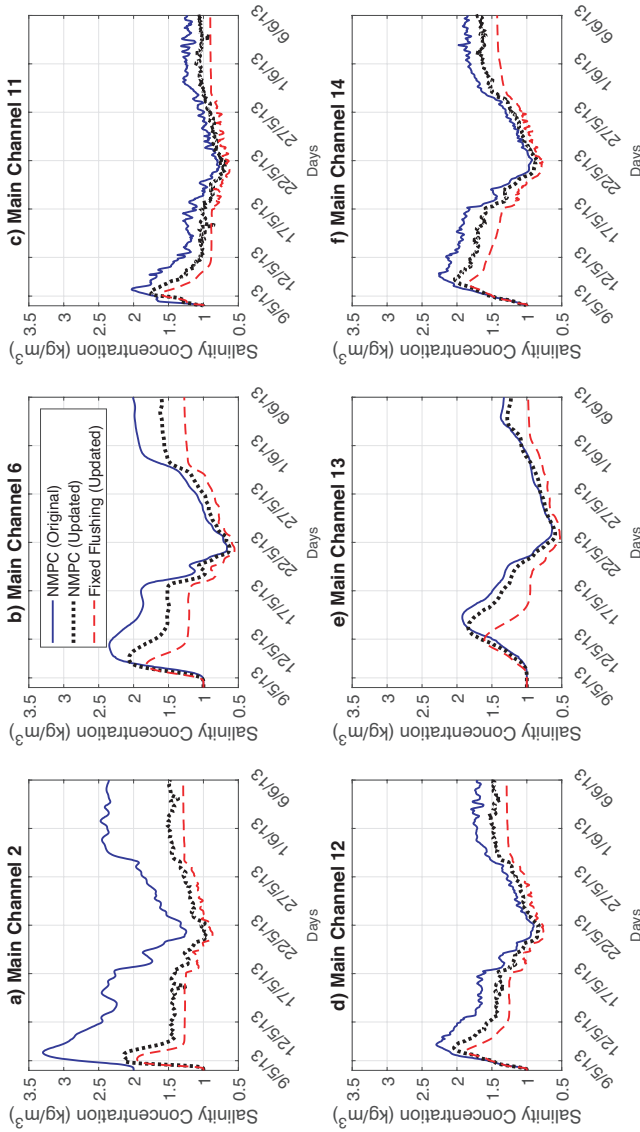
Figure 3.9: Controlled salinity concentrations over the simulation period at six different channels of Lisser-tocht catchment for the updated system compared with the original configuration and fixed flushing using the updated capacities. a) Channel 2, b) Channel 6, c) Channel 11, d) Channel 12, e) Channel 13 and f) Channel 14. Channel numbers are shown in Figure 3.3.

presently in operation in the Lissertocht catchment. We believe that the framework presented in this chapter is one of the first steps towards the application of NMPC schemes to better management of freshwater in irrigation polders.

3

4

OPTIMAL SALINITY SENSOR PLACEMENT FOR POLDER NETWORKS

No man ever steps in the same river twice,
For it is not the same river and he is not the same man.

Heraclitus

We present a systematic approach for salinity sensor placement in a polder network, where the objective is to estimate the unmeasured salinity levels in the main polder channels. We formulate this problem as optimization of the estimated salinity levels using Root Mean Square Error (RMSE) as the "goodness of fit" measure. Starting from a hydrodynamic and salt transport model of the Lissertocht catchment (a low-lying polder in the Netherlands), we use principal component analysis (PCA) to produce a low-order PCA model of the salinity distribution in the catchment. This model captures most of the relevant salinity dynamics and is capable of reconstructing the spatial and temporal salinity variation of the catchment. Just using three principal components (explaining 93 % of the variance of the dataset) for the low-order PCA model, three optimally placed sensors with a greedy algorithm make the placement robust for modeling and measurement errors. The performance of the sensor placement for salinity reconstruction is evaluated against the detailed hydrodynamic and salt transport model and is shown to be close to the global optimum found by an exhaustive search with a RMSE of 82.2 mg/l.

4.1. Introduction

Optimal use of available freshwater resources is essential for sustainable agriculture. Understanding the system state correctly before decision making is crucial and depends on the quality of the collected data and thus on the quality of the monitoring network. Such understanding enables reconstruction of the current state of the system from available measurements. Therefore, the primary purpose of a salinity monitoring network for optimal and real time control of a polder is to provide real time information about the current salinity state of the system. This information combined with the polder system characteristics (hydrodynamical conditions, salinity thresholds for agriculture) can be used by real time control schemes to update the flushing water intake and/or pumping station settings to keep the salinity levels below predefined thresholds. The flushing of the polders is often done by a fixed flushing scheme and can result in an excess use of freshwater and unnecessary pumping costs [19]. A fixed flushing strategy does not rely on any measurements of salinity and cannot react to the spatial and temporal variability of salinity in the polder system. The excess use of freshwater and costs associated with polder flushing can be reduced by real time control strategies such as model predictive control (MPC) where [57] demonstrated that up to 45 % savings in freshwater usage can be achieved by a MPC scheme for flushing control considering the water quality and quantity. The controller needs to be coupled with a monitoring network (for salinity and water level measurements) to update the system states in real time for calculation of the optimum control action. Water level in a polder system is kept within a predefined narrow margin and does not vary too much throughout the polder and therefore can be monitored easily. On the other hand, the spatial and temporal variation of salinity can be high and depends on the season of the year, access to flushing water and distance from boils resulting in a requirement of an efficient salinity monitoring network. However, considering the economic feasibility, an optimal monitoring network is required for most comprehensive salinity state updates of the system using the minimum number of sensors.

Sensor placement problems in water systems have been addressed using different approaches such as statistical methods (model reduction with proper orthogonal decomposition (POD) or principal component analysis (PCA)), optimization methods (with single or multiple objective(s)) and information theory (entropy theory) applications. Some of the examples include: water quality monitoring [75–77], water level monitoring [78], stream flow monitoring [79, 80], fluid dynamic applications [81, 82] and predicting the dynamic variations of a groundwater system [83]. Comprehensive reviews can be found in [84–86] for different water systems. Entropy theory developed by [87] is used for water quality monitoring networks optimization in rivers [75, 88, 89], in a bay [90], in sewer systems [91, 92] and groundwater [93–95]. PCA is used in [76, 77] for river water quality monitoring network analysis. To the best knowledge of the authors, no attention has been given to salinity monitoring in polder systems.

In the literature, entropy theory is adopted for sensor placement by providing measures of the information content that can be delivered from a monitoring station or a network. Model reduction techniques are used to identify the key parameters or system dynamics from a statistical analysis of the dataset of the system considered. The results of the statistical analysis are interpreted to determine desirable sensor locations. Cre-

ating a salinity monitoring system with appropriate efficiency for a polder system can be achieved by evaluation of the major variables and system dynamics of the system through a multivariate statistical method such as PCA explaining most of the variance [77]. PCA reduces dimensionality of the dataset by transforming it to a new set of variables, principal components (PCs), ordered such that the first few components retain most of the variation in the original dataset [96] and are orthogonal to each other. In this present work, we posed the following question: can we represent the salinity dynamics of a catchment with a low-order PCA model, computed using simulation dataset over a specified time interval, to decide on optimum locations of sensors for salinity monitoring? Solving a sensor optimization problem requires analyzing extremely large dimensional search spaces that increases with the number of sensors, m, and possible sensor locations, n. Exhaustive search algorithms fail to succeed, while heuristic optimization methods like greedy algorithm (GA) can be used for optimizing sensor locations, in sewer systems [97, 98], in water distribution systems [99] and in discharge monitoring networks [79]. GA is being used in sensor optimization problems due to its simplicity and low algorithmic complexity. Although greedy heuristics generally do not guarantee optimality of solutions, in many applications some structure or hierarchy can be exploited to find good or near optimal solutions. In this work, we use the orthogonality property of principal components and their order with respect to variance or information content to look for each additional sensor location in a sequence; resulting in 'near optimal' solutions. In Section 4.3.4, considering the case of placing only three sensors and a SOBEK (available from: https://www.deltares.nl/nl/software/sobek-suite/) model with fewer calculation nodes where it is possible to do exhaustive search, we demonstrate that the sensor placement achieved by the greedy solution is 'near optimal' compared to the global optimum found by the exhaustive search.

In this chapter, we investigate optimum salinity sensor placement in a polder catchment combining PCA and a GA. Optimum in this study is defined as the locations that give the best reconstruction of salinity in the main channels of the catchment. The process of evaluation of model behaviour and performance is done through comparisons of estimated and observed values by a mathematical measure [100] such as Nash-Sutcliffe Efficiency (NSE), coefficient of determination (R^2), or Root Mean Square Error (RMSE). The differences, advantages and disadvantages between different efficiency measures are given in [100] and is not a focus of this study. In PCA, the low order model is approximated in a least square sense with a similar approach like RMSE. Therefore, we use RMSE of the estimated (reconstructed) salinity states as the "goodness of fit" measure for the optimization.

We conduct the statistical analysis on the Lissertocht catchment (Figure 4.1), a low lying polder in the Netherlands with salinization problem due to saline groundwater exfiltration. A salinity dataset produced by a detailed hydrodynamic and salt transport model of the area is used for PCA and the first dominant PCs of the PCA are used to reproduce essential salinity dynamics in the catchment by means of a low-order PCA model. This model is used for the optimization of the sensor locations.
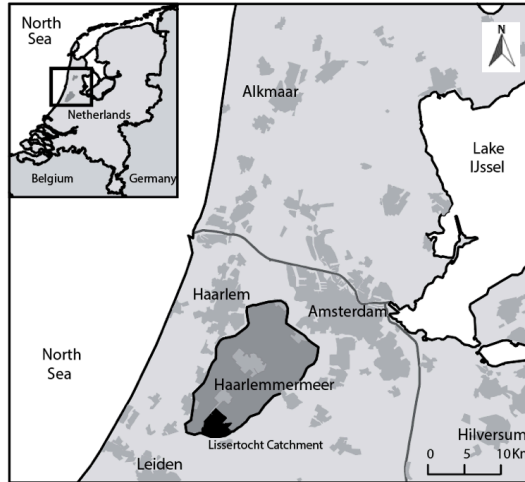
Figure 4.1: Location of the case study area (Lissertocht catchment) shown in Netherlands (Adopted from [19]).

4.2. Methodology

4.2.1. Case Study Area and Salinization Problem

The Lissertocht catchment, with a surface area of 10 km^2, is a part of the former lake Haarlemmermeer (Figure 4.1), reclaimed in 1852, and is located approximately 25 km southwest of the city of Amsterdam. Relief in the catchment ranges between 6 3.5 meter below sea level (BSL), salinity concentrations in the ditches vary between 136 and 5453 g/m^3 [23]. Mean annual precipitation and mean annual potential evapotranspiration amount to 840 mm and 590 mm respectively [23]. A system of tile drains and ditches is used to quickly drain the excess precipitation. Two pumping stations with capacities 1.48 m^3/s and 0.42 m^3/s maintain the water level relatively constant at 6.55 m BSL (October April) and 6.4 m BSL in summer (April October). The latter is an auxiliary pumping station, which is used only in extreme discharge events. Freshwater is diverted into the catchment through five inlets from April to October for maintaining surface water levels and improve water quality. The main land use in the study area is agriculture and the water quality and quantity requirement of the farmers varies depending on the crop cultivated.

The Lissertocht catchment is representative for deep polders in the Netherlands, where the main salinity input is deep saline groundwater exfiltration through boils (small vents directly connecting the groundwater system with surface water) [22]. Discharge of boils is low, but this is offset by their high salt concentration. Boil input (both discharge and concentration) is rather constant, as both groundwater head in the groundwater system and surface water level do not vary much. Spatial variation is large and boils are spread across ditches depending on the subsurface characteristics and surface elevation [101]. Groundwater flow directly into the ditches (diffusive seepage below the ditch itself) constitutes a second source of salts, but concentrations are lower than boils. This input is temporally more variable than boils, as it depends on the groundwater level in

the adjacent field. Spatial variation of the ditch exfiltration is low. Drainage through agricultural drains (exfiltration of shallow phreatic groundwater) is the most variable input, transporting the bulk of water (and salt) during discharge events. This water is more or less fresh. In general, one ditch receives drainage water from two adjacent parcels, while the next ditch receives no drainage. Freshwater is also let into the water system of the Lissertocht catchment, through five inlet culverts, with a total capacity of approximately 0.1 m^3/s (less than 10 % of total pumping capacity). Ditch layout in the study area consist of ditches bordering parcels (NW-SE); these are mostly closed on one side. Perpendicular to these so-called parcel-ditches, larger ditches collect water and transport it to the two earlier-mentioned pumping stations [19]. Electrical conductivity (EC) measurements (the electrical conductivity of the ditch water is correlated to the salinity of the same water) of the surface water in the catchment have shown clear preferential pathways of water, with inlet water being mostly confined to the direct route between inlet and pumping stations. Residence times are therefore also markedly different between ditches. Residence time in transport ditches (main channels) are in the order of days, while, in parcel ditches (drainage channels) residence time can reach up to weeks or even months.

4.2.2. MODELING SPATIAL AND TEMPORAL SALINITY DISTRIBUTIONS

The surface water salinity distribution in the case study area is modeled using a 1D hydrodynamic and a salt transport model of the area. A SOBEK model is used to calculate the salt concentrations, water levels and flows in the area with a 10 min simulation time. SOBEK model calculates the flow and water levels and followed by the salt transport calculations by SOBEK 1DWAQ. In addition to this model, the input of water and salt through tile drainage and ditch exfiltration is calculated by the Rapid Saline Groundwater Exfiltration Model (RSGEM) [58]. For the calibration of RSGEM, 100.000 simulations were performed using different parameters and a generalized likelihood uncertainty estimation was conducted to select the parameter set used in this study following [23]. The layout of the catchment network with all structures is based on the records of the responsible water authority of the area, The Rijnland District Water Control Board. Boil locations are placed in the model in accordance with the EC routing map created in May 2011 and confirmed by additional EC routing and distributed temperature sensing (DTS) measurements conducted during this study. The layout of the Lissertocht catchment, showing the inlet culverts, pumping stations and boil locations, is shown in Figure 4.2. The chloride concentration of different sources of water (inlet, precipitation, boil, drain and ditch exfiltration) are used as given in [23]. The salt transport model is calibrated using EC routing maps of the area produced in May 2011, EC measurements collected at 5 locations in the catchment over 2011 and 2012 and groundwater levels collected at 6 locations. The model is validated using the precipitation and evaporation data from the close by weather station located at Schipol airport, situated approximately 15 km northeast of the study area from 01/01/2011 until 01/01/2014 and used for calculation of the water flow and salinity in the catchment. A detailed description of the calibration of the model can be found in [102].
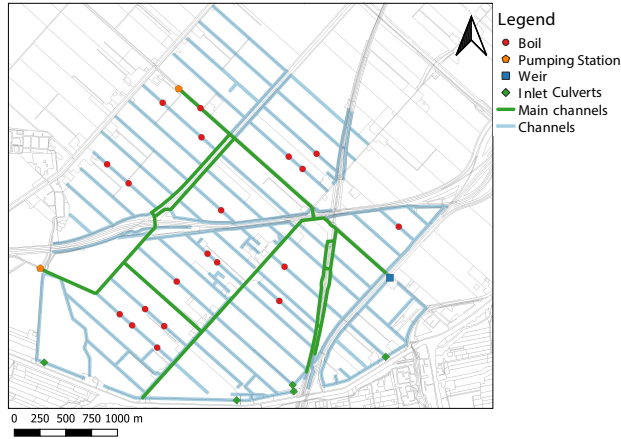
Figure 4.2: The layout of the Lissertocht catchment showing the structures, main channels and boil locations.

4.2.3. Principal Component Analysis for Estimating Salinity

Designing an optimal sensor placement requires analyzing a large-scale dynamical system of interest. Such a system is usually derived by the discretization of nonlinear partial differential equations resulting in high-dimensional discrete time models. However, the dynamics of the system can be approximated by a low-dimensional system by means of model reduction. PCA is used in this study to identify locations that capture characteristics of (annual) variations of salinity in the ditches of the catchment. Identifying the correlation between the ditches (reflecting a similar response to meteorological events, flushing water intake or proximity to boil locations) is essential for optimal estimation of the system dynamics, minimizing the number of necessary sensors by minimizing the measurement of similar, and hence redundant, system dynamics. Another important property of the PCA that is useful in sensor placement is the variance captured and represented by the PCs. Variance at a location is related to system dynamics, as it explains how much the salt concentration varies from the mean salt concentration in that location. A location with higher variance is more interesting to measure the salinity since more dynamics could potentially be captured.

We construct a low-order PCA model to reproduce the spatial salinity variation of the catchment by using the location dependent values and time dependent coefficients of the PCs. Considering the dynamical system of partial differential equations (i.e. Saint-Venant (SV) and Advection-Diffusion (AD) model, driven by boundary conditions), we restrict ourselves to states of the system describing salinity only. More information on dynamics of salt transport and control in open channels is given by Hot, see [60]. Let $x_s(t) \in \mathbb{R}^n$ represent the states of the dynamical system (average daily salinity) at time t, where n is the total number of nodes in the SOBEK model. The first step of PCA is to center the measurements such that all of the measurements have zero mean; we therefore consider the variables

$$x(t) = x_s(t) - \bar{x}$$

where $\bar{x} \in \mathbb{R}^n$ is the mean value of the salinity levels over time; i.e. the ith element of $\bar{x}$ represents the time mean of salinity at the ith location/node. Simulation of the system model for N discrete time steps results in a time-snapshots dataset $X \in \mathbb{R}^{n \times N}$ such that:

$$X := \begin{bmatrix} x(1) \, x(2) \, \ldots x(N) \end{bmatrix}$$

It can be shown that the data X can be decomposed into an orthonormal basis (also called principal components or empirical eigenfunctions) $\underline{\theta}_j \in \mathbb{R}^n$, $j = 1, 2, \ldots, n$ such that $x(t) = \sum_{j=1}^{n} \alpha_j(t) \underline{\theta}_j$, $t = 1, 2, \ldots, n$. That is [103, Sec. 2]:

$$X = \begin{bmatrix} x(1) \, x(2) \, \ldots x(N) \end{bmatrix} = \underbrace{[\underline{\theta}_1 \ldots \underline{\theta}_n]}_{\Theta_n} \underbrace{[\underline{\alpha}_1 \ldots \underline{\alpha}_N]}_{A_{n \times N}}, \quad \Theta'_n \Theta_n = I_n \tag{4.1}$$

where $\underline{\alpha}_t := [\alpha_1(t) \ldots \alpha_n(t)]' \in \mathbb{R}^n$ are the coefficient vectors for time index t and can be thought of as time dependent coefficients for reconstructing the time-snapshots via a linear combination of the time-invariant eigenvectors $\underline{\theta}_j$. Here I_n stands for the identity matrix of size n.

In PCA, we seek a low rank approximation of the basis Θ_n such that a low order model can approximate the dataset X in the least squares sense, i.e. we find

$$X \approx \hat{X} = \underbrace{[\underline{\theta}_1 \ldots \underline{\theta}_p]}_{\Theta_p \in \mathbb{R}^{n \times p}} \underbrace{\begin{bmatrix} \alpha_{1,1} & \ldots & \alpha_{1,N} \\ \vdots & \ddots & \vdots \\ \alpha_{p,1} & \ldots & \alpha_{p,N} \end{bmatrix}}_{A \in \mathbb{R}^{p \times N}}, \quad p << n \tag{4.2}$$

such that $\|X - \hat{X}\|_F$ is minimized [103], where $\|B\|_F = \sqrt{\sum_{i=1}^{} \sum_{j=1}^{} B_{ij}^2}$ and salinity at i^{th} location can be estimated by

$$x(t) \approx \sum_{j=1}^{p} \alpha_{j,t} * \underline{\theta}_j, \quad t = 1, 2, \ldots, N \tag{4.3}$$

In this standard PCA approach, we may desire to replace this least squares minimization of the reconstruction error by a weighted least squares where errors at some locations are penalised more than others. For the weighted PCA and dealing with the presence of measurement errors, please see [103].

Although the matrix factorization of X in (4.1) is not unique, one approach of generating and approximating it as in (4.2) is to employ the Singular Value Decomposition (SVD). Let the centered dataset X have the SVD given by $X = U\Sigma V^T$, where $U \in \mathbb{R}^{n \times r}$ and $V \in \mathbb{R}^{N \times r}$ have orthonormal columns, $\Sigma = \text{diag}(\sigma_1, \ldots, \sigma_r) \in \mathbb{R}^{r \times r}$, with $\sigma \geq \ldots \sigma_r > 0$, $r = \text{rank}(X)$ [103]. In our example, the number of snapshots is greater than the number of states considered (i.e. $N > n$) and therefore $r \leq n$. It can be shown that there is no better rank $p < r$ approximation for X in (4.2) than the truncation of the SVD; the first p columns of U are the eigenvectors (i.e. $\Theta_p := U(:, 1 : p)$ and the first p rows of $\Sigma V'$ span A.

Assuming that the singular values of in Σ decay rapidly, the principal components of the dataset θ_i, $i = 1, \ldots, p$, $p << r$, will capture all the significant features of the dataset and possibly the system dynamics. The number of PCs, p, is selected such that the the the total variance explained by the selected PCs exceed a user defined threshold (for example, we used 90 % in this study). Each PC is a column vector with n elements and the ith row of the PCs are linearly combined through the time dependent coefficients $\underline{\alpha}_t$ to reconstruct the salinity for the ith location. That is

$$x(t) \approx \hat{x}(t) = [\underline{\theta}_1 \ldots \underline{\theta}_p]\underline{\alpha}(t), \quad \underline{\alpha}(t) \in \mathbb{R}^p \tag{4.4}$$

4.2.4. Sensor Placement using a Greedy Algorithm

After constructing the low-order PCA model, we then aim to use this low-order model to reconstruct the spatial variation of salinity in the catchment using a limited number of measurements ($m \ll n$) available. The procedure of reconstructing the salinity state (reconstructed) vector, $\hat{x} \in \mathbb{R}^n$, in all discretization points of the catchment using m measurements taken at time step t is below.

If we assume the salinity measurements are $y(t) = Cx_s(t), C \in \mathbb{R}^{m \times n}$, then we have

$$y(t) \approx C\hat{x}_s(t), \tag{4.5}$$

$$y(t) \approx C[\underline{\theta}_1 \ldots \underline{\theta}_p]\underline{\alpha}(t) + C\bar{x} \tag{4.6}$$

Therefore, in the absence of measurement errors, we can estimate the states $\hat{x}_s(t)$ by first estimating the time-dependent coefficients $\underline{\alpha}(t)$. If the number of measurements is the same as the number of principal components in our PCA model, i.e. $m = p$, then we simply have $\underline{\alpha}(t) = (C[\underline{\theta}_1 \ldots \underline{\theta}_p])^{-1}(y(t) - C\bar{x})$. However, if the number of measurements is greater than the number of principal components in the model, we will have an over-determined least squares problem, where we estimate $\underline{\alpha}(t)$ by solving a linear least-squares optimization problem. Once the time-dependent coefficients, $\underline{\alpha}(t)$, for the current time step t are calculated, using the PCs, salinity at all locations can be reconstructed using (4.4).

We then use this estimation model to find the optimal set of sensors required to reconstruct salinity in the catchment. In this present study, we have formulated the objective of the sensor placement as finding the set of node indices $J \in \mathbb{N}^m$, $J \subset \{1, 2, \ldots, n\}$ for sensor locations so that the salinity state estimation (reconstruction) through (4.6) is optimal in the sense that it has the minimum Root Mean Square Error (RMSE) (Equation (4.7)) in the main channels (See Figure 4.2 for the main channels). We implemented this restriction (focusing on main channels instead of all channels) by considering the water availability in the channels for irrigation. The drainage channels are very shallow and are used for draining and then transferring mainly the excess rainwater to the main channels. On the other hand the main channels have deeper water levels and connection to the freshwater inlets of the catchment, which will allow the farmers to get water for irrigating their lands. Using the locations indexed in J, measurements , $y(t)$, will be collected and used to reconstruct the salinity at the main channels. The objective function

that is used to evaluate the performance of the selection is given by:

$$\min_{J} RMSE = \sqrt{\sum_{j=1} \frac{\sum_t (x_s(j,t) - \hat{x}_s(j,t))^2}{n}} \qquad (4.7)$$

where $x_s(j,t)$ is the observed or simulated salinity states at location j and time t, $\hat{x}_s(j,t)$ is the reconstructed/estimated salinity state and n is the total number of nodes that salinity is estimated. RMSE is always non-negative and smaller values indicate a better accuracy of the predictions.

In this study, we employed a greedy algorithm (GA) to evaluate the selection of m sensor locations. The algorithm is greedy in the sense that it sequentially places the sensors one by one. In the first step, a single sensor (location) that gives the maximum gain to the objective function is selected out of all the possible n locations. In the following step, having fixed the previous selection, the next sensor location is determined (from the remaining n-1 locations) that gives the largest improvement to the objective function [97]. This procedure continues until the last sensor location is determined. Algorithm 1 summarizes the pseudo code tailored for placing salinity sensors in the catchment with a greedy algorithm. Determining the (globally) optimal m locations requires finding solution to a computationally challenging combinatorial optimization problem, using an exhaustive search with m possible combinations of n possible sensor locations. As an example, placing $m = 3$ sensors for Lissertocht catchment (with $n = 755$ nodes) results in 2262 iterations with a GA (line 7 to 12 of Algorithm 1) while the exhaustive search requires 71.443.385 iterations, where each such calculation involves estimating the coefficients $\underline{\alpha}(t)$ from measurements $\underline{y}(t)$ for all $t = 1, \dots, N$, estimating the corresponding states using (4.4) and then computing the objective function (4.7) (line 11 of Algorithm 1). The combination with the best f is the global optimum for the exhaustive search. The difference in computation time and the efficiency of using a GA compared to exhaustive search is illustrated in section 4.3.4.

4.3. Results and Discussions
4.3.1. Reference Scenario
The reference scenario is generated by simulating the Lissertocht catchment using the SOBEK model of the area from 01/01/2011 to 01/01/2014. During the simulation, a fixed flushing strategy is applied (freshwater is introduced to the system from the intakes at their maximum capacity starting from 1st April until 1st October) and the pump is operated according to the water level measurement near the pumping station following assigned water level thresholds. Figure 4.3 illustrates the spatial variation of salinity in the Lissertocht catchment for a snapshot taken from the reference scenario in a dry period using the SOBEK model.

The reference scenario is used to identify system behaviour and the effect of flushing on the system (the pathway of flushing water and the ditches that have no or limited access to the flushing water) using the layout given in Figure 4.2. Interpretation of the results revealed that the salinity in the catchment increases during the summer period


Algorithm 1: Pseudo Code of Sensor Placement

Input: Salinity dataset, $X \in \mathbb{R}^{n \times N}$, of n nodes for N discrete time steps.
Output: Set of sensor locations (J) optimizing the objective in Equation (4.7)

Initialization
1 Divide data matrix X into two sets of time periods, X_{train} and $X_{test} \in \mathbb{R}^{n \times N/2}$.
   Low-order PCA Model from X_{train}
2 Run PCA on X_{train} and record the first p PCs ($\underline{\theta}_1 \ldots \underline{\theta}_p$) for the low-order PCA
   model (4.4)
   Sensor Placement with Greedy Algorithm
3 $J = \emptyset$;   // m sensor locations to be determined
4 **for** $i = 1$ to m **do**
5 | $Performance = [] \in \mathbb{R}^n$
6 | **for** $j \in \{1 : n\} \setminus J$ **do**   // index set of all nodes minus J considered
7 | | $\tilde{J} = J + j$
8 | | Take measurement(s) $y(t)$ from location(s) $\tilde{J}$ of data X_{test}
9 | | Calculate time dependent coefficient(s), $\underline{\alpha}(t)$, $\forall t$ as in Equation (4.6)
10 | | Estimate salinity states, $\hat{x}_s$, at all n locations using (4.4)
11 | | Compute objective f and record $Performance(j) = f$
12 | **return** loc ;   // $loc \leftarrow j$ such that $Performance(j)$ is the best
13 | $J \rightarrow J \cup loc$;   // i^{th} sensor is placed
14 **return** J ;   // All of the m sensors are placed
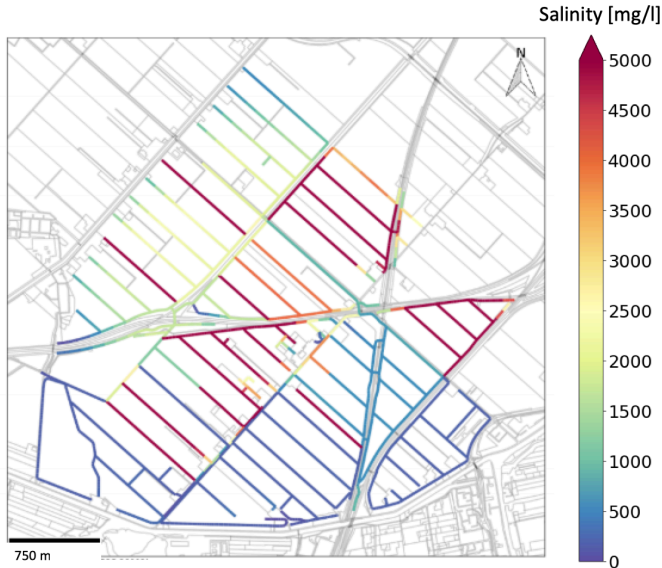
Figure 4.3: The spatial variation of salinity in the Lissertocht catchment for a snapshot (daily average of 15/07/2012) taken from the reference scenario; modeled with the SOBEK model.
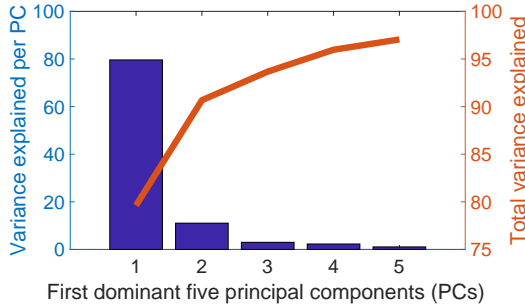
Figure 4.4: Variance explained by the first five PCs. The solid line represents the total variance explained
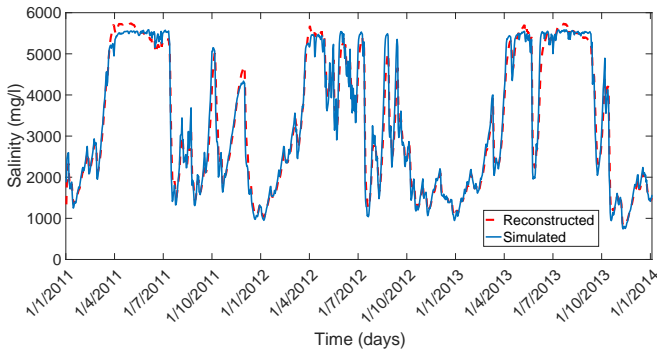

Figure 4.5: Comparison of the reconstructed salinity using 3 PCs and the simulated salinity at node 172.

despite the flushing. The main reason for this is the lack of drained precipitation that flushes the whole system naturally. Especially the small stagnant drainage ditches with boils get no or very limited amount of fresh flushing water and thus the salinity in those ditches can increase up to 5500 mg/l during summer. The high saline water from these stagnant ditches eventually flows to the pumping station, resulting in increased salinity concentration also in the main ditches.

4.3.2. PRINCIPAL COMPONENT ANALYSIS

The SOBEK model consists of $n = 755$ nodes where the average daily salinity is calculated for the whole simulation period ($N = 1097$ days). This simulation results in a salinity dataset of dimension 755 by 1097. As in equation (4.1), this multidimensional data set can be decomposed into 755 PCs. The percentage of variance explained by the first five PCs is shown in Figure 4.4. The first three PCs of this dataset explains more than 93 percent of the variance in the data (Figure 4.4). Figure 4.5 also illustrates the quality of the reconstructed salinity level over time at node 172; this is an example of reconstruction using 3 PCs via equation (4.4).

Interpretation of the coefficients and the principal components (shown in Figure 4.6 and 4.7, respectively,) and the simulations are used to identify the hydrological be-
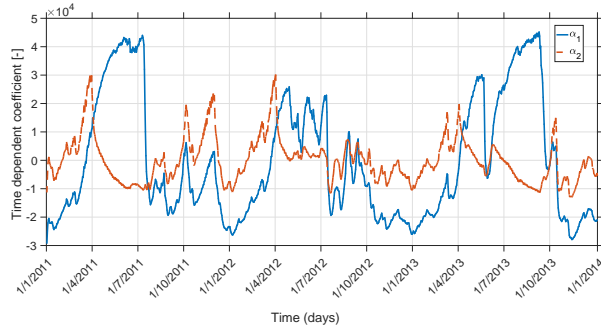
Figure 4.6: Time dependent coefficients , $\underline{\alpha}(t)$, of the first two PCs.
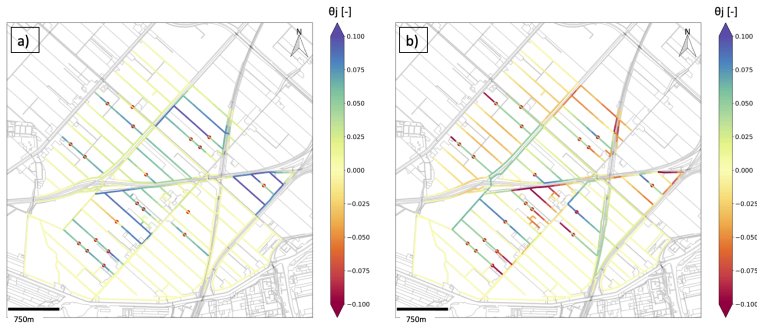

Figure 4.7: Principal component values, $\underline{\theta}_j$, corresponding to each location for a)first b)second principal components. The boil locations are also shown with red dots in the ditches.

haviour of the catchment. As can be seen in Figure 4.6, the time dependent coefficient signal of the first component starts to increase in winter (wet period) and reaches to its peak during the summer (dry period) of each year. This behaviour is in accordance with the drainage channels with high salinity problem (due a boil or a nearby boil in the channel). This can also be seen in Figure 4.7-a showing the PC location dependent values of the first PC is high in drainage channels with a boil. These channels are naturally flushed when it rains (mostly in wet period) and the salinity increases during summer period. The time dependent coefficient signal of the second PC decreases immediately after 1st of April just after the flushing of the catchment begins (Figure 4.6). Moreover, as can be seen in Figure 4.7-b the PC location dependent values of the second PC are high in channels that are sensitive to flushing (main channels connecting the freshwater intakes to the rest of the catchment and drainage channels with access to flushing water). This shows that PCA can be helpful in understanding system behaviour, as was also shown by [76, 77] in other applications.

Table 4.1: Effective sensor placements for 3 sensors by minimizing RMSE.

Node Number(s)	RMSE [mg/l]
543	140.02
543 - 131	84.31
543 - 131 - 731	82.18

4.3.3. OPTIMUM SENSOR PLACEMENT BASED ON THE LOW-ORDER PCA MODEL

The low-order PCA model described in equation (4.4) is based on the first three PCs of the original salinity dataset ordered according to the variance each PC explains (i.e. see the SVD in Section 4.2.3 with ordered eigenvalues forming the variance of each PC). We selected the first three PCs for the low-order PCA model since the variance explained by the first three PCs exceeds the threshold of 90 % that we defined for this study. This property of the low-order PCA model is important in sensor placement selection using a GA. The first 3 PCs, capturing 93 % of the variance, are used for the low-order PCA model. Selection of a new sensor locations in the GA can be conducted such that the variance covered is increased while the covariance between the selected locations are decreased by GA to place 3 sensors. To test the performance of sensor placements, we splitted the salinity dataset into two sets on time. PCA of the first part of the dataset is used to select the most dominant PCs and their corresponding location dependent coefficients. The second part is used to test different sensor placement layouts. Table 4.1 show the performance of the placement considering the objective function given in equation (4.7) with a GA.

The overall performance of the placements increases with the number of sensors placed (Table 4.1). To illustrate the performance of the sensor placement for salinity reconstruction of three different nodes on the main channels (blue squares in Figure 4.8), Figures 4.9 - 4.11 are provided. The estimation of the placement at location 51 has small mismatches compared to the simulated values with errors less than 30 mg/l. This location is close to the inlets of the catchment where the water is fresh and the salinity variance is low compared to the rest of the catchment. Therefore, the principal component values of the first two PCs is low at this location (Figure 4.7). The estimation of salinity is better at locations that are identified by the PCs used for the low-order PCA model like locations 170 and 445. For locations 170 (Figure 4.10) and 445 (Figure 4.11) estimations of sensor placement is very close to the simulated values. The salinity dynamics are represented accurately capturing the peaks as well as the lower salinity values observed at that location during the simulation period. Optimum sensor locations are selected such that the objective function given in (4.7) is satisfied over the main channels. However, if there exists a specific location of interest, the objective function can be modified for maximizing the salinity estimation performance at that location instead of evaluating the objective over the main channels.
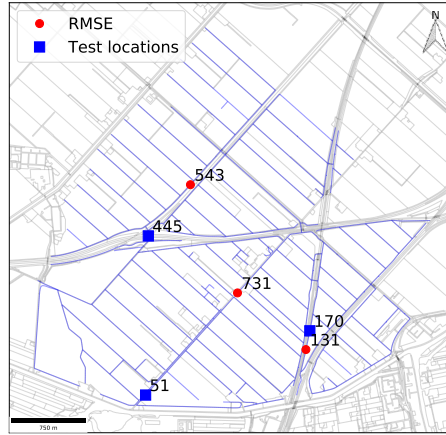
Figure 4.8: Optimum sensor locations obtained by minimization of RMSE (indicated by red circles) and three test locations (blue squares) for showing the performance of the placement.
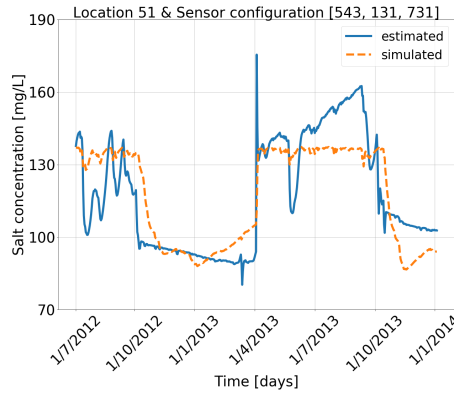

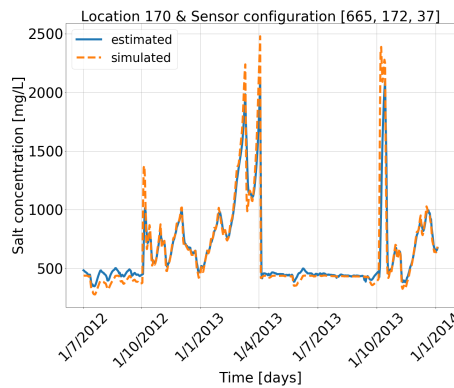Figure 4.9: Performance of the sensor placement at node 51.

Figure 4.10: Performance of the sensor placement at node 170.
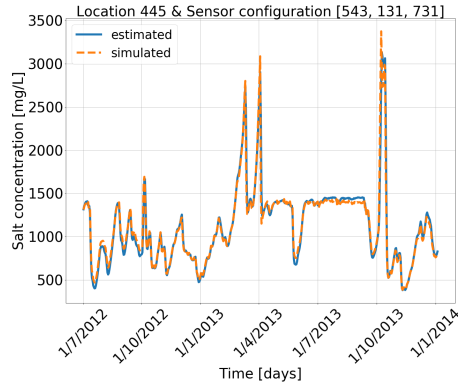
Figure 4.11: Performance of the sensor placement at node 445.
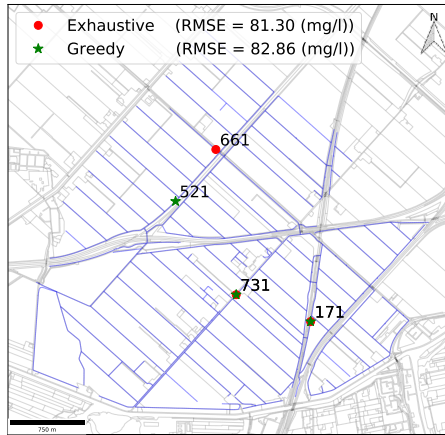
Figure 4.12: Comparison of optimization results using an exhaustive search and greedy algorithm.

4.3.4. OPTIMALITY OF PLACEMENTS USING GREEDY ALGORITHM

To illustrate the solution obtained by the greedy algorithm is near optimal, we repeated the optimization using an exhaustive search by simplifying the search space used in the optimization. Every consecutive 5th node in the catchment is represented by 1 node and the search space is decreased to n=151 nodes. With this reduction in the search space, the total number of possible combinations to place 3 sensors decreased from 71.443.385 (3 combination of 755) to 562.475 (3 combination of 151). All combinations of the reduced search space were evaluated and the best was selected with the exhaustive search. For a fair comparison, we repeated the optimization using GA for the reduced space too and evaluated the performance of the selection in the full system. The locations obtained and the corresponding performances (See legend of Figure 4.12) by using the exhaustive search and GA are shown in Figure 4.12.

As expected, better performing locations are obtained by using an exhaustive search than the greedy algorithm. However, the difference in the objective values of the loca-

tions are very close. As can be seen in Figure 4.12 same locations are selected for the two sensors (nodes 731 and 171) and only the last sensor locations are different for GA versus the exhaustive search. The slight improvement in the objective for exhaustive search is achieved in exchange for a big difference in computation time. Finding the optimum lasted more than three days for the exhaustive search while it took only a few minutes for the GA. All the computations performed within Python Spyder 3.3.2 for macOS High Sierra (v 10.13.6) installed on a 2.9 GHz Intel Core i5. In a larger network with larger search space and many more sensors to be placed, the application of an exhaustive search is not feasible due to the combinatorial computational burden, while a near optimal solution can easily be achieved within a limited time using our greedy heuristic.

4.3.5. A POSTERIORI ASSESSMENT OF ROBUSTNESS OF SENSOR PLACEMENT TO MEASUREMENT AND MODELING ERRORS

The SOBEK model used in this study is calibrated for the reference scenario. This model is used to create the salinity dataset of the reference scenario, which is then used for the sensor placement given in Section 4.3.3 without any consideration of uncertainties related to measurements or model errors. Therefore, to investigate the effect of possible measurement and model errors on the performance of the sensor placements, a robustness analysis is conducted in this section. Firstly, for the assessment of robustness to measurement errors, we added a random Gaussian error to the measurements used in equation (4.6) with a zero mean and a standard deviation of 10. The estimated coefficients, $\underline{\alpha}(t)$, are computed using measurements with errors. We created a total of 100 measurement datasets and calculated the performance sensor placement using measurements from these datasets with errors. A decline in the performance is observed since the original placement was obtained assuming full system knowledge and without any uncertainties. RMSE increased from 82.18 mg/l to 111.86 mg/l with a standard deviation of 1.92 mg/l. In reality, it is possible that the measurement errors can be identified and filtered out, which will reduce the performance reduction demonstrated here.

Secondly, the effect of possible modeling errors related to boil flux, flushing discharge and boil locations are investigated using a total of five scenarios. We started with simulating the SOBEK model by changing boil flux (halving or doubling of the reference scenario), flushing discharge (halving or doubling of the reference scenario) and boil locations (change locations of 4 boils). The results of these scenarios are used to create new salinity datasets for the robustness analysis with different dynamics than the reference scenario. Later, the performance of the optimum sensor placement was tested for reconstructing the salinity for these scenarios. Changing boil flux affects the total salt load entering the catchment directly. A higher and a lower mean salinity in the catchment is observed due to increased and decreased boil flux, respectively. Similarly, mean salinity in the catchment decreased in case of doubling the flushing while it increased due to half flushing. These changes affected the variance and the salinity dynamics in the catchment and resulted in changes in the performance of placements. The performance with respect to the scenarios representing possible model mismatches including the reference scenario and the mean performance of the measurement error analysis are given in Figure 4.13.

For all the scenarios, sensor placement performs well with small fluctuations in RMSE.
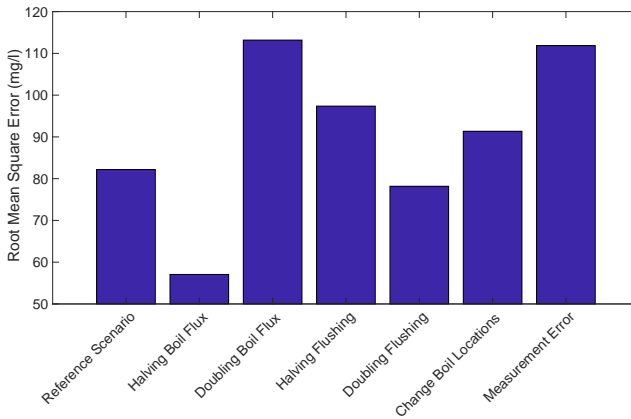
Figure 4.13: Robustness of placement (543-131-731) to model errors using RMSE as the performance index

The mean of the RMSE for all the scenarios is 87.57 mg/l with a standard deviation of 17.34 mg/l, indicating that the placement is robust to measurement errors and some model uncertainties. An expected performance drop for the scenarios with changing boil locations and measurement error is observed compared to the reference scenario because of the change of variance (due to changed boil locations) and uncertainty added to the measurements. This is in accordance with the results of PCA. The first PC (with the biggest variance) is attributed to the drainage channels with high salinity problems due to a boil. Depending on the presence of a boil in or a nearby drainage channel, the salinity dynamics in that channel varies considerably, which effects the variance of salinity at that location. Physically, a sensor placed upstream of a boil will not capture the high salt load and will miss variance information for capturing the dynamics caused by the boil. Low-order PCA model relies on maximizing the variance captured (dynamics), therefore, lower performances are observed for scenarios changing the distribution of variance over the catchment in comparison to the reference scenario. Higher and lower RMSE values calculated for the rest of the scenarios are related to the mean salinity in the catchment. Changing the boil flux affects the total salt load entering the catchment resulting in a higher RMSE in case of doubling boil flux and a lower RMSE in case of halving the boil flux. Similar effects are observed due to the changes in flushing, resulting in a lower RMSE due to increased freshwater intake (doubling flushing) and a higher RMSE due to decreased freshwater intake (halving flushing).

4.4. CONCLUSION AND OUTLOOK

In this chapter, we investigated an optimal placement of salinity sensors to represent the salinity in the main channels of a typical low-lying polder in the Netherlands. Using the salinity dataset obtained by a hydrodynamic and a salt transport model of the Lissertocht catchment, a principal component analysis was performed. PCA results showed that more than 93% of the variance of the dataset can be represented with a system of

three principal components and can be used to describe the essential salinity dynamics in the catchment by means of a low-order PCA model. The accuracy of the low-order PCA model increases with the number of PCs used, and this number depends on the user defined threshold for the variance explained by the selected PCs (90 % in this study). Using the low-order PCA model, optimum sensor placement of three sensors is achieved using RMSE of the estimated salinity levels as the "goodness of fit" measure. The performance of the sensor placement for salinity reconstruction is evaluated against the detailed hydrodynamic and salt transport model and is shown to yield good results with a RMSE of 82.2 mg/l.

A posteriori assessment showed that the sensor placement is robust to measurement and model errors. Increased uncertainty due to modelling and measurement errors resulted in small deviations of the performance of the placement. The placement succeeded in reconstructing the salinity of the main channels for different scenarios and are robust. Capturing the variance and related dynamics in the catchment is very important for the placements done using the low-order PCA model. Therefore, most significant performance drop of the placement is observed in case of changing boil locations. Wrong estimation of boil locations results in lack of important variance information, which is crucial for capturing the dynamics caused by the boils resulting in worse salinity estimation performance for the sensor placement. This is an important outcome illustrating the importance of the hydrodynamic and salt transport model used for simulations and creating salinity datasets and of correctly locating boil sites. A good model is a must for the methodology described in this study. Extra caution and efficient ways of detecting boils is necessary for future applications.

The optimum sensor placement formulated in this study will be used in combination of a model predictive control (MPC) scheme in a follow-up research and applied to the Lissertocht catchment. Salinity and water transport dynamics will be formulated with a similar strategy developed in [57]. A state estimator (for example a Kalman Filter) in accordance with the dynamical system should be implemented for better reconstruction of the salinity state of the catchment that will be used by the MPC scheme.

5

CONCLUSION AND OUTLOOK

You cannot make everyone happy,
You are not a pizza!

...

5.1. CONCLUSIONS ON MODEL PREDICTIVE CONTROL OF POLDER FLUSHING

SURFACE water flushing is a significant part of total freshwater demand (about 15 % in the Netherlands). If the flushing is done only when it is necessary, the amount of freshwater required could significantly decrease, and this could then create a buffer of freshwater supply especially in drought periods. To achieve a better management practice for low-lying irrigation polder networks, salinity and water level control is studied in this thesis by explicitly considering freshwater conservation using Model Predictive Control (MPC). MPC is considered here because of its proven capability of handling constraints and time delays in the system and of using predictions of states and disturbances, which all leads to a better operation of complex water systems. Research questions outlined in Section 1.6 have been answered. Here, a summary of the conclusions related to the application of MPC for polder flushing are given.

In Chapter 2, a linear MPC scheme is developed using the linearized and discretized De Saint Venant and Advection Dispersion equations for controlling the salinity and water level in a test canal. This chapter presents the first successful application of physically-based internal model for integrated water quality and quantity control in real time, thanks to the increased computational power of personal computers and efficient linear program solvers. In addition to the application of physically-based internal model, the MPC formulation presented in Chapter 2 introduces a simple but innovative solution for the third objective of polder flushing, being the minimization of freshwater usage. Using a combination of soft constraints for freshwater usage and salinity concentration, up to 46 % freshwater usage savings is achieved with MPC compared to the fixed flushing, which is current common practice.

In Chapter 3, a nonlinear Model Predictive Control (NMPC) formulation is developed and implemented to control polder flushing in the Lissertocht catchment Haarlemmermeer Polder, Province of North-Holland, The Netherlands) as a case study. A network model for salinity and water transport coupled with a saline groundwater exfiltration model is developed, also considering the mixing at the connection nodes. The network model is used to optimize multiple objectives on water level, salinity and freshwater control using NMPC. The resulting nonlinear programming (NLP) problem is solved with a receding horizon implementation. Despite the savings in freshwater usage compared to the fixed flushing, the performance for the case study was found to be insufficient for salinity control (salinity above the salinity threshold due to the insufficient flushing capacity). Using the results of NMPC and analyzing the polder network, a design update for two out of five intake capacities would significantly improve the salinity control performance. Without violating the constraints of the system, water level and salinity would after the design update be controlled with around 20 % saving in freshwater usage.

5.1.1. LINEAR VS NONLINEAR MODEL PREDICTIVE CONTROL

In this thesis, we used both linear and nonlinear MPC formulations. In Chapter 2, a single canal is controlled using a linear state space model while in Chapter 3 a NMPC formulation is preferred. Linear models are more efficient in terms of computational complexity and can be solved efficiently. To control salinity and water level in single

canals or canals connected in series, the MPC formulation described in Chapter 2 can be used and global optimum for the linearized system can be found satisfying the constraints.

In operation of a polder network, different salinity thresholds can be considered according to the farmer needs resulting in time-varying set points. Moreover, spatial and temporal variation of saline groundwater disturbances and different cross sections and flow depths of the canals in the polder network make local linearization around a fixed operation point (as applied in Chapter 2) inaccurate in terms of future system behavior predictions. Therefore, in Chapter 3, NMPC strategy is selected to control a real polder network, the Lissertocht catchment. Constraints on inputs, outputs and states are implemented in the optimization problem and the resulting NLP is solved on-line at each control time step. Compared to the linear MPC, NMPC requires more computational power and time. Finding a global optimal solution to the nonlinear control problem is not guaranteed in NMPC. However, as demonstrated in Chapter 3, by applying the control actions (that can be local optimum for the optimal control problem solved) satisfactory performance for salinity and water level control of the Lissertocht catchment is achieved within the constraints of the system.

Selection of linear or nonlinear MPC depends on the problem considered, computational resources and the required accuracy. If the system controlled can be represented by a linear model with the required accuracy, linear MPC can be selected to gain efficiency in computation time.

5.1.2. CHOOSING WEIGHTS IN THE OBJECTIVE FUNCTION

Weights used in the objective function of the MPC determines the behavior of the controller. Physical dimensions or the requirements of the controlled water system can be used for tuning the controller using the Maximum Allowed Value Estimate (MAVE) [28]. Starting from an initial estimate of a weight that normalize all the states and inputs, users can tune the weights that results to a satisfactory performance (user defined). For the simple test canal, all objectives of polder operation as defined in this thesis are satisfied. Water level and salinity concentration were kept close to their predefined threshold while the flushing was done only when it is necessary resulting in great savings in freshwater usage.

For the real case of polder network control, a selection for set of weights is made that ensures a satisfactory performance for dry periods. The performance of the controller with these weights in a wet period (excessive rainfall resulting in natural flushing) seemed unsatisfactory in terms of freshwater savings. When the salinity concentration in the polder was below the threshold due to the natural flushing, it was expected that the controller should decrease the flushing amount as in the case of simple test canal to save freshwater. To overcome this problem, a penalty increase on flushing discharge is implemented. However, doing so resulted in decreased flushing not only when the salinity was below but also when it is above the threshold. Therefore, a choice is made that works better for the dry period, which is more critical in terms of salinity control.

5.2. CONCLUSIONS ON SENSOR PLACEMENT

The quality and availability of measurements are crucial for the application of MPC. Every control time step, the optimization has to be updated with the most recent measurements of the states (water level and salinity). Measuring water level in a polder is not a challenging task since the water level is kept within a predefined narrow margin and the water level does not vary throughout the polder. On the other hand, spatial and temporal variation of salinity in a polder network, depending on the season, access to freshwater and distance to the salinity sources, makes salinity measurements a challenging process. In Chapter 4, considering the economic feasibility, we investigated an optimal placement of salinity sensors for the Lissertoch catchment. We showed that, a low-order Principal Component Analysis (PCA) model can be used to represent the salinity dynamics of the Lissertocht catchment. The low-order PCA model is used to find optimal locations of salinity sensors in this catchment. Salinity concentration measurements from the optimal locations are used to represent salinity concentrations (not measured) at all main channels. We developed a Greedy Algorithm (GA) to place the salinity sensors using Root Mean Square Error (RMSE) as the goodness of fit measure. To compare the results obtained by GA, we repeated the search with an exhaustive search, which finds the global optimum by trying all of the possible combinations for placing the sensors. We showed the placement using GA performs equally well compared to the exhaustive search in exchange for a big difference in computational time (three days versus minutes). This comparison was only possible for placing three sensors for a decreased search space (possible alternatives to place sensors were decreased by five). In a larger network or for placing more sensors, using exhaustive search would be computationally practically impossible.

A posterior assessment revealed the importance of detecting boil locations for the robustness of the sensor placement. The most significant performance drop of the placement is observed in case of boil locations. This shows the importance of the accuracy of the collected (boil) data and models representing the saline groundwater exfiltration, which directly affects the salinity sensor placement performance.

5.3. WHERE TO START AND WHAT TO DO IN A NEW AREA?

This thesis focuses on control of the surface water system of a polder network with saline groundwater exfiltration. The control algorithms developed in this thesis are not case specific and can be applied elsewhere in other low-lying delta areas. On the other hand, the disturbance of the controlled system, saline groundwater exfiltration, is case specific and is related to the groundwater characteristics of the area. To understand the groundwater and salinity exfiltration characteristics of a new area of interest, following steps should be completed (in brief) before applying the control and sensor placement methodologies developed in this thesis:

- point salinity measurements to keep track of seasonal variability,

- sampling the quality and quantity of surface water for analyzing the different sources of salinity to identify the variation of salinity in the area and especially salty boils, for instance using

- Electrical Conductivity (EC) measurements

- Distributed Temperature Sensing (DTS) measurements (the difference between the temperature of surface water and the salty boils can be used to identify the locations of the boils [101])

- Electro-Magnetic (EM) measurements

- Taking samples of the surface water at certain locations

- hydrodynamics and salt transport of the surface water system, using a calibrated model,

- determination of land use, required salinity thresholds according to the farmer needs, and finally, points of special interest such as environmental quality requirements, irrigation intake points for controlling salinity.

Current developments in monitoring and measuring groundwater salinity distributions using tools like airborne electromagnetic (AEM) surveys [104] will increase the speed and accuracy of detecting spatial variation of salinity in a new area and thus will increase the applicability of the methodologies developed in this thesis.

5.4. RECOMMENDATIONS FOR FURTHER RESEARCH

5.4.1. UNCERTAINTY IN MODELING AND PREDICTIONS

In Chapters 2 and 3, the controlled system is represented by a simulation model, which made it possible to extract all the salinity and water level measurements at all discretization points. For the application of MPC, a deterministic approach is used, while perfect knowledge of the predictions and measurements about the controlled system is assumed. On the other hand, this is not the case in reality and uncertainties related to measurements, predictions and/or modeling errors has to be considered for the real-life applications of the developed control schemes.

Although this was not the focus of this thesis, for the application of MPC to a real system, further research is needed related to the possible sources and effects of uncertainty. Uncertainties related to the predictions, model mismatches and unknown disturbances (wrong estimation of exfiltration fluxes and concentrations, errors in actual structure flows) can be handled by using tools like tree based MPC [46, 105] or offset-free MPC [38] applied to polder flushing.

5.4.2. OBJECTIVE FUNCTION OF MPC

In this thesis, a quadratic cost function is used as the objective function of the MPC schemes developed to keep the states at their predefined steady-state. Controller penalizes the deviation of the error of the states from their corresponding steady-state values (trajectory tracking). The optimal steady state or trajectory (water level set point or salinity concentration threshold) is provided by some previous experience or another management system and does not include the real economy of the controlled process. For an increasing number of applications, this hierarchical separation of first setting a trajectory and then trying to track that is not optimal or desirable [106]. Recently, Economic MPC (EMPC) formulations for different industrial applications are proposed that

combines the economy of the process and the performance together with an economic objective function [106, 107]. EMPC operates the system in a possible time-varying fashion by not forcing the process to operate at a predefined steady-state (without tracking a set point) but by directly optimizing the economic performance of the process [107].

In polders, tracking the water level set point is necessary for safety reasons discussed earlier in this thesis. On the other hand, trying to keep salinity concentrations at a level according to the traditional behavior of farmers that want to continue cultivating the same salt intolerant crops may not be economically feasible. EMPC can include the real economy of flushing by directly considering all of the costs of all processes (flushing, energy used, damage to crops, revenue of the cultivated crops) involved in polder management. EMPC of polder flushing is worth attempting to achieve an economical and sustainable management of irrigation polder networks.

A

APPENDIX

Saint Venant and Advection Dispersion equations are discretized using a staggered grid scheme. A discretization matrix (see Eqn. (2.5)) for n discretization points is obtained with the terms given as:

For i=1

$$sv_{i,i} = 1 + \frac{\Delta t}{A_{s,i}^n} A_i^k f u_{i+1/2} , \quad sv_{i,i+1} = -\frac{\Delta t}{A_{s,i}^k} A_i^k f u_{i+1/2}, \quad sv_f = -\frac{\Delta t}{A_{s,i}^n},$$

$$d_i = -\frac{\Delta t}{A_{s,i}^k} A_i^k r u_{i+1/2} + \frac{\Delta t Q_{l,i}^k}{A_{s,i}^k},$$

$$ad_{i,i} = 1 + \frac{\Delta t}{V_i^k}(\frac{1}{\Delta x}(K_{i+1/2}^{k+1} A_{i+1/2}^{k+1} + K_{in}^{k+1} A_i^{k+1}) + Q_{i+1/2}^{k+1}), \quad ad_{i,i+1} = -\frac{\Delta t}{V_i^n \cdot \Delta x} K_{i+1/2}^{k+1} A_{i+1/2}^{k+1}$$

$$ad_f = \frac{\Delta t}{V_i^k}(C_i^k - C_{in}^{k+1}), \quad ad_{i,i}^k = 1 + \frac{\Delta t(Q_{i+1/2}^{k+1})}{V_i^k},$$

$$d_{i+n} = \frac{\Delta t}{V_i^n}(\frac{1}{\Delta x} K_{in}^{k+1} A_i^{k+1})(C_{in}^{k+1} - c_{\text{ref}}) + \frac{Q_{l,i}^k \Delta t(C_{l,i}^n - C_i^n)}{V_i^n}$$

For i=2:n-1

$$sv_{i,i} = 1 + \frac{\Delta t}{A_{s,i}^k} A_{i-1}^k f u_{i-1/2} + \frac{\Delta t}{A_{s,i}^k} A_i^k f u_{i+1/2}, \quad sv_{i,i-1} = -\frac{\Delta t}{A_{s,i}^k} A_{i-1}^k f u_{i-1/2},$$

$$sv_{i,i+1} = -\frac{\Delta t}{A_{s,i}^k} A_i^k f u_{i+1/2}, \quad d_i = \frac{\Delta t}{A_{s,i}^k} A_{i-1}^k(r u_{i-1/2}) - \frac{\Delta t}{A_{s,i}^k} A_i^k(r u_{i+1/2}) + \frac{\Delta t Q_{l,i}^k}{A_{s,i}^k},$$

$$ad_{i,i} = 1 + \frac{\Delta t}{V_i^k}(\frac{1}{\Delta x}(K_{i+1/2}^{k+1} A_{i+1/2}^{k+1} + K_{i-1/2}^{k+1} A_{i-1/2}^{k+1}) + Q_{i+1/2}^{k+1}),$$

$$ad_{i,i-1} = -\frac{\Delta t}{V_i^k}(\frac{1}{\Delta x} K_{i+1/2}^{k+1} A_{i-1/2}^{k+1} + Q_{i-1/2}^{k+1})$$

$$ad_{i,i+1} = -\frac{\Delta t}{V_i^k} \frac{1}{\Delta x} K_{i+1/2}^{k+1} A_{i+1/2}^{k+1}, ad_{i,i}^k = 1 + \frac{\Delta t((Q_{i+1/2}^{k+1}) - (Q_{i-1/2}^{k+1}))}{V_i^k}, d_{i+n} = \frac{Q_{l,i}^k \Delta t(C_{l,i}^k - C_i^k)}{V_i^k}$$

For i=n

$$sv_{i,i} = 1 + \frac{\Delta t}{A_{s,i}^k} A_{i-1}^k f u_{i-1/2}, sv_{i,i-1} = -\frac{\Delta t}{A_{s,i}^k} A_{i-1}^k f u_{i-1/2}, sv_o = \frac{\Delta t}{A_{s,i}^k},$$

$$d_i = \frac{\Delta t}{A_{s,i}^k} \theta A_{i-1}^k(r u_{i-1/2}) + \frac{\Delta t Q_{l,i}^k}{A_{s,i}^k}, \quad ad_{i,i} = 1 + \frac{\Delta t}{V_i^k}(\frac{1}{\Delta x}(K_{i-1/2}^{k+1} A_{i-1/2}^{k+1}),$$

$$ad_{i,i-1} = -\frac{\Delta t}{V_i^k}(\frac{1}{\Delta x} K_{i-1/2}^{k+1} A_{i-1/2}^{k+1} + Q_{i-1/2}^{k+1}), ad_o = \frac{\Delta t}{V_i^k}(C_i^{k+1} - C_i^k), ad_{i,i}^k = 1 - \frac{C_i^k \Delta t(Q_{i-1/2}^{k+1})}{V_i^n},$$

$$d_{i+n} = \frac{Q_{l,i}^k \Delta t(C_{l,i} - C_i^k)}{V_i^n}$$

Where

$$fu_{i+1/2}^k = \frac{g\Delta t}{\Delta x \left(1 + g\frac{v_{i+1/2}^k}{Cz^2 R}\right)}$$

$$ru_{i+1/2}^k = \frac{\frac{1}{A_{i+1/2}^k}\left(\frac{\bar{Q}_{i+1}^k v_{i+1/2}^k - \bar{Q}_i^k v_{i-1/2}^k}{\Delta x} + v_{i+1/2}^k \frac{\bar{Q}_{i+1}^k - \bar{Q}_i^k}{\Delta x}\right) + v_{i+1/2}^k}{\left(1 + g\frac{v_{i+1/2}^k}{Cz^2 R}\right)}$$

$$\bar{Q}_i^k = (Q_{i+1/2}^k - Q_{i+1/2}^k)/2$$

$$\bar{A}_{i+1/2}^k = (A_{i+1/2}^k - A_{i+1/2}^k)/2$$

K_{in} and C_{in} are the dispersion coefficient and the concentration of the incoming water

REFERENCES

[1] J. A. Leggett and N. T. Carter, *Rio+ 20: The united nations conference on sustainable development, june 2012,* (Library of Congress, Congressional Research Service, 2012).

[2] R. Nicholls and C. Small, *Improved estimates of coastal population and exposure to hazards released,* Eos **83**, 301 (2002).

[3] Y. Wada, L. P. H. van Beek, N. Wanders, and M. F. P. Bierkens, *Human water consumption intensifies hydrological drought worldwide,* Environmental Research Letters **8**, 034036 (2013).

[4] Z. Huang, M. Hejazi, Q. Tang, C. R. Vernon, Y. Liu, M. Chen, and K. Calvin, *Global agricultural green and blue water consumption under future climate and land use changes,* Journal of Hydrology **574**, 242 (2019).

[5] E. Custodio, *Aquifer overexploitation: What does it mean?* Hydrogeology Journal **10**, 254 (2002).

[6] P. G. B. De Louw, S. Eeman, B. Siemon, B. R. Voortman, J. Gunnink, E. S. Van Baaren, and G. H. P. Oude Essink, *Shallow rainwater lenses in deltaic areas with saline seepage,* Hydrology and Earth System Sciences **15**, 3659 (2011).

[7] J. Schewe, J. Heinke, D. Gerten, I. Haddeland, N. W. Arnell, D. B. Clark, R. Dankers, S. Eisner, B. M. Fekete, F. J. Colón-González, S. N. Gosling, H. Kim, X. Liu, Y. Masaki, F. T. Portmann, Y. Satoh, T. Stacke, Q. Tang, Y. Wada, D. Wisser, T. Albrecht, K. Frieler, F. Piontek, L. Warszawski, and P. Kabat, *Multimodel assessment of water scarcity under climate change.* Proceedings of the National Academy of Sciences of the United States of America **111**, 3245 (2014).

[8] G. Forzieri, L. Feyen, R. Rojas, M. Flörke, F. Wimmer, and a. Bianchi, *Ensemble projections of future streamflow droughts in Europe,* Hydrology and Earth System Sciences **18**, 85 (2014).

[9] P. M. Barlow, *Ground water in freshwater-saltwater environments of the Atlantic coast*, Vol. 1262 (Geological Survey (USGS), 2003).

[10] A. G. Bobba, *Numerical modelling of salt-water intrusion due to human activities and sea-level change in the godavari delta, india,* Hydrological Sciences Journal **47**, S67 (2002).

[11] P. M. Barlow and E. G. Reichard, *Saltwater intrusion in coastal regions of north america,* Hydrogeology Journal **18**, 247 (2010).

[12] G. H. P. Oude Essink, E. S. Van Baaren, and P. G. B. De Louw, *Effects of climate change on coastal groundwater systems: A modeling study in the Netherlands,* Water Resources Research **46**, 1 (2010).

[13] V. Post and E. Abarca, *Preface: Saltwater and freshwater interactions in coastal aquifers,* Hydrogeology Journal **18**, 1 (2010).

[14] J. R. Delsman, M. J. Waterloo, M. M. Groen, J. Groen, and P. J. Stuyfzand, *Investigating summer flow paths in a Dutch agricultural field using high frequency direct measurements,* Journal of Hydrology **519**, 3069 (2014).

[15] P. G. B. De Louw, S. Eeman, G. H. P. Oude Essink, E. Vermue, and V. E. a. Post, *Rainwater lens dynamics and mixing between infiltrating rainwater and upward saline groundwater seepage beneath a tile-drained agricultural field,* Journal of Hydrology **501**, 133 (2013).

[16] F. Klijn, E. van Velzen, J. ter Maat, J. Hunink, G. Baarse, V. Beumer, P. Boderie, J. Buma, J. R. Delsman, J. Hoogewoud, *et al.*, *Zoetwatervoorziening in Nederland: aangescherpte landelijke knelpuntenanalyse 21e eeuw*, Tech. Rep. (Deltares, 2012).

[17] Delta Programme Commissioner, *Delta Programme 2020 - Continuing the work on the delta: down to earth, alert, and prepared*, Tech. Rep. (Delta Programme Commissioner, 2019).

[18] Contributors,Wikipedia, *Polders — Wikipedia, the free encyclopedia,* (2020), [Online; accessed 16-April-2020].

[19] J. R. Delsman, *Saline Groundwater - Surface Water Interaction in Coastal Lowlands* (IOS Press, Inc., Amsterdam, 2015) pp. 1–188.

[20] A. H. Lobbrecht, M. D. Sinke, and S. B. Bouma, *Dynamic control of the Delfland Polders and storage basin, The Netherlands,* in *Water Science and Technology*, Vol. 39 (1999) pp. 269–279.

[21] E. V. R. Vellinga, C. Toussaint, and K. Wit, *Water quality and hydrology in a coastal region of the netherlands,* Journal of Hydrology **50**, 105 (1981).

[22] P. de Louw, G. Oude Essink, P. Stuyfzand, and S. van der Zee, *Upward groundwater flow in boils as the dominant mechanism of salinization in deep polders, The Netherlands,* Journal of Hydrology **394**, 494 (2010).

[23] J. R. Delsman, G. H. P. Oude Essink, K. J. Beven, and P. J. Stuyfzand, *Uncertainty estimation of end-member mixing using generalized likelihood uncertainty estimation (GLUE), applied in a lowland catchment,* Water Resources Research **49**, 4792 (2013).

[24] J. de Halleux, C. Prieur, J.-M. Coron, B. d'Andréa Novel, and G. Bastin, *Boundary feedback control in networks of open channels,* Automatica **39**, 1365 (2003).

[25] J. Schuurmans, O. Bosgra, and R. Brouwer, *Open-channel flow model approximation for controller design,* Applied Mathematical Modelling **19**, 525 (1995).

[26] J. Schuurmans, *Control of water levels in open channels (PhD Dissertation)*, Ph.D. thesis, The Netherlands: Delft Univesity of Technology (1997).

[27] A. J. Clemmens and B. T. Wahlin, *Simple Optimal Downstream Feedback Canal Controllers: ASCE Test Case Results,* Journal of Irrigation and Drainage Engineering **130**, 35 (2004).

[28] P. J. van Overloop, *Model Predictive Control on Open Water Systems*, Ph.D. thesis, The Netherlands: Delft University of Technology (2006).

[29] H. Ghorbanidehno, A. Kokkinaki, P. K. Kitanidis, and E. Darve, *Optimal estimation and scheduling in aquifer management using the rapid feedback control method*, Advances in Water Resources **110**, 310 (2017).

[30] L. Kong, X. Lei, Q. Yang, H. Wang, *et al.*, *Automatic feedback control algorithm for canal for a quick upstream water supply interruption in the case of an emergency*, in *MATEC Web of Conferences*, Vol. 246 (EDP Sciences, 2018) p. 02026.

[31] Z. Wang, M. M. Polycarpou, J. G. Uber, and F. Shang, *Adaptive control of water quality in water distribution networks*, IEEE transactions on control systems technology **14**, 149 (2005).

[32] M. M. Polycarpou, J. G. Uber, Z. Wang, F. Shang, and M. Brdys, *Feedback control of water quality*, IEEE Control Systems Magazine **22**, 68 (2002).

[33] K. J. Åström and R. M. Murray, *Feedback systems: an introduction for scientists and engineers* (Princeton university press, 2010).

[34] E. Bautista, T. Strelkoff, and A. Clemmens, *General characteristics of solutions to the open-channel flow, feedforward control problem*, Journal of irrigation and drainage engineering **129**, 129 (2003).

[35] J. Soler, M. Gómez, and J. Rodellar, *Goroso: Feedforward control algorithm for irrigation canals based on sequential quadratic programming*, Journal of irrigation and drainage engineering **139**, 41 (2013).

[36] X. Tian, *Model predictive control for operational water management*, Ph.D. thesis, The Netherlands: Delft University of Technology (2015).

[37] E. Camacho and C. Bordons, *Model Predictive control*, 2nd ed., Advanced Textbooks in Control and Signal Processing (Springer London, London, 2007) p. 405.

[38] B. E. Aydin, P. J. van Overloop, M. Rutten, and X. Tian, *Offset-Free Model Predictive Control of an Open Water Channel Based on Moving Horizon Estimation*, Journal of Irrigation and Drainage Engineering , B4016005 (2016).

[39] R. Negenborn, P. van Overloop, T. Keviczky, and B. De Schutter, *Distributed model predictive control of irrigation canals*, Networks and Heterogeneous Media **4**, 359 (2009).

[40] X. Tian, P. J. van Overloop, R. R. Negenborn, and N. van de Giesen, *Operational flood control of a low-lying delta system using large time step Model Predictive Control*, Advances in Water Resources **75**, 1 (2014).

[41] M. Breckpot, O. M. Agudelo, P. Meert, P. Willems, and B. De Moor, *Flood control of the Demer by using Model Predictive Control*, Control Engineering Practice **21**, 1776 (2013).

[42] T. B. Blanco, P. Willems, B. De Moor, and J. Berlamont, *Flooding prevention of the demer river using model predictive control,* IFAC Proceedings Volumes **41**, 3629 (2008).

[43] M. Xu, P. J. Van Overloop, N. C. Van De Giesen, and G. S. Stelling, *Real-time control of combined surface water quantity and quality: Polder flushing,* Water Science and Technology **61**, 869 (2010).

[44] M. Xu, P. van Overloop, and N. van de Giesen, *Model reduction in model predictive control of combined water quantity and quality in open channels,* Environmental Modelling & Software **42**, 72 (2013).

[45] S. Galelli, A. Castelletti, and A. Goedbloed, *High-Performance Integrated Control of water quality and quantity in urban water reservoirs,* Water Resources Research **51**, 9053 (2015).

[46] L. Raso, D. Schwanenberg, N. van de Giesen, and P. J. van Overloop, *Short-term optimal operation of water systems using ensemble forecasts,* Advances in water resources **71**, 200 (2014).

[47] E. Kayacan, E. Kayacan, H. Ramon, and W. Saeys, *Learning in centralized nonlinear model predictive control: Application to an autonomous tractor-trailer system,* IEEE Transactions on Control Systems Technology **23**, 197 (2014).

[48] E. Shamir, S. B. Megdal, C. Carrillo, C. L. Castro, H.-I. Chang, K. Chief, F. E. Corkhill, S. Eden, K. P. Georgakakos, K. M. Nelson, *et al.*, *Climate change and water resources management in the upper santa cruz river, arizona,* Journal of Hydrology **521**, 18 (2015).

[49] P. O. Malaterre and J. Rodellar, *Multivariable predictive control of irrigation canals. Design and evaluation on a 2-pool model,* Proceedings of the International Workshop on Regulation of Irrigation Canals: State of the Art of Research and Applications , 239 (1997).

[50] P. J. van Overloop, K. Horváth, and B. E. Aydin, *Model predictive control based on an integrator resonance model applied to an open water channel,* Control Engineering Practice **27**, 54 (2014).

[51] K. Horváth, E. Galvis, M. G. Valentín, and J. Rodellar, *New offset-free method for model predictive control of open channels,* Control Engineering Practice **41**, 13 (2015).

[52] X. Tian, R. R. Negenborn, P. J. van Overloop, J. M. Maestre, and E. Mostert, *Model Predictive Control for Incorporating Transport of Water and Transport over Water in the Dry Season,* in *Operations Research/ Computer Science Interfaces Series*, Vol. 58 (2015) pp. 191–210.

[53] X. Tian, P. J. Van Overloop, R. Negenborn, and P. M. Torreblanca, *Incorporating transport over water in the multi-objective water management of the Lake IJssel*

area in the Netherlands, 2013 10th IEEE International Conference on Networking, Sensing and Control, ICNSC 2013 , 649 (2013).

[54] D. Schwanenberg, M. Xu, T. Ochterbeck, C. Allen, and D. Karimanzira, *Short-term management of hydropower assets of the federal columbia river power system,* Journal of Applied Water Engineering and Research **2**, 25 (2014).

[55] D. Schwanenberg, F. M. Fan, S. Naumann, J. I. Kuwajima, R. A. Montero, and A. A. Dos Reis, *Short-term reservoir optimization for flood mitigation under meteorological and hydrological forecast uncertainty,* Water Resources Management **29**, 1635 (2015).

[56] A. Ficchì, L. Raso, D. Dorchies, F. Pianosi, P.-O. Malaterre, P.-J. Van Overloop, and M. Jay-Allemand, *Optimal operation of the multireservoir system in the seine river basin using deterministic and ensemble forecasts,* Journal of Water Resources Planning and Management **142**, 05015005 (2016).

[57] B. E. Aydin, X. Tian, J. Delsman, G. H. Oude Essink, M. Rutten, and E. Abraham, *Optimal salinity and water level control of water courses using Model Predictive Control,* Environmental Modelling & Software **112**, 36 (2018).

[58] J. R. Delsman, P. G. de Louw, W. J. de Lange, and G. H. Oude Essink, *Fast calculation of groundwater exfiltration salinity in a lowland catchment using a lumped celerity/velocity approach,* Environmental Modelling and Software **96**, 323 (2017).

[59] P. G. B. De Louw, Y. Van Der Velde, and S. E. A. T. M. Van Der Zee, *Quantifying water and salt fluxes in a lowland polder catchment dominated by boil seepage: A probabilistic end-member mixing approach,* Hydrology and Earth System Sciences **15**, 2101 (2011).

[60] A. Hof and W. Schuurmans, *Water quality control in open channels,* Water Science and Technology, 42- 153-159 , 153 (2000).

[61] H. B. Fischer, E. J. List, R. C. Koh, J. Imberger, and N. H. Brooks, *Mixing in Inland and Coastal Waters* (Elsevier, 1979) pp. 1–483.

[62] G. S. Stelling and S. P. a. Duinmeijer, *A staggered conservative scheme for every Froude number in rapidly varied shallow water flows,* International Journal for Numerical Methods in Fluids **43**, 1329 (2003).

[63] J. M. Maciejowski, *Predictive control with constraints* (Prentice Hall, New York, 2002) p. 331.

[64] A. K. Sampathirao, P. Sopasakis, A. Bemporad, and P. P. Patrinos, *Gpu-accelerated stochastic predictive control of drinking water networks,* IEEE Transactions on Control Systems Technology **26**, 551 (2017).

[65] C. Shang, W.-H. Chen, A. D. Stroock, and F. You, *Robust model predictive control of irrigation systems with active uncertainty learning and data analytics,* IEEE Transactions on Control Systems Technology (2019).

[66] D. Delgoda, H. Malano, S. K. Saleem, and M. N. Halgamuge, *Irrigation control based on model predictive control (mpc): Formulation of theory and validation using weather forecast data and aquacrop model,* Environmental Modelling & Software **78**, 40 (2016).

[67] D. Tavernini, M. Metzler, P. Gruber, and A. Sorniotti, *Explicit nonlinear model predictive control for electric vehicle traction control,* IEEE Transactions on Control Systems Technology **27**, 1438 (2018).

[68] E. Nederkoorn, J. Schuurmans, J. Grispen, and W. Schuurmans, *Continuous nonlinear model predictive control of a hybrid water system,* Journal of Hydroinformatics **15**, 246 (2012).

[69] Y. Wang, V. Puig, and G. Cembrano, *Non-linear economic model predictive control of water distribution networks,* Journal of Process Control **56**, 23 (2017).

[70] D. Q. Mayne, J. B. Rawlings, C. V. Rao, and P. O. Scokaert, *Constrained model predictive control: Stability and optimality,* Automatica **36**, 789 (2000).

[71] J. T. Betts, *Practical methods for optimal control and estimation using nonlinear programming*, Vol. 19 (Siam, 2010).

[72] A. Wächter and L. T. Biegler, *On the implementation of an interior-point filter line-search algorithm for large-scale nonlinear programming,* Mathematical programming **106**, 25 (2006).

[73] B. E. Aydin, H. Hagedooren, M. M. Rutten, J. R. Delsman, G. H. P. Oude Essink, N. van de Giesen, and E. Abraham, *A greedy algorithm for optimal sensor placement to estimate salinity in polder networks,* Water **11**, 1101 (2019).

[74] Deltares, *Sobek, user manual,* (2014).

[75] N. Mahjouri and R. Kerachian, *Revising river water quality monitoring networks using discrete entropy theory: The Jajrood River experience,* Environmental Monitoring and Assessment **175**, 291 (2011).

[76] R. Noori, M. S. Sabahi, A. R. Karbassi, A. Baghvand, and H. T. Zadeh, *Multivariate statistical analysis of surface water quality based on correlations and variations in the data set,* Desalination **260**, 129 (2010).

[77] Y. Ouyang, *Evaluation of river water quality monitoring stations by principal component analysis,* Water Research **39**, 2621 (2005).

[78] L. Alfonso, A. Lobbrecht, and R. Price, *Optimization of water level monitoring network in polder systems using information theory,* Water Resources Research **46**, 1 (2010).

[79] L. Alfonso, L. He, A. Lobbrecht, and R. Price, *Information theory applied to evaluate the discharge monitoring network of the Magdalena River,* Journal of Hydroinformatics **15**, 211 (2013).

[80] L. Raso, S. V. Weijs, and M. Werner, *Balancing costs and benefits in selecting new information: Efficient monitoring using deterministic hydro-economic models,* Water Resources Management **32**, 339 (2018).

[81] K. Cohen, S. Siegel, and T. McLaughlin, *A heuristic approach to effective sensor placement for modeling of a cylinder wake,* Computers & Fluids **35**, 103 (2006).

[82] B. Yildirim, C. Chryssostomidis, and G. E. Karniadakis, *Efficient sensor placement for ocean measurements using low-dimensional concepts,* Ocean Modelling **27**, 160 (2009).

[83] S. Gangopadhyay, A. Das Gupta, and M. Nachabe, *Evaluation of Ground Water Monitoring Network by Principal Component Analysis,* Ground Water **39**, 181 (2001).

[84] A. K. Mishra and P. Coulibaly, *Developments in Hydrometric Network Design : a Review,* , 1 (2009).

[85] J. Keum, K. C. Kornelsen, J. M. Leach, and P. Coulibaly, *Entropy applications to water monitoring network design: A review,* Entropy **19**, 1 (2017).

[86] W. E. Hart and R. Murray, *Review of Sensor Placement Strategies for Contamination Warning Systems in Drinking Water Distribution Systems,* Journal of Water Resources Planning and Management **136**, 611 (2010).

[87] C. E. Shannon, *A Mathematical Theory of Communication,* Bell System Technical Journal **27**, 379 (1948), arXiv:9411012 [chao-dyn] .

[88] C. Lee, K. Paik, D. G. Yoo, and J. H. Kim, *Efficient method for optimal placing of water quality monitoring stations for an ungauged basin,* Journal of Environmental Management **132**, 24 (2014).

[89] M. Memarzadeh, N. Mahjouri, and R. Kerachian, *Evaluating sampling locations in river water quality monitoring networks: Application of dynamic factor analysis and discrete entropy theory,* Environmental Earth Sciences **70**, 2577 (2013).

[90] A. Boroumand and T. Rajaee, *Discrete entropy theory for optimal redesigning of salinity monitoring network in San Francisco bay,* Water Science and Technology: Water Supply **17**, 606 (2017).

[91] B. K. Banik, L. Alfonso, A. S. Torres, A. Mynett, C. Di Cristo, and A. Leopardi, *Optimal placement of water quality monitoring stations in sewer systems: An information theory approach,* Procedia Engineering **119**, 1308 (2015).

[92] J. H. Lee, *Determination of optimal water quality monitoring points in sewer systems using entropy theory,* Entropy **15**, 3419 (2013).

[93] F. Masoumi and R. Kerachian, *Assessment of the groundwater salinity monitoring network of the Tehran region: Application of the discrete entropy theory,* Water Science and Technology **58**, 765 (2008).

[94] Y. Mogheir and V. P. Singh, *Application of information theory to groundwater quality monitoring networks,* Water Resources Management **16**, 37 (2002).

[95] R. R. Owlia, A. Abrishamchi, and M. Tajrishy, *Spatial-temporal assessment and redesign of groundwater quality monitoring network: A case study,* Environmental Monitoring and Assessment **172**, 263 (2011).

[96] I. T. Jolliffe, *Springer Series in Statistics*, Springer Series in Statistics, Vol. 98 (Springer-Verlag, New York, 2002) p. 487, arXiv:arXiv:1011.1669v3 .

[97] B. K. Banik, L. Alfonso, C. Di Cristo, and A. Leopardi, *Greedy algorithms for sensor location in sewer systems,* Water (Switzerland) **9**, 1 (2017).

[98] B. K. Banik, L. Alfonso, C. Di Cristo, A. Leopardi, and A. Mynett, *Evaluation of Different Formulations to Optimally Locate Sensors in Sewer Systems,* Journal of Water Resources Planning and Management **143**, 04017026 (2017).

[99] J. Uber, R. Janke, R. Murray, and P. Meyer, *Greedy Heuristic Methods for Locating Water Quality Sensors in Distribution Systems,* Critical Transitions in Water and Environmental Resources Management **40737**, 1 (2004).

[100] P. Krause, D. Boyle, and F. Bäse, *Comparison of different efficiency criteria for hydrological model assessment,* Advances in geosciences **5**, 89 (2005).

[101] O. Hoes, W. Luxemburg, M. C Westhof, N. van de Giesen, and J. Selker, *Identifying seepage in ditches and canals in polders in the netherlands by distributed temperature sensing,* Lowland Technology International **11**, 21 (2009).

[102] I. Kelderman, *Slimmer inlaten in de Haarlemmermeerpolder Slimmer inlaten in de Haarlemmermeerpolder*, Tech. Rep. (Deltares, 2015).

[103] M. Udell, C. Horn, R. Zadeh, S. Boyd, *et al.*, *Generalized low rank models,* Foundations and Trends® in Machine Learning **9**, 1 (2016).

[104] J. King, G. Oude Essink, M. Karaolis, B. Siemon, and M. F. Bierkens, *Quantifying geophysical inversion uncertainty using airborne frequency domain electromagnetic dataapplied at the province of zeeland, the netherlands,* Water Resources Research **54**, 8420 (2018).

[105] J. Maestre, L. Raso, P. Van Overloop, and B. De Schutter, *Distributed tree-based model predictive control on a drainage water system,* Journal of Hydroinformatics **15**, 335 (2012).

[106] J. B. Rawlings, D. Angeli, and C. N. Bates, *Fundamentals of economic model predictive control,* in *2012 IEEE 51st IEEE conference on decision and control (CDC)* (IEEE, 2012) pp. 3851–3861.

[107] M. Ellis, H. Durand, and P. D. Christofides, *A tutorial review of economic model predictive control methods,* Journal of Process Control **24**, 1156 (2014).

ACKNOWLEDGEMENTS

Welcome to the end of this story. Its been a long one with a lot of challenges but thanks to you it was full with a lot of good memories. So if you are here looking at this page to find the answer "if Boran have written something for me?", most probably the answer will be yes and I just want to let you know that I am very thankful for meeting with you.

Everything started with an email sent on July 2012, which had three actors involved. The first person was the receiver of the email, late dr. ir. Peter Jules van Overloop. I am very grateful to him for seeing and responding to that email out of many similar ones and helping me to start a guest researcher position here at TU Delft. Due to unexpected circumstances we could not finish what we had started. You were a brilliant scientist, a good friend and I also have to admit you were the one that pointed the importance of Thursdays and colloquiums for me. We ended up having different reasons but I ended up treating Thursdays as the end of the week for a long time as you once said. Thank you for everything and rest in peace.

Second person was Bilge Çelik. Back then sharing similar dreams, you were the one chasing for me what I am finishing now. Following you and getting all kind of support from you at the beginning, this thesis would not be possible without you. Now far from where we started, once again I would use this opportunity to tell how important you were in this story.

Last person involved in that email was the sender, Ekin as his family calls him. I will briefly thank him for being him. Showing some of the important properties of people from his region in Turkey, he was able to adapt, adjust and resist to whatever was coming while keeping the child in him alive. Thank you for the joy, I have no regrets.

My supervision team, a bit larger than normal, at different stages of this journey guided me with right questions and answers and made this work scientifically relevant and solid. First of all, I will thank to my promoter, Prof. Nick van de Giesen for giving me the chance to officially join the Water Management Department as a PhD candidate at a moment where I was thinking all the doors were closing. Thank you for the trust and the support in the following years. Then, I will thank to my daily supervisors and co-promoters (in order of appearance).

Dr. ir. Martine Rutten, I don't know what you did right or wrong to find three PhD's to be supervised as you started your new role in the department but I feel very lucky to have you there on my side. When we first met, I had no idea what I was doing and what I will be doing but you helped me first finish what I started with PJ and then advised me to structure my research that led to this thesis. Thank you for your guidance.

Once the long awaited signature confirming the start of WaterNexus project was there, I met with Dr. ir Gualbert H.P. Oude Essink. You were able to recognize me from a distance while I was trying to approach you to introduce myself in Joost's PhD defence. Maybe it was obvious that I was the outsider in that room and it was an easy guess, but that was enough to impress me with the way you had an overview over things around

you. Thank you for the critical view, guidance and the push outside TU Delft. I know there is not enough subsurface, groundwater and global in this thesis, but that part I left for the new generations that will also be lucky enough to meet with their supervisor in one of the best bar's in Den Haag on a Saturday night.

Almost half way through my PhD, I got luckier with my supervision and started working with Dr. ir. Edo Abraham. After first meetings, you already had enough questions and ideas to keep me busy until the end. Luckily, your door was always open and there was always time for me. You were 'the eye' that knew what I was and wasn't doing. Your push to convince me that what we achieved at the end was possible helped me a lot to get where I am now. I am looking forward to a long future of friendship and collaboration with you.

I will thank to Dr. Xin Tian, the person who welcomed me when I first entered 4.71, not only as an office mate and a friend but also with his very critical role in helping me understand and solve any problem with MPC. Whenever I left Edo's room with more questions in mind, I knew Tian was there. Your contribution to this work is more than you think.

Summer 2015 was understanding Dr. Joost Delsman thesis on saline groundwater exfiltration, and try to shape my research over that. I am very thankful for your help, effort and model that I used almost every stage of this thesis.

I will also thank Hugo Hagedooren, the one and only master student I supervised. His hard work and motivation brought me one step closer to the end.

Water management department would not be like this if we didn't have two beautiful colleagues helping us all the time. First of all Betty, thank you for the constant smile in your face and I want you to know that when you also offered me a slice of your apple at the lunch table, I felt special. It was a pleasure to be around you. Then comes Lydia, I know I am loud sometimes but when Lydia is there I feel normal. Its a good feeling to have that kind of friends around you where you feel comfortable. Thank you for all the joy you are bringing to us.

Starting from a hate relation in Vienna because of a wasted ice cream, I managed to change his mind in Luxembourg while chopping onions. Juancho, meneer, I believe what we achieved in Luxembourg will stay as a legend. Until your responsibilities increased as a father, having a friend always ready to talk about food or actually better to eat and drink together was amazing. Our complicated numbering system, and missed opportunities of 'bitterballen's' will always be following us as we grow older.

Bart, I met with you as a brewer that has a lot to tell about beers but then I realized you have a lot to tell about everything, impressive! Sometimes too much but after years, you know what I will say and get your position wisely. The project of making cider from the apples of my village is valid until we go and collect those apples.

Bas, sitting on a terrace or walking in the city or enjoying a boat ride, it is always easy and fun to be with you. TU Delft story for both of us is coming to an end, but I am sure this was just the start.

David, my friend!, what to say for you. You are awesome and you know it. I am sorry for ruining your Mr.Tasty pleasure! Now I am gone you can go back and enjoy again. Although I still think pizza is a better choice for closing Thursday's.

Carina, walking in the corridor with smiling and curious eyes and a piercing on your

nose! I already knew you were not a normal PhD and the time we spent proved nothing less. I think you are the starting point of my German/Austrian sympathy.

Remco and Cesar, thank you guys! In addition to having an important role on Thursdays (which is followed by Jerom and he knows how crucial that role is and he nails it!), it was a pleasure to watch you guys be the second team at fitterij with my beautiful team mate Anna. Not once but twice and I am sure that was your destiny, sorry guys.

Ase, my beautiful office mate! It took a while to change your judgmental view on me to an "okay what is there to celebrate and lets celebrate it fancy" mode, but it worth the effort.

Paul, Antonella, Sergio, Monica, Jessica, Robert, Ties, Tamara, Elisa, Sandra Junier, Laurene, Bahareh, Juan Carlo, Martin, Jeff, Dengxiao, Chealsea, Camille, Sandra de Vries, Gaby, Banafsheh, Nay, Petra, Coco, Tim, Yingrong, Anjana, Andreas, Saeed, Alexandra, Changrang and all other WM friends... It was a pleasure to have a beer (I know some of you drink more than one) or a coffee at the coffee corner or eat something together. We have more than this but I am sure once you will be writing your acknowledgement at some point you will also run out of words and start fast forwarding :) I love you! No broken hearts please.

Being from a different culture, it took a while to get used to having a friendly talk with the big names in the department. Its a unique experience and always a pleasure! Erik (I am not sure why your jokes are not more popular? I love them!), Maurits, Saket, Susan (special thanks for the best high five ever), Huub (a true inspiration for how to open and enjoy a beer), Miriam, Rolf, Ruud, Wim and Thom thank you for everything.

Les agas de den haag, Comert and Nilhan... Different timings and different roles but you reminded me the feeling of having close friends around you that you can speak your language. Extra credit goes to Cemo for making 33 as my best age so far.

Nazli, Salih, Korhan, Haki, Ismail, Burcu, Taner, Sevil, Ebru... The Turkish-Dutch or Dutch-Turkish friends, friends that have similar stories why we are settling here... It is precious to find the smell of home in one glass raki we share. Şerefinize!

Erdal, being the only one to return back and being the one to support me while I needed someone to talk deserves a special thanks. What you did and how you helped me is unforgettable.

All WaterNexus friends for the headache at the second day of the general assemblies, special thank goes to Daniel Zamrsky. Thank you for inviting me to your birthday party and also it was a nice competition with you for being the -best PhD.

Everything I achieved was possible with the unconditional support and love of my parents and elder brother.

Anne! Baba! Bir çocuğun sevildiğini bilmesi kadar kıymetli bir duygu yok. Ben sizin sevginizi ve desteğinizi her zaman yanımda hissediyorum. İyi ki varsınız ve iyi ki beni olduğum kişi olabilmem konusunda koşulsuz desteklediniz. Sizi seviyorum benim ilk ve en büyük öğretmenlerim.

Her zaman yanmda olan Ağbim, Ozan Emre. Çaldığın bağlamanın sesiyle uyuduğum küçük odamızda, senden öğrendim doğru ve şefkatli olmayı. Küçücük ellerinle tutup boyundan çok büyük bir sorumlulukla okula götürdüğün kardeşin sonunda okul hayatını bitiriyor. Herşey için sağol.

And Luisa... with this thesis I am obtaining a PhD, the highest university degree, but

you are the one making me feel smart. Thank you for your support, understanding and love.

CURRICULUM VITÆ

Boran Ekin AYDIN

22-03-1985	Born in Macka, Trabzon, Turkey.

EDUCATION

2000–2003	Science High School Yomra Science High School, Trabzon, Turkey
2003–2008	B.Sc. in Civil Engineering, Civil Engineering Faculty Middle East Technical University, Ankara, Turkey
2008–2010	MSc. in Civil Engineering, Civil Engineering Faculty Middle East Technical University, Ankara, Turkey
2015–2020	PhD. in Civil Engineering, Civil Engineering and Geosciences Faculty Delft University of Technology

WORK EXPERIENCE

2013-2015	Guest Researcher, Water management department Delft University of Technology, Delft, The Netherlands
2012	Post Master Researcher, Environmental and Infrastructure Engineering Department Politecnico di Milano, Milano, Italy
2011	Energy Consultant Resel Project & Energy Consultancy, Ankara, Turkey
2010-2011	Civil Engineer / Energy Expert Turkerler Holding, Ankara, Turkey

LIST OF PUBLICATIONS

PEER REVIEWED JOURNAL ARTICLES

6. **B.E. Aydin**, J. Delsman, G.H.P. Oude Essink, N. van de Giesen and E. Abraham, *Nonlinear Model Predictive Control of Polder Flushing*, submitted to IEEE Transactions and Control Engineering.

5. **B.E. Aydin**, H. Hagedooren, M.M. Rutten, J. Delsman, G.H.P. Oude Essink, N. van de Giesen, and E. Abraham, *A greedy algorithm for optimal sensor placement to estimate salinity in polder networks*, Water (Switzerland) **11**, 1 (2019).

4. **B.E. Aydin**, X. Tian, J. Delsman, G.H.P. Oude Essink, M.M. Rutten, and E. Abraham, *Optimal salinity and water level control of water courses using model predictive control*, Environmental Modelling and Software **112**, 36 (2018).

3. **B.E. Aydin**, P. J. van Overloop, M.M. Rutten, and X. Tian, *Offset-Free Model Predictive Control of an Open Water Channel Based on Moving Horizon Estimation*, Journal of Irrigation and Drainage Engineering, **143**,3, B4016005 (2016).

2. X. Tian, **B.E. Aydin**, R.R. Negenborn, N. van de Giesen, and J.M. Maestre *Model predictive control for water level control in the case of spills*, Journal of Irrigation and Drainage Engineering, **143**,3, B4016006 (2016).

1. P. J. van Overloop, K. Horváth, and **B.E. Aydin**, *Model predictive control based on an integrator resonance model applied to an open water channel*, Control Engineering Practice, **44**,pp.54-60, (2014).

PEER REVIEWED CONFERENCE PAPERS

4. **B.E. Aydin**; M.M. Rutten, and E. Abraham, *Model Predictive Control of Salinity and Water Level in a Hypothetical Polder Ditch: Is it Possible to Use the Discretized Linearized Physical Equations for Optimization*, In Proceedings of 13th International Conference on Hydroinformatics, Palermo, Italy (2018).

3. **B.E. Aydin**, M.M. Rutten, E. Abraham, G.H.P. Oude Essink and J. Delsman, *Model predictive control of salinity in a polder ditch under high saline groundwater exfiltration conditions: A Test case.*, In Proceedings of 20th World Congress The International Federation of Automatic Control. Toulouse, France, IFAC-PapersOnLine, **50**, 1 (2017).

2. **B.E. Aydin**, M.M. Rutten, G.H.P. Oude Essink and J. Delsman, *Polder Flushing: Model Predictive Control of Flushing Operations to Effective and Real Time Control of Salinity in Polders.*, In Proceedings of 12th International Conference on Hydroinformatics, Incheon, South Korea, Procedia Engineering, **154**, 1 (2016).

1. **B.E. Aydin**, P. J. van Overloop, and X. Tian, *Offset Free Model Predictive Control of an Open Water Reach.*, In Proceedings of 11th International Conference on Hydroinformatics, New York, USA, (2014).